Dissertation

Crosstalk Between Gut Microbiome Bile Acids and Metabolome in Sarcopenia in Liver Cirrhosis

Submitted by

Aliwa, Benard Ochieng

for the Academic Degree of

Doctor of Philosophy (Ph.D.)

at the

Medical University of Graz

Department of Gastroenterology and Hepatology

under the supervision of

Prof. Dr. STADLBAUER-KÖLLNER, Vanessa

2023.

DECLARATION

I hereby declare that this thesis is my original work and that I have fully acknowledged by name all those individuals and organizations that have contributed to the research for this thesis. Due acknowledgment has been made in the text of all other material used. Throughout this thesis and in all related publications, I followed the Medical University of Graz guidelines on Good Scientific Practice.

Graz, August 16, 2023

DISCLOSURES

Parts of this thesis were published in :

Aliwa B, Horvath A, Traub J, Feldbacher N, Habisch H, Fauler G, Madl T, Stadlbauer V. Altered gut microbiome, bile acid composition and metabolome in sarcopenia in liver cirrhosis. J Cachexia Sarcopenia Muscle. 2023 Sep 28. doi: 10.1002/jcsm.13342. PMID: 37767786.

Co-authors who contributed to these publications:

Angela Horvath[1,2,] Julia Traub[3] , Nicole Feldbacher[1,2], Hansjörg Habisch[4] , Günter Fauler[6] , Tobias Madl[4,5] , Vanessa Stadlbauer[1,2]*

[1]Division of Gastroenterology and Hepatology, Department of Internal Medicine, Medical University of Graz, Austria

[2]Centre for Biomarker Research in Medicine (CBmed), Graz, Austria

[3]Department of Clinical Medical Nutrition, University Hospital Graz, Graz, Austria

[4]Gottfried Schatz Research Center, Molecular Biology and Biochemistry, Medical University of Graz, Austria

[5]BioTechMed-Graz, Graz, Austria

[6]Clinical Institute for Medical and Chemical Laboratory Diagnostics, Graz, Austria

ACKNOWLEDGEMENTS

I am deeply grateful to everyone who has played a role in completing my dissertation. First and foremost, my heartfelt appreciation goes to my supervisor, Prof. Dr. Stadlbauer-Köllner, Vanessa. Her unwavering trust, guidance, support, and encouragement throughout my Ph.D. journey have brought this dissertation to fruition. I would also like to extend my thanks to all my colleagues at the Medical University of Graz and the University Hospital of Graz, specifically Dr. Angela Horvath, Nicole Feldbacher, Rosa Haller, Christian Pacher, Kristina Žukauskaitė', and Hazia Olha. Their constant presence and support, both during challenging times and moments of success, have been invaluable. My gratitude extends to the esteemed members of my thesis committee, Prof. Priv.-Doz. Mag. Tobias Madl, Prof. Dr. Castellani Christoph, and Dr. Angela Horvath for their guidance and valuable insights throughout this project. I want to thank Dr. Hansjörg Habisch for his assistance with metabolome wet lab analysis and Gunter Fauler for his technical support regarding serum and stool bile acids measurements. Their expertise has been essential to the success of my research. I am thankful to the entire faculty and students of the MOLMED Ph.D. program for their friendship and stimulating scientific discussions.

Additionally, I extend my gratitude to the Office for Doctoral Studies at the Medical University of Graz for their continuous support. Special thanks are due to the Core Facilities of the Center for Medical Research (ZMF) and the Clinical Institute of Medical and Chemical Laboratory Diagnostics at the Medical University of Graz. Their assistance with the technical aspects of the experiments and analyses has been invaluable. I am profoundly grateful to my parents, Mr. Ernest Aliwa Ayuge and Mrs. Lilian Aketch Aliwa, for their unwavering support and encouragement. Their boundless love, prayers, and unwavering trust in me have been my pillars of strength. Finally, I acknowledge the financial support from the Austrian Science Fund (FWF, Grant ID: KLI741), the Medical University of Graz through the Ph.D., Program Molecular Medicine (DK-MOLMED)., Austrian Research Promotion Agency (FFG, Grant 864690).

In closing, I am reminded of a Swahili proverb encapsulating the spirit of unity and collaboration that has shaped this dissertation: "Umoja ni nguvu." Translated as " Unity is strength," this proverb perfectly embodies my dissertation committee and lab colleagues' collective efforts, teamwork, and shared accomplishments.

TABLE OF CONTENTS

ABBREVIATIONS AND DEFINITIONS

EWGSOP	European working group on sarcopenia in older people
COPD	Chronic obstructive pulmonary disease
HBV	Hepatitis B virus
HCV	Hepatitis C virus
NASH	Non-alcoholic steatohepatitis
MELD	Model end-stage liver disease
BAs	Bile acids
AAs	Amino acids
BCAAs	Branched-chain amino acids
AAAs	Aromatic amino acids
SCFAs	Short-chain fatty acids
LPS	Lipopolysaccharide
LBP	Lipopolysaccharide-binding protein
sCD14	Soluble CD14
TLR	Toll-like receptor
NF-κB	Nuclear factor kappa B
IL	Interleukin
TNF-α	Tumor necrosis factor-alpha
Akt-	Protein kinase B
mTOR	Mammalian target of rapamycin
CRP	C-reactive protein
IGF-1	Insulin growth factor 1
DAO	Diamine oxidase
GSK3βG	Glycogen synthase kinase
FGF-21	Fibroblast growth factor 21
FNDC5	Fibronectin type III domain-containing protein 5
AST	Aspartate aminotransferase
ALT	Alanine aminotransferase
GGT	Gamma-glutamyl transferase
Hct	Hematocrit

PEM	Protein-energy malnutrition
T-UDCA	Total ursodeoxycholic acid
GUDCA	Glycodeoxycholic acid
TUDCA	Taurodeoxycholic acid
UDCA	Deoxycholic acid
Total DCA	Total deoxycholic acid
GDCA	Glycodeoxycholic acid
TDCA	Taurodeoxycholic acid
DCA	Deoxycholic acid
Total LCA	Total lithocholic acid
GLCA	Glycodeoxycholic acid
TLCA	Taurodeoxycholic acid
LCA	Lithocholic acid
Total CA	Total cholic acid
GCA	Glycocholic acid
TCA	Taurocholic acid
CA	Cholic acid
Total CDCA	Total chenodeoxycholic acid
GCDCA	Glycochenodeoxycholic acid
TCDCA	Taurochenodeoxycholic acid
CDCA	Chenodeoxycholic acid
Total BA	Total bile acid (Total UDCA + total CA+ total CDCA + total DCA + total LCA)
T-UDCA	Total ursodeoxycholic acid (TUDCA + GUDCA + TUDCA)
Total CA	(CA + GCA + TCA)
Total CDCA	(CDCA + GCDCA + TCDCA)
Total DCA	(DCA + GDCA+ TDCA)
Total LCA	(LCA + GLCA + TLCA)
Primary unconjugated BAs	(CA and CDCA)
Primary conjugated BAs	(GCA, TCA, GCDCA, and TCDCA)
Total primary BAs	Total primary bile acids (Total CA + total CDCA)
Secondary unconjugated BAs	(DCA, LCA, and UDCA)
Secondary conjugated BAs	(TDCA, GDCA, GLCA, TLCA, GUDCA, and TUDCA)

Total sec BAs	(DCA + GDCA + TDCA + LCA + GLCA +TLCA +UDCA + GUDCA + TUDCA)
12 α OH-BAs	12 alpha hydroxylated bile acid
12 alpha hydroxylated bile acid	(CA and DCA)
Non-12 alpha hydroxylated bile acid	(Total CDCA, total LCA, and total UDCA)
12-oxoLCA	12 oxo-lithocholic acid
3-oxoLCA	3 oxo-lithocholic acid
3-oxoDCA	3-oxo-deoxycholic acid
CA: CDCA	Ratio of cholic acid to c
DCA: CA	Ratio of deoxycholic acid to cholic acid
LCA: CDCA	Ratio of lithocholic acid to chenodeoxycholic acid
GDCA: DCA	Ratio of glycodeoxycholic acid to deoxycholic acid
TDCA: DCA	Ratio of taurodeoxycholic acid to deoxycholic acid
GLCA: LCA	Ratio of glycodeoxycholic acid to lithocholic acid
TLCA: LCA	Ratio of taurolithocholic acid to lithocholic acid
TCDCA: CDCA	Ratio of taurochenodeoxycholic acid to chenodeoxycholic acid
GCDCA: CDCA	Ratio of glycochenodeoxycholic acid to chenodeoxycholic acid
12 α OH-BAs: non 12 α OH-BAs	Ratio of 12 alpha hydroxylated bile acid to non-12 alpha hydroxylated bile acid
T-UDCA: total sec BAs	Ratio of total ursodeoxycholic acid to total secondary bile acid
BSH	Bile salt hydrolase
BaiCDE	Bile acid inducer operon CD and E
3 α-HSDH	3 alpha-hydroxysteroid dehydrogenases
3 β-HSDH	3 betta-hydroxysteroid dehydrogenases
7 α-HSDH	7 alpha-hydroxysteroid dehydrogenases
5 AR	5 alpha reductases
7 β-HSDH	7 betta-hydroxysteroid dehydrogenases
12 α-HSDH	12 alpha-hydroxysteroid dehydrogenases
HSD3B7	Hydroxy-delta-5 steroid dehydrogenase, 3 Beta isomerase 7

CYP27A1	Sterol-27-hydroxylase
CYP7A1	cholesterol 7α-hydroxylase
CY7B1	Oxysterol 7 alpha-hydroxylase
BAAT	Bile acid acyl-CoA-synthase amino acid transferase
SULT2A1	Sulfotransferase
CA7S	Sulfated cholic acid
FXR receptor	Farnesoid X receptor
TGR5 receptor	G-protein coupled receptor specific for bile acids
SHP	Small heterodimer partner
GLP 1	Glucagon-like peptide 1
ASBT	Apical sodium-dependent bile acid transporter
NTCP	Sodium taurocholate co-transporting polypeptide
OATP	Organic anion transporting polypeptide
ERK	Extracellular signal-regulated protein kinase
pSK1	Ribosomal protein S 6 kinase 1
cAMP	Cyclic adenosine monophosphate
AMPK	Adenosine monophosphate-activated protein kinase
MURF1	Muscle ring finger 1
T_H17	T helper cell 17
RORγt	Retinoic acid receptor-related orphan receptor
GPR41	G-coupled protein receptor 41
FOXO 3	Foxhead box transcriptional factors 3
ROS	Reactive oxygen species
CoQ10	Ubiquinone coenzyme 10
G-6-pase	Glucose 6 phosphatase
MHC	Myosin heavy chain
CT	Computerized tomography
MRI	Magnetic resonance imaging
NMR	Nuclear magnetic resonance
BCLC	Barcelona clinic liver cancer stage
16S rRNA	16 S ribosomal ribonucleic acid
DNA	Deoxyribonucleic acid
ELISA	Enzyme-linked immunosorbent assay

HPLC-MS/MS	High-performance liquid chromatography-tandem mass spectroscopy
BMI	Body mass index
MAMC	Mid-arm muscle circumference
GMS	Graz malnutrition screening
RFH-NPT	Royal free hospital global assessment
TSFT	Triceps skinfold thickness
HGS	Hand grip strength
qPCR	Quantitative polymerase chain reaction
dsDNA	Double-stranded DNA
MEOH	Methanol
NaOH	Sodium hydroxide
TMSP	Trimethylsilyl propionic acid
PCoA	Principal coordinate analysis
O-PLSA-DA	Orthogonal projection latent structure discriminant analysis
LDA	Linear discriminant analysis
LEfSe	Linear discriminant analysis effect size
ANCOM	Analysis of the composition of the microbiome
LASSO	Least absolute shrinkage and selection operator
ASV	Amplicon sequence variants
KEEG	Kyoto encyclopedia of genes and genomes
HMDB	Human metabolome database
MSEA	Metabolite set enrichment analysis
PPI	Proton pump inhibitor

LIST OF FIGURES

LIST OF TABLES

ZUSAMMENFASSUNG

Sarkopenie bei Leberzirrhose ist mit einer verringerten Lebensqualität und einem hohen Sterblichkeitsrisiko verbunden. Die Pathogenese ist noch nicht vollständig geklärt. Wir stellten die Hypothese auf, dass sich das Darmmikrobiom, die Gallensäurezusammensetzung und die Metaboliten zwischen Leberzirrhosepatienten mit und ohne Sarkopenie unterscheiden und zur Pathogenese beitragen.

Patient*innen mit Leberzirrhose mit (n=78) und ohne (n=38) Sarkopenie und nicht-zirrhotische Kontrollpersonen mit (n=39) und ohne (n=20) Sarkopenie (diagnostiziert anhand der Kriterien der europäischen Arbeitsgruppe zu Sarkopenie bei älteren Menschen) wurden eingeschlossen. Die Zusammensetzung des Darmmikrobioms wurde durch 16S-rRNA-Sequenzierung, die Zusammensetzung von Serum- und Stuhlgallensäuren durch Hochleistungsflüssigkeitschromatographie-Tandem-Massenspektrometrie (HPLC-MS/MS) und die Metabolomzusammensetzung in Serum, Stuhl und Urin durch Magnetresonanz (NMR)-Spektroskopie untersucht.

Bacteroides fragilis, Blautia marseille, Sutterella spp und Veillonella parvula traten bei Patient*innen mit Leberzirrhose und Sarkopenie vermehrt auf, wohingegen Bacteroides ovatus bei Patient*innen mit Leberzirrhose ohne Sarkopenie häufiger vorkam. In ähnlicher Weise waren Alistipes putredinis, Alistipes onderdonkii subspp vulgaris, Ruminococcaceae, Bacteroides coccae und Eubacterium coprostanoligenes mit nicht zirrhotischen Kontrollen ohne Sarkopenie assoziiert. Wir beobachteten signifikant erhöhte sekundäre Gallensäurespiegel), Desoxycholsäure (DCA, p = 0,01) und Lithocholsäure (LCA, p = 0,02) und die Verhältnisse von Desoxycholsäure zu Cholsäure (DCA: CA, p = 0,04), Lithocholsäure zu Chenodesoxycholsäure (LCA: CDCA, p = 0,03) und 12 alpha-hydroxyliert zu Nicht-12 alpha-hydroxylierte BAs (12 α-OH: Nicht-12 α-OH BAs, p = 0,04) im Serum von Patient*innen mit Leberzirrhose und Sarkopenie im Vergleich zu Patient*innen mit Leberzirrhose ohne Sarkopenie, was auf eine verstärkte Umwandlung von primären in sekundären Gallensäuren durch das Darmmikrobiom hinweist . Primäre Gallensäuren wie CA (p = 0,02), Verhältnisse von CA: CDCA (p = 0,03) und Gesamt-Ursodesoxycholsäure zu gesamten sekundären BAs (T-UDCA: Gesamt-sec-BAs, p = 0,03) waren im Stuhl von Patient*innen mit Leberzirrhose und Sarkopenie im Vergleich zu Patient*innen mit Leberzirrhose ohne Sarkopenie signifikant reduziert. In ähnlicher Weise waren GDCA:DCA und GLCA:LCA im Serum der nicht-zirrhotischen Kontrollgruppe mit Sarkopenie signifikant erhöht im Vergleich zu nicht-zirrhotischen Personen ohne Sarkopenie. Außerdem waren Valin und

Acetat im Serum von Patient*innen mit Leberzirrhose und Sarkopenie im Vergleich zu Patienten mit Leberzirrhose ohne Sarkopenie signifikant reduziert ($p = 0,01$ bzw. $p = 0,03$). Die multivariate logistische Regression bestätigte weiterhin die Assoziation von Bacteroides ovatus ($p = 0,01$), Verhältnisse von CA: CDCA ($p = 0,03$), 12 α-OH: Nicht-12 α-OH-BAs ($p = 0,04$), T-UDCA: insgesamt -sec-BAs ($p = 0,01$) und Serumvalin ($p = 0,04$) mit Sarkopenie bei Leberzirrhose, selbst wenn für die Schwere der Lebererkrankung und Medikamenteneinnahme korrigiert wurde.

Unsere Studie legt eine mögliche funktionelle Wechselwirkung veränderten Darmmikrobiom, den Gallensäureprofilen und Aminosäuren bei Sarkopenie nahe, was auf ein mögliches mechanistisches Zusammenspiel beim Verständnis der Sarkopenie-Pathogenese hinweist.

ABSTRACT

Sarcopenia in liver cirrhosis is associated with low quality of life and high mortality risk. The pathogenesis has yet to be fully understood. We hypothesized that gut microbiome, bile acid composition, and metabolites differ between cirrhotic patients with and without sarcopenia and contribute to pathogenesis.

Sarcopenia was diagnosed according to the European working group on sarcopenia in older people. Cirrhotic patients with (n=78) and without (n=38) sarcopenia and non-cirrhotic controls with (n=39) and without (n=20) sarcopenia. Fecal microbiome composition was studied by 16S rRNA gene sequencing, serum, and fecal bile acids (BAs) composition by high-performance liquid chromatography-tandem mass spectrometry (HPLC-MS/MS), and metabolome composition in serum, feces, and urine by nuclear magnetic resonance (NMR).

Bacteroides fragilis, Blautia marseille, Sutterella spp*,* and *Veillonella parvula* were associated with cirrhotic patients with sarcopenia, whereas *Bacteroides ovatus* was more abundant in cirrhotic patients without sarcopenia. Similarly, *Alistipes putredinis*, *Alistipes onderdonkii* subspp *vulgaris*, *Ruminococcaceae*, *Bacteroides coccae*, and *Eubacterium coprostanoligenes* were associated with non-cirrhotic controls without sarcopenia We observed significantly elevated secondary (BAs), deoxycholic acid (DCA, p = 0.01), and lithocholic acid (LCA, p = 0.02), and the ratios of deoxycholic acid to cholic acid (DCA: CA, p = 0.04), lithocholic acid to chenodeoxycholic acid (LCA: CDCA, p = 0.03), and 12 alpha-hydroxylated to non-12 alpha-hydroxylated BAs (12 α-OH: non-12 α-OH BAs, p = 0.04) in serum of cirrhotic patients with sarcopenia compared to cirrhotic patients without sarcopenia indicating an enhanced transformation of primary to secondary (BAs) by the gut microbiome. Primary BAs CA (p = 0.02), ratios of CA: CDCA (p = 0.03), and total ursodeoxycholic acid to total secondary BAs (T-UDCA: total-sec-BAs, p = 0.03) were significantly reduced in the stool of cirrhotic patients with sarcopenia compared to cirrhotic without sarcopenia. Similarly, GDCA: DCA and GLCA: LCA were significantly increased in serum of non-cirrhotic control with sarcopenia than non-cirrhotic without sarcopenia. Also, valine and acetate were significantly reduced in the serum of cirrhotic patients with sarcopenia compared to cirrhotic patients without sarcopenia (p = 0.01 and p = 0.03, respectively). Multivariate logistic regression further confirmed the association of *Bacteroides ovatus* (p = 0.01), ratios of CA: CDCA (p = 0.03), 12 α-OH: non-12 α-OH BAs (p = 0.04), T-UDCA: total-sec-BAs (p = 0.01), and serum valine (p = 0.04) with sarcopenia in liver cirrhosis even when corrected for the severity of liver disease and drug use.

Our study suggests a potential functional gut microbiome-host interaction linking sarcopenia with the altered gut microbiome, bile acids profiles, and amino acids, pointing towards a possible mechanistic interplay in understanding sarcopenia pathogenesis.

INTRODUCTION

Sarcopenia is the progressive loss of muscle mass and function commonly observed in older people, although it can also occur early in life due to various factors (2-6). There are two main categories of sarcopenia: primary, which is related to aging, and secondary, which is caused by metabolic disorders, malignant diseases, poor nutrition, and lifestyle factors such as physical inactivity (3, 5-7). The prevalence of sarcopenia increases with age, and the loss of muscle mass and function is more pronounced after age 50, with a decline of up to 15% per year (8-10). By age 80, there can be a 50% loss of muscle mass and function (11, 12). Based on appendicular lean mass measurements, 23-30% of adults above 60 suffer from sarcopenia (13, 14). However, the prevalence of sarcopenia is significantly lower (5-10 %) when diagnosed according to the European Working Group on Sarcopenia in Older People 2 (EWGSOP 2) criteria (6). Diagnosing sarcopenia requires analyzing body composition using established and validated tools and techniques and determining appropriate cut-off values for the sarcopenia (muscle mass, function, or strength) parameters (3, 6). The practical clinical diagnosis of sarcopenia, as established by the EWGSOP in 2010, involves muscle function (strength and power) and loss of muscle mass. (15, 16). This two-parameter diagnostic approach is necessary due to the non-linear relationship between muscle function (strength and power) and loss of muscle mass (15).

Furthermore, secondary sarcopenia is considered when there is evidence of causal factors other than aging, including metabolic and malignant diseases (10, 15). The conditions associated with secondary sarcopenia include liver cirrhosis, chronic kidney disease, cancer, osteoporosis, pancreatitis, hypertension, hypercholesteremia, diabetes type II, Hashimoto thyroiditis, chronic obstructive pulmonary disease (COPD), among others (2, 6, 10, 17). Therefore, treating the underlying conditions is necessary to control secondary sarcopenia (10). In contrast to age-related sarcopenia, secondary sarcopenia causes a gradual, non-linear loss of muscle mass that is of a larger magnitude and maybe be reversed (10, 18).

Sarcopenia in liver cirrhosis

Liver cirrhosis is a chronic and life-threatening liver disease caused primarily by chronic hepatitis B (HBV) or hepatitis C (HCV) virus infections, as well as alcoholic and non-alcoholic steatohepatitis (NASH) (19). However, liver cirrhosis patients also frequently suffer from sarcopenia, which affects 50-70% of cases (6, 20, 21). Sarcopenia poses a risk of disability, frailty, extended hospital stays, and lower quality of life among liver cirrhotic patients (22). Moreover, sarcopenia is an independent risk factor for mortality in patients with liver cirrhosis (2, 23), and it worsens other cirrhosis-associated complications, such as encephalopathy, ascites, and portal hypertension (21, 24). Therefore, sarcopenia was suggested to add ten additional points to the Model End-Stage Liver Disease (MELD) score calculation, accounting for the enhanced mortality risk in cirrhosis (25).

In liver cirrhosis, various metabolic changes can affect skeletal muscle cell growth and differentiation, leading to sarcopenia (2, 3, 26). For instance, dysregulation in bile acids (BAs) synthesis, glucose metabolism, selective utilization of aromatic amino acids (AAs), and increased breakdown of muscle-branched-chain amino acids (BCAAs) as an energy source are some of the metabolic changes that occur (2, 3, 21). Malnutrition, hypermetabolism, hyperammonemia, inflammation, and hormonal changes are other factors that may contribute to sarcopenia in cirrhosis (2, 3). Although the pathogenesis of sarcopenia in cirrhosis is multifactorial, its exact molecular mechanisms are not fully understood yet. Several factors, such as the altered gut microbiome, inflammation, changes in hormonal and nutritional status, bile acid (BA), and metabolome, may potentially mediate sarcopenia in cirrhosis (Fig. 1) (2).

Potential molecular mechanisms of sarcopenia in liver cirrhosis

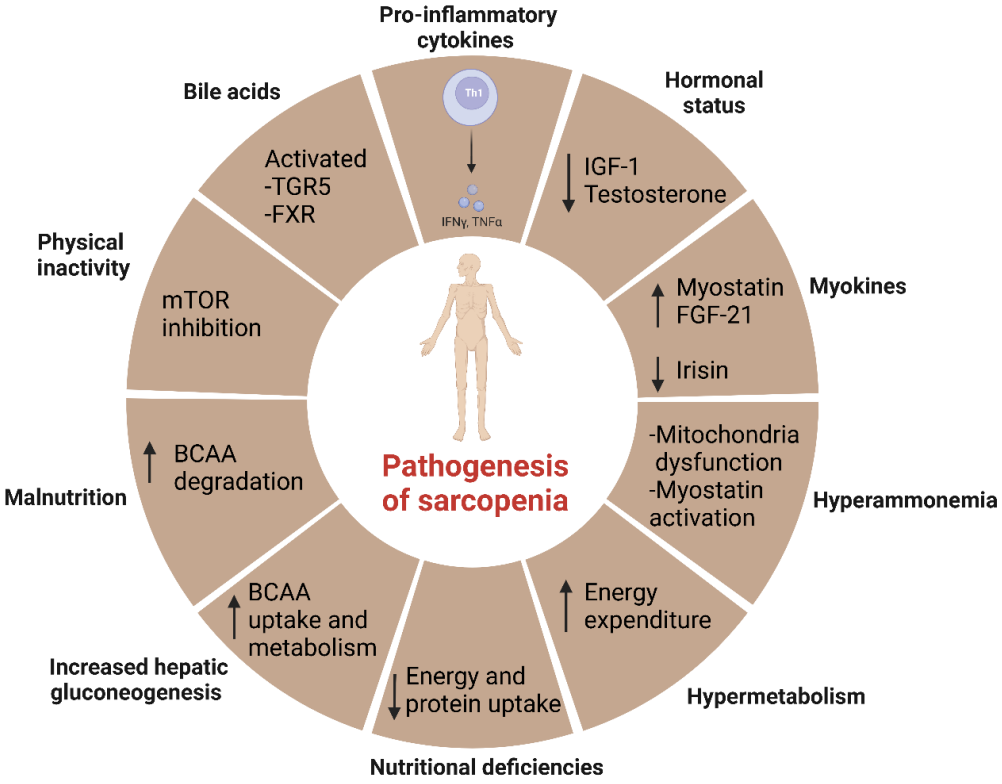

Figure 1. Overview of potential mediators of sarcopenia in liver cirrhosis. It was created with Biorender.com.

Altered gut microbiome and inflammation

The gut microbiome is a term used to describe trillions of microbes, including bacteria, viruses, archaea, and fungi, and their genetic material found in the gastrointestinal tract (27-29). Most of the gut microbiome comprises facultative and anaerobic bacteria, with Firmicutes and Bacteroidetes being the most common phyla, while Proteobacteria and Actinobacteria are less prevalent (30). The gut microbiome is known to potentially affect the host's metabolic processes and immune responses (31, 32). However, changes in the gut microbiome composition may shift those physiological processes, activating cirrhotic-associated malnutrition and worsening cirrhotic complications like sarcopenia (31, 33, 34). Notably, altered gut microbiome composition has been associated with loss of muscle mass and function or strength in cirrhotic patients (29, 34).

Furthermore, altered gut microbiome composition has been demonstrated in age-related sarcopenia in humans and rats (35-37). The gut microbiome produces inflammatory mediators and bioactive metabolites that regulate host cellular physiological processes, including inflammation (32, 38, 39). The alteration of the gut microbiome composition has been associated with inflammation, with the gut microbiome of liver cirrhotic patients exhibiting an increase in potential pathogenic species compared to healthy controls (40-42). *Escherichia coli*, *Enterobacteriaceae*, *Staphylococcus* spp, and *Veillonellaceae* are significantly more abundant in cirrhotic patients than in healthy controls (42-44). Similarly, increased abundance of *Enterobacteriaceae* and *Streptococcaceae* and reduced *Lachnospiraceae* and *Ruminococcaceae* were reported in cirrhotic patients with sarcopenia (34). *Fusobacterium*, *Ruminococcus*, and *Anaerostipes* have also been reported as critical discriminating features to predict the risk of sarcopenia in cirrhosis (34).

Intestinal motility, increased portal pressure, and altered bile acid composition may contribute to the alteration of gut microbiome composition in liver cirrhosis (42, 44). Additionally, host extrinsic factors, such as antibiotic use, lifestyle, disease etiology, and disease severity, have been shown to influence gut microbiome composition (45). Broad-spectrum antibiotics use has immediate and long-term effects on the gut microbiota composition (45). Furthermore, the altered gut microbiome composition has also been linked to disease etiology and severity, such as cirrhosis, alcoholic liver disease, and non-alcoholic fatty liver disease (33, 46, 47). Individual marker taxa may be linked to specific disease etiologies and their severity (33, 40, 48). Changes in the gut microbiome composition may have clinical implications, such as the overgrowth of pathogenic bacterial species in decompensated liver disease (42). Furthermore, alteration of gut microbiome composition has been associated with increased gut permeability, intestinal bacterial translocation (BT), and inflammation (43, 49). The increased gut permeability may lead to the passage of viable bacteria and bacterial products, including lipopolysaccharides (49). Lipopolysaccharide (LPS) promotes the expression of lipopolysaccharide-binding protein (LBP), which can bind with LPS to form LPS-LBP complexes that interact with immune cell membrane protein CD14. This interaction can cause the release of pro-inflammatory cytokines via the toll-like receptors-nuclear factor kappa-β (TLRs-NF-kB) pathway (50). Pro-inflammatory cytokines, such as interleukins 1 (IL 1), interleukin 6 (IL-6), interleukin 17 (IL-17), and tumor necrosis factor-alpha (TNF-α), can mediate skeletal muscle protein degradation primarily by upregulating the ubiquitin-proteasome pathway, caspase-mediated protein cleavage, and autophagy (51, 52). Increased serum pro-inflammatory cytokines have been reported in sarcopenic patients compared to healthy controls in the aged population (51). Additionally, increased levels of C-

reactive protein (CRP), an inflammatory biomarker, have been linked to loss of muscle strength in sarcopenic patients (53).

Besides inflammation, the gut microbiome has a significant metabolic capacity (54-56). The gut microbiome is responsible for metabolizing and bioavailability of specific metabolites, which are crucial for the physiological processes (55-57). One of the essential functions of the gut microbiome is the metabolism and bioavailability of specific amino acids, including branched-chain amino acids (58). Changes in gut microbiome composition and amino acid metabolism may contribute to sarcopenia in liver cirrhosis (34). Cirrhotic patients with sarcopenia have been found to have significantly reduced levels of BCAAs (leucine, valine, and isoleucine) and the amino acids alanine, proline, and tryptophan (34). Another critical metabolite of the gut microbiome fermentation is short-chain fatty acids (SCFAs), such as acetate, propionate, and butyrate. These SCFAs are essential for gut health and integrity of the epithelial barrier, regulation of skeletal muscle metabolism and function, and immunomodulation (59, 60).

Hormones and myokines

Muscle protein turnover refers to the balance between protein synthesis and degradation, loss of muscle mass because of enhanced skeletal muscle protein degradation is a hallmark of sarcopenia (3, 61). In addition to inflammation and metabolites, changes in hormonal status may also play a role in regulating muscle protein turnover (26, 41, 62). Hormones, including insulin growth factor 1 (IGF-1) and testosterone, have been shown to regulate skeletal muscle mass (2, 26, 62). Moreover, skeletal muscle cells can adapt to external changes in nutrition and exercise by secreting myokines, including myostatin, fibroblast growth factor-21 (FGF-21), and irisin (26, 63). These myokines have both autocrine and endocrine effects, enabling them to regulate skeletal muscle protein turnover (26, 63).

IGF-1

IGF-1, an anabolic hormone, can mediate skeletal muscle protein synthesis and prevent protein degradation, acting as a positive regulator (62, 64). The role of IGF-1 in muscle growth and differentiation has been demonstrated through gain-and-loss-of-function approaches. Inactivation of the IGF-1 receptor resulted in muscle atrophy (65), while overexpression of IGF-1 has been shown to result in muscle hypertrophy in vitro. (66). IGF-1 mediates skeletal muscle growth and protein synthesis through a mechanism that depends on the upregulation of the protein kinase B-

mammalian target of the rapamycin (Akt-mTOR) pathway (2, 62, 64). Apart from stimulating skeletal muscle protein synthesis, IGF-1 inhibits the production of transcription factors such as fork-head box protein 3 (FOXO3), thus suppressing the ubiquitin-proteasome system-dependent skeletal muscle protein degradation (62, 64, 67). IGF-1 may also inhibit myostatin production, preventing skeletal muscle atrophy (64).

Glycogen synthase kinase-3β (GSK3β) is a critical downstream pathway dependent on IGF-1 activation. Phosphorylation and inhibition of GSK3β activities have been associated with skeletal muscle hypertrophic conditions (68, 69). Reduced levels of IGF-1 in serum were reported in age-related sarcopenia, compared to non-sarcopenic individuals (70). Furthermore, muscle mass and function have been independently associated with IGF-1, indicating the potential role of IGF-1 as a mediator of sarcopenia in liver cirrhosis (62, 70).

Myostatin

Myostatin is a transforming growth factor-β superfamily member and is a negative regulator of skeletal muscle growth and differentiation (62, 63, 71). It achieves this by inhibiting myoblast proliferation, differentiation, and fusion and preventing satellite cell differentiation and proliferation (72-74). Additionally, myostatin mediates muscle atrophy by inhibiting the Akt-mTOR pathway and promoting the ubiquitin-proteasome system-dependent muscle protein degradation (63, 75). The myostatin-Smad3 pathway also contributes to muscle atrophy by inhibiting skeletal muscle protein synthesis and decreasing myotube size (76, 77).

In humans, loss-of-function mutations of myostatin have been associated with increased skeletal muscle mass (63, 78). Furthermore, in a mouse model of Duchenne muscular dystrophy (DMD), myostatin inhibition has ameliorated muscle dystrophy by increasing muscle mass, size, and strength (71).

FGF-21

Apart from myostatin, skeletal muscle cells also secrete fibroblast growth factor-21 (FGF-21) when influenced by external stimuli such as hormones, exercise, and nutrients (63, 79-81). FGF-21 is a member of the FGF superfamily and is mainly expressed in many organs, including the liver and skeletal muscle (79). FGF-21 regulates muscle mass, muscle glucose uptake, and mitochondrial muscle functions. (63, 80). Moreover, mitochondrial dysfunction and stress

response have been associated with increased secretion of FGF-21 from the muscle (63). In vitro, studies have shown that FGF-21 is upregulated by Akt pathway activation (79). However, increased serum FGF-21 is associated with the loss of muscle mass and mitochondrial dysfunction, indicating the catabolic effect of FGF-21 on human skeletal muscle health (63, 82, 83).

Irisin

Irisin is a myokine derived from a precursor fibronectin type III domain-containing protein 5 (FNDC5) with autocrine function (84, 85). Skeletal muscle secrets irisin in response to external stimuli, including nutrients and exercise (84, 86). Skeletal muscle also secrets irisin in increased protein catabolic conditions (63). Increased irisin promotes myogenic differentiation and inhibits skeletal muscle protein degradation (63, 84). Furthermore, irisin increases cell energetics associated with increased energy metabolism and glucose uptake (63, 84, 85, 87). Conversely, irisin knockout mice showed worsened loss of muscle mass, whereas irisin treatment ameliorated sarcopenia in aging mice through inhibition of myostatin and ubiquitin-proteosome system protein-degradation (87). Furthermore, reduced irisin has been associated with sarcopenia. Hence a potential biomarker to predict sarcopenia in liver cirrhosis (88, 89).

Malnutrition

Besides inflammation and hormonal and myokine status changes, protein-energy malnutrition (PEM) is a common feature associated with cirrhosis (21, 90, 91). PEM occurs in 65-90% of patients with chronic liver disease, and causes include malabsorption, loss of appetite, decreased hepatic protein synthesis, and hypermetabolism (74). Furthermore, PEM is associated with an increased risk of complications such as ascites, hepatic encephalopathy, and increased mortality (91). A positive linear relationship between the severity of liver disease and malnutrition has been reported, with 51% of liver cirrhotic patients experiencing significant protein malnutrition (91). Liver cirrhotic patients with PEM suffer from the loss of muscle mass (74, 91). Since cirrhosis is associated with a hypermetabolic state and accelerated malnutrition, increased energy expenditure may likely further impair protein synthesis with increased protein breakdown resulting in muscle atrophy (2, 21, 92).

Furthermore, reduced total energy intake has been associated with sarcopenia in liver cirrhosis, and the potential mediators include reduced dietary calorie intake, nausea, and anorexia (74). Starvation is also a critical risk factor for protein depletion, with short periods of starvation leading to protein breakdown in cirrhosis (93). Consequently, such catabolic state results in an increased breakdown of muscle BCAA as a source of energy (94). Increased whole-body protein turnover characterized by increased ketogenesis and amino acid consumption as an energy source has been reported in liver cirrhosis (21, 95). Notably, liver cirrhosis patients have a lower ratio of branched-chain amino acids (BCCA) to aromatic amino acids (AAA) compared to controls because of a metabolic switch leading to the degradation of BCAAs for gluconeogenesis (21, 96). The increased degradation of muscle BCCAs may result in loss of skeletal muscle mass, leading to sarcopenia (21, 96).

Bile acid in liver cirrhosis

Given the significant role of BAs in inflammation, energy metabolism, and muscle physiology, it is not surprising that BA-receptor-activated pathways are of great interest in understanding molecular mechanisms for the pathogenesis of liver disease and associated complications such as sarcopenia (97-100). BAs have varied effects on hepatocytes and skeletal muscle cells based on the degree of hydroxylation and hydroxyl group orientation (101-103). Furthermore, the cytotoxicity of the BAs to hepatocytes is proportional to their hydrophobic-hydrophilic balance (101, 102). Total serum BAs have been used as a marker for hepatocyte injury (104). The hydrophilicity of unconjugated and conjugated BAs decreases in the order UDCA>CA>CDCA>DCA>LCA and taurine conjugated>glycine conjugated > unconjugated BAs species (101, 105, 106). Accumulation of hydrophobic cytotoxic BAs has been linked to liver injury and inflammation (100). Furthermore, increased plasma hydrophobic BAs were reported to be increased in chronic liver disease patients compared to healthy controls (107). Elevated plasma cholic acid (CA), chenodeoxycholic acid (CDCA), glycocholic acid (GCA), taurocholic acid (TCA), glycochenodeoxycholic acid (GCDCA), and taurochenodeoxycholic acid (TCDCA), lithocholic acid (LCA), and deoxycholic acid (DCA) were reported in chronic liver disease (102, 107). UDCA improved the overall hydrophilicity of the BA pool and liver function indices in patients with chronic liver disease (101, 108).

Even though the relationship between BAs and sarcopenia in liver cirrhosis is still being investigated, quantification of BAs levels may potentially be a useful diagnostic tool for identifying patients at risk for sarcopenia in liver cirrhosis. The total and individual BAs species are potential

biomarkers for the diagnosis and prognosis of cirrhosis (100, 109). Serum BA can be used to diagnose liver disease, and the normal range of fasting BA is 1.0-6.0 μmol/; in cholestasis, the level of BA is elevated to more than 10 μmol/l (110). The elevated DCA and LCA indicate an increased risk of sarcopenia in liver cirrhosis (99, 103).

Bile acid synthesis and conjugation

BAs are steroidal molecules synthesized from cholesterol in the liver through enzymatic-dependent reactions (105, 111). It converts insoluble cholesterol into water-soluble and readily secreted molecules (111, 112). Cholesterol is converted to BAs through hydroxylation, epimerization of the 3-hydroxyl group, and the oxidative cleavage of the 3-C side chain (97, 105, 112, 113). Typically, the human liver synthesizes up to 200-600mg of BAs daily through the classical and alternative pathways (106, 112, 114). The classical pathway is responsible for about 75% of daily total BAs production, favoring the production of cholic acid (CA) (105, 106). However, through 27 hydroxylases (CYP27A1) enzymatic activities, chenodeoxycholic acid (CDCA) can also be produced through the classical pathway; otherwise, the alternative pathway is the main pathway responsible for CDCA synthesis (106, 113).

The first reaction step in the classical pathway is the 7α-hydroxylation catalyzed by cholesterol 7α-hydroxylase (CYP7A1). CYP7A1 hydroxylation is a rate-limiting enzymatic reaction determining the quantity of BAs daily output (98, 105). Whereas the alternative pathway is initiated by mitochondrial sterol-27 hydroxylase (CYP27A1) and oxysterol 7α- hydroxylase (CYP7B1), forming 27-hydroxycholesterol (98, 113). The cholesterol and oxysterol-derived 7α-hydroxylated intermediates are further modified through several reaction steps, including sterol ring modification, side-chain oxidation, and shortening (105, 106, 113). While epimerization of the CDCA results in UDCA production (105). The alternative pathway contributes 10% to the compensation of BAs daily loss; however, in cirrhosis, it is the major contributing pathway (105).

The bile acid acyl-CoA-synthase amino acid transferase (BAAT) is critical in the two-step BAs conjugation (105, 113, 115). Synthesized primary BAs are conjugated with glycine or taurine for easy transportation (97, 105). The physiological benefit of BAs conjugation is increased solubility; in humans, 75% are conjugated with glycine, whereas 25% with taurine (105). Besides conjugation, BAs are also transformed by the liver enzyme sulfotransferase 2A1 (SULT2A1) through sulfation processes (116). Even though BAs are retained within the enterohepatic circulation, less than 10% spill over into the circulatory system and are subsequently excreted into the urine by the kidney (114, 117). For increased hydrophilicity and reduced cytotoxicity, the

leaked BAs in the circulatory system are largely sulfated by SULT2A1 in healthy conditions (106, 116-118). More than 70% of urinary BAs are sulfated, and the degree of sulfation depends on the BA's hydrophobicity (116). Sulfation changes BAs' structural, physiochemical, and functional characteristics (118, 119). Sulfotransferase 2A1 (SULT2A1) is the predominant hepatic sulfation enzyme catalyzing sulfation of BAs at different positions at 3-OH and 7-OH in humans and mice, respectively (106, 116, 117). The function of BAs can be altered after sulfation; for example, sulfated cholic acid (CA7S) can potentially activate TGR5 upregulating the production of glucagon-like peptide 1 (GLP) (54).

Regulation of bile acid synthesis in the liver

Bile acid synthesis in the liver is regulated through FXR dependent negative feedback mechanism (97, 98, 105). FXR is a transcriptional factor that binds to the promoter region of target genes and is mainly expressed in the liver and ileum (98). When BAs activate, FXR induces the expression of a small heterodimer partner (SHP) that represses the expression of CYP7A1 and CYP8B1 in the liver (98, 120). Furthermore, the binding of BAs to FXR induces enterocytes secreting FGF15/19, inhibiting liver CYP7A1 and CYP8B1, acting as a complementary mechanism to the liver FXR-SHP BAs synthetic inhibition pathway (98, 114). Therefore, repression of BAs synthesis through a negative feedback mechanism may require complementary activation of the liver and ilium FXR (113, 114). Through FXR-FGF15/21-dependent mechanism, alteration of the gut microbiome composition can regulate BAs synthesis and composition (114).

Bile acid biotransformation

After BAs synthesis in the liver, the gut microbiome metabolizes primary to secondary BAs and oxo-BAs (97, 114, 121). BAs biotransformation includes deconjugation through bile salt hydrolase (BSH), dehydroxylation through 7-alpha dehydroxylase, and oxidation/epimerization of the hydroxyl groups at C-3, C-7, and C-12 (106, 113, 114, 121). A diverse array of anaerobic bacteria within the intestines is responsible for executing deconjugation and oxidation reactions. BSH genes are widely distributed in a broad spectrum of bacterial and archaeal species. However, the process of bile acid 7α-dehydroxylation is confined to a specific subset of anaerobic bacteria, constituting a minor portion of the overall colonic microbial population (100, 105, 121-123). BSH hydrolyses the C-24 N-acyl amide bond linking primary BAs with either glycine or taurine to release free primary BAs and glycine or taurine (55, 105). The deconjugation of primary BAs is critical in preventing their active reabsorption from the small intestines through apical sodium-dependent bile acid transporter (ASBT) (113). Notably, approximately 95% of biliary secreted BAs

are actively reabsorbed from the ileum to the liver through a portal vein by specific BAs transporter known as apical sodium-dependent bile acid transporter (ASBT), whereas 5% of BAs escape ASBT-reabsorption ending up in the colon (57, 113).

Besides deconjugation and sulfation, BAs are dehydroxylated; 7α-dehydroxylase producing bacteria metabolize primary BAs to secondary BAs and their intermediate BAs species 7-deoxy BAs (113, 122-124). The 7α-dehydroxylation of primary BAs results in the formation of DCA (3α,12α-dihydroxy-5β-cholanoic acid) from CA and LCA (3α-hydroxy-5β-cholanoic acid) from CDCA (124-126). *Clostridium, Ruminococcus,* and *Eubacterium* are the primary producers of 7α-dehydroxylase (122, 124, 126). Unlike epimerization/oxidation, dehydroxylation of BAs by the 7α-dehydroxylase is confined to unconjugated primary BAs (127). Notably, 7α-dehydroxylation activities are widespread among bacterial species (128). Furthermore, isomerization of the 7α-OH group in the CDCA results in the formation of ursodeoxycholic acid (UDCA), while conversion of UDCA to LCA is through 7β-dehydroxylation (113, 129, 130). Deoxycholic acid (DCA) and lithocholic acid (LCA), 12-oxoLCA, and 3-oxoLCA are the most abundant secondary BAs produced daily, representing more than 40% of the BAs pool and more than 25% in the gallbladder (123-125). The gut microbiome capable of producing both BSH and 7-α dehydroxylase individually or communally successfully metabolizes primary to secondary BAs (105, 127).

The gut microbiome also metabolizes oxo-(keto) BAs through epimerization/oxidation of the hydroxyl group (131). The oxidation of the hydroxyl groups in positions 3,7 or 12 is a complex process-aided bacterial hydroxysteroid dehydrogenase (HSDH) (105, 124, 131). In a time-reversible reaction catalyzed by HSDH, epimerization/oxidation of the BAs hydroxyl changes from α to the β configuration (105). HSDH is produced mainly by members of *Actinobacteria, Bacteroides* spp*, Ruminococcus*, *Clostridium scindens, Clostridium hylemonae, Eggerthella lenta, Ruminococcus gnavus, and Eubacterium centum* (113, 124, 126). Moreover, *Clostridium scindens, Eggerthella lenta, Alistipes* spp*,* and *Ruminococcus gnavus* produce 3α-HSDH, 3β-HSDH, and 5α-reductase catalyzing the production of 3-oxoDCA from DCA, and 3-oxoLCA from LCA, isoalloDCA from 3-oxoDCA and isalloLCA from 3-oxoLCA (124, 132). Similarly, *Parabacteroides distasonis* metabolizes LCA and DCA to form 7-oxo-lithocholic acid (7oxo-LCA) and 7-oxo-deoxycholic acids (7oxo-DCA), respectively (132). The formation of oxo-BAs through an oxidative reaction catalyzed by gut microbiome HSDH is reversible (113, 124, 132). However, despite advanced analytical methods, the quantification of oxo-BAs in samples is limited due to the limited availability of standards (113).

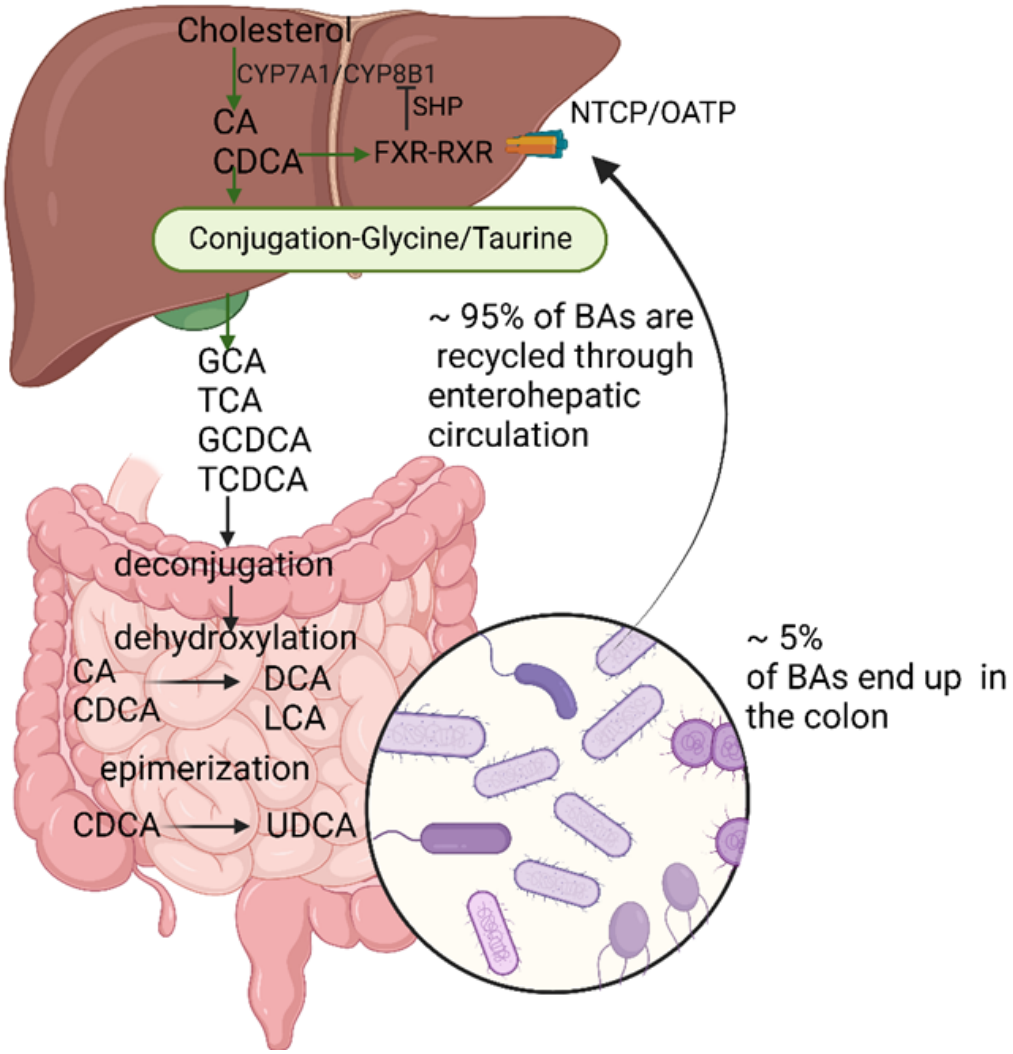

Figure 2. An overview of bile acid metabolism. This figure was created with BioRender.com.

Direct effects of bile acids on skeletal muscle

BAs may directly influence skeletal muscle physiology (56, 99, 103, 133). Previous studies have shown that BAs can promote the loss of muscle mass and function, which are critical features of sarcopenia (99, 103, 133). The difference in BAs structural diversity and affinity towards FXR and TGR5 receptors underscores the ability of individual BAs to have varied effects on skeletal muscle mass and function (98, 112, 127). However, the order of BAs potency to activate FXR differs from TGR-5, suggesting that the two receptors are engaged differently to regulate skeletal muscle physiology upon BAs activation (97, 134, 135). The ability of bile acids to activate FXR receptors is in the order as follows CDCA>DCA> LCA>CA (114, 134). At the same time, secondary BAs are the most potent TGR5 agonists, conjugated and unconjugated BAs, LCA>DCA>CDCA>CA

in the order of potency. BAs activated-FXR leads to the secretion of FGF15/19 in the liver and ileum (113, 114, 133). Increased expression of FGF15/19 has been shown to induce phosphorylation of extracellular signal-regulated protein kinase 1/2 (ERK 1/2) and increased production of ribosomal protein S6 kinase 1 (pSK1), leading to increased skeletal muscle protein synthesis and growth (56, 133, 136). Furthermore, BA activated FXR-FGF15/19 signaling pathway promotes skeletal muscle protein synthesis indicating the potential as a therapeutic target for sarcopenia.

BAs can also directly induce skeletal muscle atrophic conditions through TGR5-dependent mechanisms (99, 103). After BAs binding, TGR5 linked Gαs protein causes increased production and rise in cAMP, leading to downstream upregulation of effectors including Akt and mTOR (97, 137, 138). The activation of the Akt-mTOR pathway promotes skeletal muscle protein synthesis and prevents skeletal muscle degradation by inhibiting atrogin-1 and MURF1 production (139). TUDCA and UDCA have been shown to activate the Akt-mTOR pathway promoting skeletal muscle protein synthesis and preventing ubiquitin-proteosome-dependent muscle protein degradation (139). Furthermore, the Akt-mTOR pathway activation improved mitochondrial energy metabolism and ATP production to meet the high-energy demands of skeletal muscle cells (140-142). Mitochondrial dysfunction may mediate the loss of skeletal muscle mass and function associated with sarcopenia (140-142). Skeletal muscle mitochondrial function can also be regulated through TGR5 and ubiquitin-dependent activated protein kinase (AMPK) pathway-dependent mechanism (140). CA and DCA treatment induced skeletal muscle atrophy, mitochondrial dysfunction, and increased ROS production through a TGR5-dependent mechanism in vivo (140). Increased ROS production has been shown to cause increased production of atrophic genes, including atrogin-1 and MuRF-1, leading to skeletal muscle protein degradation (103).

Indirect effects of bile acids on skeletal muscle

BAs may also indirectly influence skeletal muscle physiology; the interplay between BAs and immune cells presents a unique opportunity to understand the mechanisms involved (32, 143). Hydrophobic BAs have been shown to induce inflammatory responses, whereas hydrophilic BAs are anti-inflammatory (112). Besides hepatic, ileal, and skeletal muscle cells, immune cells, including macrophages, monocytes, natural killer cells (NKT), and T cells, also express BAs receptors FXR and TGR5 (32, 143, 144). FXR and TGR5 activation has been shown to mediate regulatory and inhibitory functions of immune cells (132, 138, 144, 145). BAs-activated TGR5 has

been shown to attenuate pro-inflammatory cytokine production in macrophages and monocytes (146, 147). Accumulation of cytotoxic BAs promotes inflammation in liver disease (148). Furthermore, cytokines, including interleukin 1β (IL-1β), interleukin 6 (IL-6), and TNF-α, promote systemic inflammation and apoptosis, leading to loss of skeletal muscle mass and function (149). Interleukin expressions are modulated by numerous transcriptional factors upon BAs-receptor binding. 3oxoLCA and isoalloLCA have been shown to prevent the differentiation of T_H17 through RORγt dependent and RORγt independent mechanisms, respectively (32, 148). IsoalloLCA and IsoDCA induce Treg cell differentiation through an FXR-dependent mechanism (32). Similarly, CDCA, TCDCA, and TUDCA-treated monocytes and macrophages have shown reduced phagocytic and pro-inflammatory cytokine production after LPS stimulation, suggesting the immunosuppressive nature of BAs (143).

Besides induction of inflammatory responses, BAs may also indirectly affect muscle mass through their effect on metabolism and nutrient absorption, energy expenditure, and glucose, which may indirectly influence muscle mass and function (112). BAs regulate lipids and fats and fat-soluble vitamin absorption; nutrients may also play an essential role in BAs synthesis (112). The bioavailability of cholesterol as a substrate has been shown to activate the CYP7A1 indicating the direct link between cholesterol and BAs synthesis in the liver (112). Similarly, BAs have been shown to activate the Akt signaling pathway, which may phosphorylate FOXO1 and prevent glucose-6-phosphatase (G-6-pase) activity from activating gluconeogenesis (112). Besides glucose metabolism, bile acid activation of TGR5 has been shown to regulate energy metabolism in human muscle cells (112).

An overview of potential intervention options to reverse sarcopenia in liver cirrhosis

Sarcopenia significantly negatively impacts the quality of life of liver cirrhotic patients (21, 41). However, limited therapeutic intervention options are available to address sarcopenia in liver cirrhosis and improve muscle health and overall well-being (2). Different nutritional and non-nutritional strategies have been shown to improve skeletal muscle mass and function, including amino acids supplementation and calorie intake, hormonal therapy, physical activity, and mechanistic targeted treatments have been investigated (2, 10, 150).

Dietary intervention and nutritional supplementation

Low energy and protein intake and malabsorption contribute to malnutrition in liver cirrhosis (2, 151). Furthermore, several factors such as ascites, micronutrient deficiency, loss of appetite, and portal hypertension mediate reduced energy and protein intake (151). However, it still needs to be made clear which of these factors plays a key role; hence all the elements should be considered when undertaking nutritional assessment and dietary interventions for cirrhotic patients (151). Nutritional interventions, including BCAA supplementation, high-energy protein, and late-night snack, have been recommended for liver cirrhotic patients (152). In liver cirrhosis, malnutrition is potentially mediated by metabolic disorders, malabsorption, impaired liver capacity to store energy, and insufficient oral intake, mainly caused by existent ascites (2). Malabsorption may contribute to low net energy despite adequate caloric intake (74). High energy and protein-rich food intake may help maintain nitrogen balance and protein synthesis in cirrhosis (2, 151). Nutrient supplementation, including BCAAs supplementation, has been shown to impact skeletal muscle health by remodeling skeletal muscle protein turnover (2, 150). In principle, BCAAs are used for muscle cell energy production and mediate muscle protein synthesis, the reduced plasma BCAA is attributed to increased muscle uptake and degradation to reduce ammonia toxication through glutamine synthase (74). In cirrhotic patients with sarcopenia, BCAA to aromatic amino acid (AAs) ratio is significantly reduced compared to healthy controls due to increased muscle BCAAs uptake (74). BCAAs supplementation targeting increased skeletal muscle protein degradation has been suggested (153-155). Using leucine as an interventional strategy is justified due to its ability to mediate skeletal protein synthesis and insulin signaling pathways (150). In cirrhotic patients, oral leucine supplementation (10g/day) has been shown to improve muscle mass and quality of life (156).

Additionally, leucine treatment has been shown to regulate skeletal muscle protein turnover and influence the transition to negative nitrogen balance in the fasting state (153-155). In humans, few studies have assessed the effect of leucine supplementation on skeletal muscle mass and function and whether a dose-dependent impact can be demonstrated (150). Although in vitro and in vivo animal studies have revealed interesting results. They may not represent the best model to study human skeletal protein metabolism and may not mimic molecular mechanisms leading to skeletal muscle wasting in humans (150).

Hormonal therapy

Changes in hormonal status are among the many factors mediating the loss of skeletal muscle mass and function (2, 157). Interventions that might reverse the loss of muscle mass and improve muscle function and promote anabolic status are potential therapeutic agents to treat sarcopenia (157). Hormonal therapy has been suggested as a possible therapeutic intervention strategy for treating sarcopenia in liver cirrhosis (2, 74, 152). The likely hormones include Insulin-like Growth Factor 1 (IGF-1), testosterone, and myostatin inhibitors (74, 152, 157). IGF-1 has been shown to regulate skeletal muscle protein turnover and promote satellite cell differentiation and proliferation, mechanisms critical in maintaining muscle mass and function (74, 157). Furthermore, IGF-1 inhibits myostatin and stimulates muscle protein synthesis through the Akt-mTOR pathway-dependent mechanism (74). In aged-population, skeletal muscle overexpression of IGF-1 has been associated with hypertrophy and maintenance of lean muscle mass (157).

Besides IGF-1, testosterone, the primary male sex hormone, has been explored as a potential therapeutic urgent for sarcopenia (2, 74, 158). Testosterone has two beneficial effects on muscle cells: activating the mTOR pathway and inhibiting myostatin (74). Myostatin is a negative regulator of satellite cell differentiation and proliferation and one of the potential mediators of sarcopenia (74). Thus myostatin inhibition has been shown to improve skeletal muscle mass and function in animal models (74). Cirrhotic patients with sarcopenia have been associated with elevated myostatin and reduced plasma IGF-1 and testosterone (74). Testosterone replacement therapy has been found to improve muscle strength, physical function, and quality of life in those with cirrhosis (152, 158, 159). Furthermore, testosterone increases lean body mass and improves physical performance and endurance (158, 160). Thus, testosterone should be considered a viable treatment option for cirrhosis patients suffering from sarcopenia (74).

Bile acids as potential therapeutic agents/targets for sarcopenia

BAs activate FXR leading to downstream upregulation of target genes liver *shp* and ileal *fgf15/19* (133, 136). The upregulated *fxr, shp,* and *fgf-19* expressions have been associated with increased skeletal muscle mass and function, indicating that the FXR signaling pathway presents a potential therapeutic target for sarcopenia (92, 112, 133, 136). Furthermore, FXR-FGF15/19 agonists may activate the phosphorylation of extracellular-signaling-regulated protein kinase (ERK) and ribosomal protein S6 kinase (pS6K1). These are two essential transcriptional regulators for the

mTOR pathway (56, 136). Activated FGF19-ERK-mTOR signaling pathway may increase skeletal muscle growth, muscle protein synthesis, skeletal muscle fibers size, and myotubes sizes (56, 92, 136). CDCA is the most potent FXR agonist, which induces the production of FGF15/19; however, obeticholic acid is synthesized from CDCA, and it is 100 times more potent FXR agonist than any other natural BAs (133, 134). BAs activated FXR-FGF15/19-ERK signaling, have been shown to have a positive impact on skeletal muscle (133). Similarly, long-term treatment with fexaramine, a commercially synthesized FXR agonist, ameliorated the loss of muscle mass and function in an FXR-FGF15/19-ERK-dependent manner (133).

Ubiquitin-proteosome kinase pathway can also be targeted since it has an essential role in skeletal muscle protein degradation, a key feature for skeletal muscle atrophy leading to loss of muscle mass and function(161). Therefore, silencing the ubiquitin-proteasome kinase pathway through PI3-Akt activation presents a potential therapeutic target for sarcopenia (161). The upregulation of the ubiquitin-proteosome kinase pathway depends on the transcriptional factor FOXO3, which may be inhibited by PI3-Akt signaling activation (161, 162). Phosphorylated FOXO3 exit nuclease into the cytoplasm, limiting the transcriptional activities along with reduced downstream expression of target genes ubiquitin ligases, including atrogin-1 and MURF1 (161, 162). Skeletal muscle proteins myosin heavy chain (MHC) and troponin are targets for ubiquitin ligases degradation (163). In principle, BAs with the ability to activate the PI3-Akt pathway are potential pharmacological agents to prevent ubiquitin ligases-dependent skeletal muscle protein degradation; notably, UDCA and TUDCA are less cytotoxic modulators of the PI3-Akt pathway in TGR5 dependent mechanism (106). TUDCA treatment reversed muscle atrophy in mice with cachexia (121). Furthermore, the UDCA mode of action may also include the activation of ERK1 and mitochondrial membrane permeability transition inhibition (164).

The other rationale for using BAs as therapeutic agents may also be for replacement therapy or alteration of BA composition (110). In replacement therapy, the BAs correct deficiencies occasioned by dysregulation in BAs metabolism (165). UDCA is an epimer of CDCA with a hydrophilic characteristic found in humans and other mammals (165, 166). When orally administered as protonated acid, it may reduce the biliary secretion of hydrophobic and cytotoxic BAs (165). Furthermore, orally administered UDCA and TUDCA can inhibit the ileal absorption of endogenous BAs altering the BA pool composition (165, 167).

Table 1. Therapeutic strategies to improve muscle mass and reverse sarcopenia in cirrhosis.

Intervention	Administration	Mechanism

High energy, high protein diet	1-1.5 g of protein per kg of body weight per day (total 35-40 kcal/kg total energy intake per day)	Improves nitrogen energy balance
Late evening snack	Complex carbohydrate snacks with protein, such as cheese on whole-meal bread	Reduces muscle breakdown during overnight fasting
BCAA supplementation	Oral granule leucine supplementation/ isoleucine /valine 7.5 g/3.75 g/3.75 g (dissolved in carbohydrate beverage)	Upregulate mTOR leading to increased muscle protein synthesis.
Testosterone replacement therapy	Testosterone decanoate or topical testosterone gel based on the manufacturer's recommendation	mTOR pathway upregulation leads to increased muscle protein synthesis. Reduced proteolysis through myostatin inhibition, and ubiquitin-proteasome pathway downregulation
IGF-1 therapy	Research use only	mTOR-Akt pathway activation with increased muscle protein synthesis. Myostatin inhibition leads to improved satellite cell differentiation and proliferation.
UDCA and TUDCA	Research use only	Protection against cytotoxic hydrophobic bile acids. Activation of extracellular signal-regulated kinases (ERK). Inhibition of mitochondrial membrane permeability transition (MMPT).

Possible therapeutic interventions to reverse sarcopenia in liver cirrhosis, adapted from Sinclair et al., 2016 (74)

HYPOTHESIS AND AIMS

The gut microbiome, bile acids, and metabolome have been shown to mediate loss of muscle mass and function, and composition is altered in cirrhotic patients. Thus, we hypothesize that the composition of the gut microbiome, bile acids, and metabolome are altered in liver cirrhosis, leading to increased gut permeability, translocation of bacterial products, and inflammation, potentially contributing to the development of sarcopenia.

The specific aims of this thesis were

1) To study the gut permeability, bacterial translocation, and inflammatory biomarkers of cirrhotic patients with and without sarcopenia and non-cirrhotic controls with and without sarcopenia.
2) To determine changes in the gut microbiome composition between cirrhotic patients with and without sarcopenia and non-cirrhotic controls with and without sarcopenia.
3) To determine changes in the composition of bile acids and metabolome between cirrhotic patients with and without sarcopenia and non-cirrhotic controls with and without sarcopenia.
4) To investigate an association between gut microbiome composition, gut permeability and bacterial translocation, bile acids, and metabolome with sarcopenia in cirrhosis.
5) To study the metabolic pathways associated with sarcopenia in liver cirrhosis and non-cirrhotic controls.

MATERIALS AND METHODS

The description of some parts of the materials and methods section is like those previously published (1)

Recruitment of study participants and study design

All liver cirrhotic patients seen between April 2017 and January 2019 at the Department of Gastroenterology and Hepatology of the Medical University of Graz were conveniently sampled and screened for eligibility. Non-cirrhotic patients with diagnoses of different diseases, including Hashimoto thyroiditis, chronic obstructive pulmonary disease (COPD), chronic kidney disease, osteoporosis, pancreatitis, hypertension, hypercholesteremia, diabetes type II, and other conditions, served as controls. Cirrhosis was diagnosed either through biopsy or through a combination of clinical + radiological signs (e.g., signs of the uneven surface of the liver on ultrasound, CT, or MRI, evidence of cirrhosis on non-invasive tests such as elastography, clinical evidence of portal hypertension or decompensation of cirrhosis (e.g., history of ascites, esophageal varices, hepatic encephalopathy). The diagnosis of cirrhosis was established before patients were included in this study by the attending physicians and documented using the ICD10 code K74. Patients over the age of 18 who were male and female, had given written informed consent, underwent a CT or MRI scan within +/- 2 months of the baseline study visit, and had been diagnosed with cirrhosis clinically, radiologically, or histologically were included in the study. The study excluded patients with liver cirrhosis who had hepatocellular carcinoma stage Barcelona clinic liver cancer stage C or D (BCLC C or D), were receiving ursodeoxycholic acid treatment, currently using probiotics or antibiotics, had hepatic encephalopathy > grade 2, or had any other cognitive disorders that prevented informed consent. The study was authorized by the Medical University of Graz's research ethics committee (29-280 ex 16/17), registered on clinicaltrials.gov (NCT03080129), and carried out in accordance with the 2013 revision of the Declaration of Helsinki.

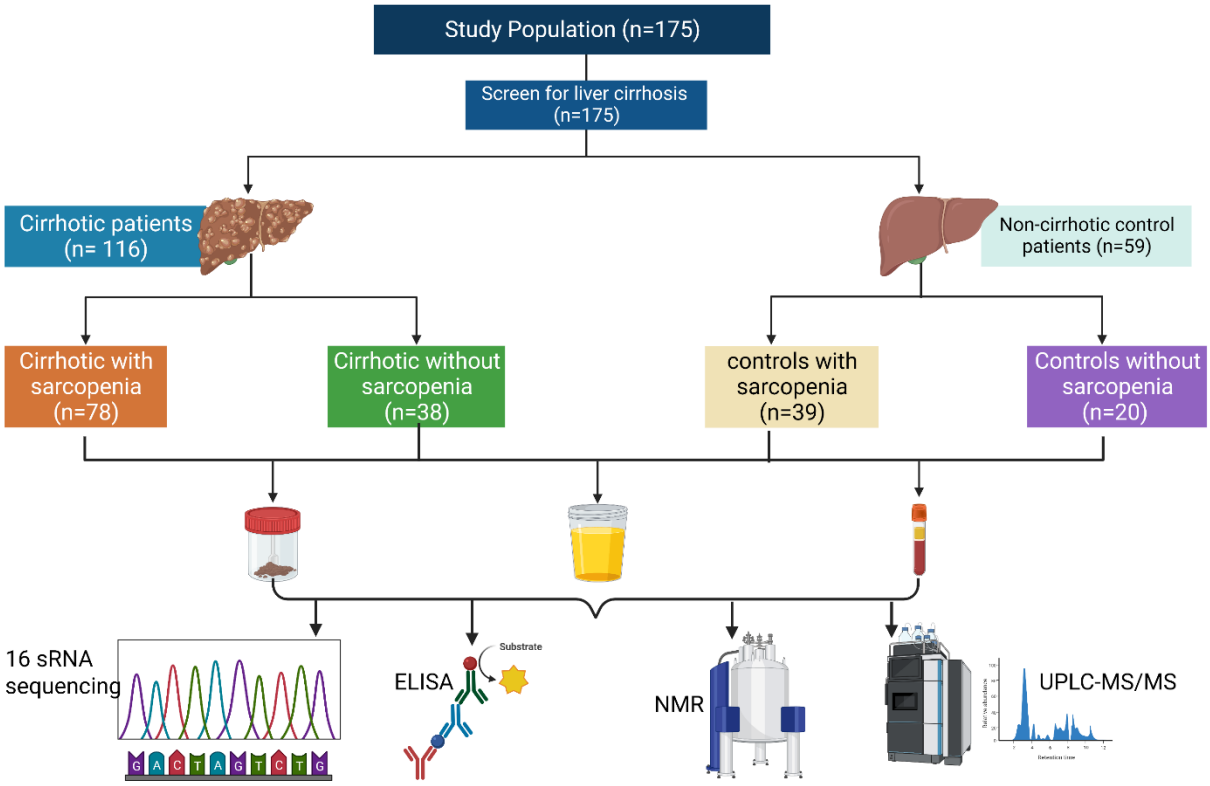

Figure 3. Flow chart diagram of study participants recruitment and study design. It was created with Biorender.com.

Sarcopenia assessment

Sarcopenia was diagnosed and assessed based on the previous recommendation by the EWGSOP 2010 (15). Sarcopenia tends to be diagnosed less frequently in individuals with liver cirrhosis when employing the 2019 criteria in comparison to the 2010 criteria, primarily due to variations in the initial parameters and threshold values utilized during the diagnostic procedure(168). The cross-sectional imaging of the L3 vertebra was used to determine the loss of muscle mass as previously described (15). For this test, muscle mass was assessed using the CT or MRI images of the L3 vertebra with an L3-muscle area of < 52.5 cm^2/m^2 for men and < 38.6 cm^2/m^2 for women, being considered as cut-off values (15, 16). Similarly, hand grip strength, a validated standard method, was used to determine muscle strength. A hydraulic dynamometer (Jamar Hydraulic Hand Dynamometer) was used for this measurement. The cut-off values of < 30 kg for men and < 20 kg for women were considered as previously described (15, 16).

Furthermore, gait speed measurements were conducted to determine muscle function. For this test, a 4-meter course was marked on the hallway with a 1-meter acceleration and 1-meter deceleration zone. For the gait speed test, the cut-off value of ≤ 0.8 m/s was considered as previously described, and the time taken to complete the 4-meter course drawn on the corridor was recorded in seconds (15, 16).

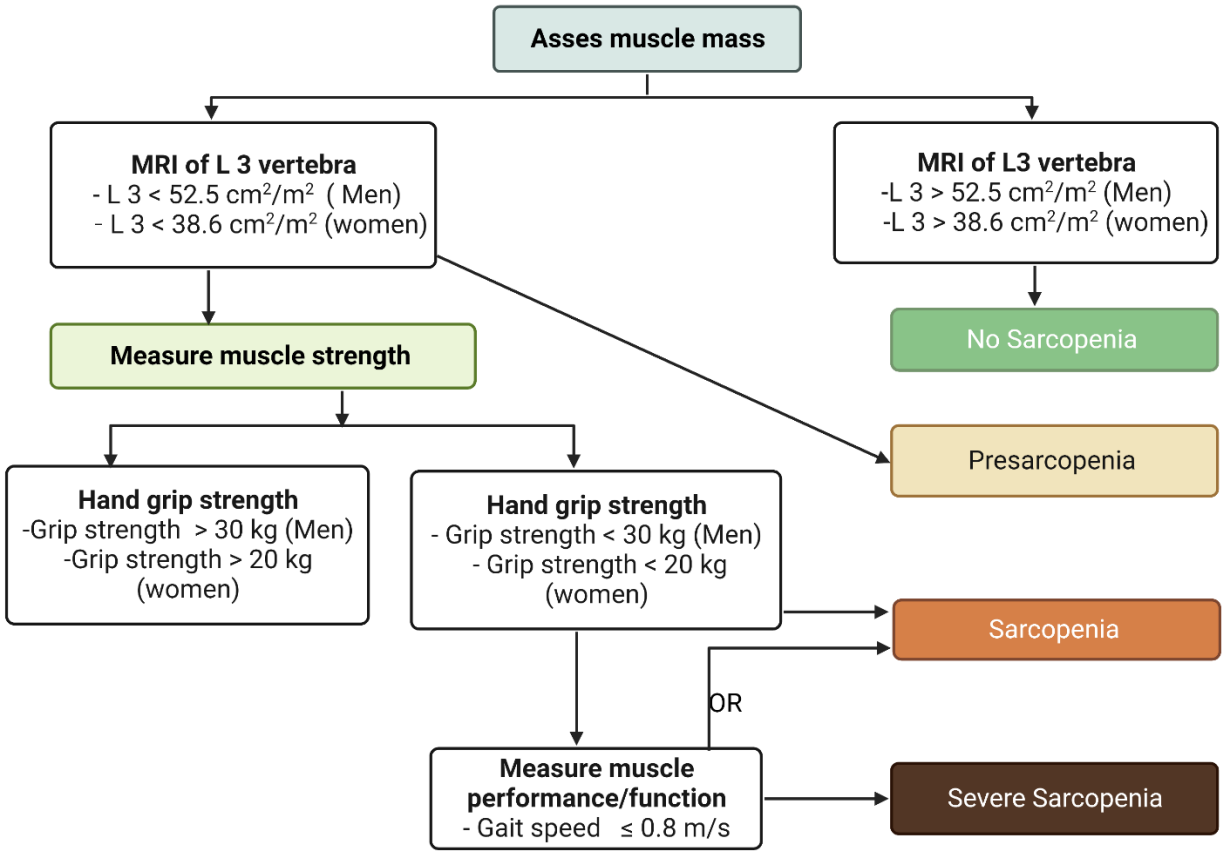

Figure 4. Flow chart of sarcopenia assessment, diagnostic parameters steps, and cut-off values. It was created with BioRender.com.

Nutritional and malnutrition status assessment

The nutritional and malnutrition status of the study populations were evaluated using various anthropometric measurements and validated screening methods (Fig 5), which included body mass index (BMI), mid-upper arm circumference (MAMC), Graz malnutrition screening (GMS), royal free hospital-subjective global assessment (RFH-NPT), and triceps skinfold thickness (TSFT) as earlier described (169). BMI was determined by calculating (kg. Body weight [BW]/[height in meter]^2) to classify malnutrition status. The cut-off value was (18.5 kg/m^2-29.5

kg/m^2) as previously described (169). MAMC was used to assess body muscle mass. MAMC has been used to predict sarcopenia and mortality in liver cirrhosis (170). Graz malnutrition screening (GMS), a validated screening tool, was used to classify the malnutrition risks in our study cohort. A total of ≥ 3 points indicated malnutrition (Table 2), as previously described (171). RFH-NPT (Fig 6) was also used as a screening tool to classify the risk of malnutritional; as previously described, the scores were marked as low (0 points), moderate (1 point), or high (2-7 points) (172). The first step involved evaluating the presence of acute alcoholic hepatitis or tube feeding, separating patients into groups with or without ascites or edema in the second step, and computing scores obtained by patients to assign them to the appropriate risk group as previously described (173). Triceps Skinfold Thickness (TSFT) was measured using skin calipers as the standard measure of fat stores and body mass; measurements were not affected by the retention of fluids in the body. The test was conducted as previously described (169).

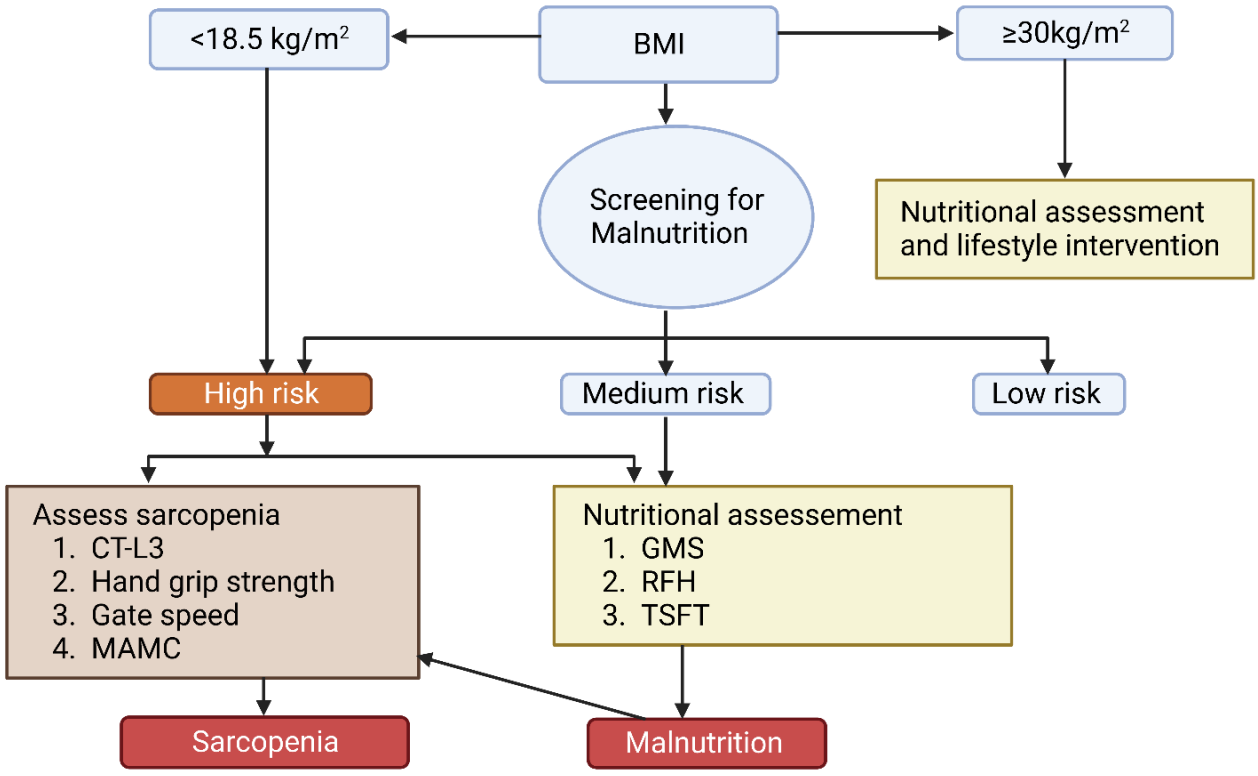

Figure 5. Flow chart of sarcopenia and nutritional assessment.

Table 2. Graz malnutrition screening (GMS) factors and scoring points.

Items	Personnel		Scoring points
Date of birth	The qualified nurses		
	Items 1 to 3		
Weight (kg)			
Height (m)			
BMI (kg/m^2)			
1. Weight loss within the last three months			
Current weight: _____	Weight lost three months ago: _____		
Evaluation weight loss		< 5 %	0 point
		5 – 10 %	1 point
		> 10 %	2 points
2. Body Mass Index (kg/m^2)			
	For patients up to 65 years:	For patients 65 years or older:	
	BMI > 20	BMI > 22	0
	BMI > 18-20	BMI > 20-22	1
	BMI < 18	BMI < 20	2
3. Decrease in food intake within the last months was due to the following:			
	Loss of appetite	No	Yes = 1 point
	Problems with chewing and swallowing	No	Yes = 1 point
	Nausea, vomiting, and diarrhea	No	Yes = 1 point
4. Severity of disease:	**International classification of disease done by a physician**		

Choose either 4a OR 4b. In 4a, the presence often this condition will be awarded 1 point, while in 4b, the existence of any of these conditions will be awarded 2 points.

a) Malignant systemic disease (without chemo/radiotherapy), preterminal renal failure (serum creatinine >5 mg/dl), acute gastrointestinal infection, maldigestion, chronic alcohol abuse, decompensated liver cirrhosis (CHILD C),

amyloidosis, COPD stage ≥ III, neurogenic dysphagia, wound NPUAP stage 1+ IV, polypharmacy > 5 drugs	1 point
b) Advanced malignant systemic disease, sepsis, wounds NPUAP stage I + II, malabsorption syndrome, chemo/ radiotherapy (longer than one week)	2 points
+ 1 If 65 years or older	1 point
GMS score ≥ 3 = malnutrition	
Summary of the items	**Values in scoring points**
Weight loss within the last three months	0 – 2
BMI	0 – 2
Changes in nutritional intake	0 – 3
1. Loss of appetite	
2. Nausea/ vomiting/ diarrhea	
3. Chewing and swallowing problems	
The severity of the disease according to the given list	0 – 2
Age > 65 years	1

This table was partly adapted from (171).

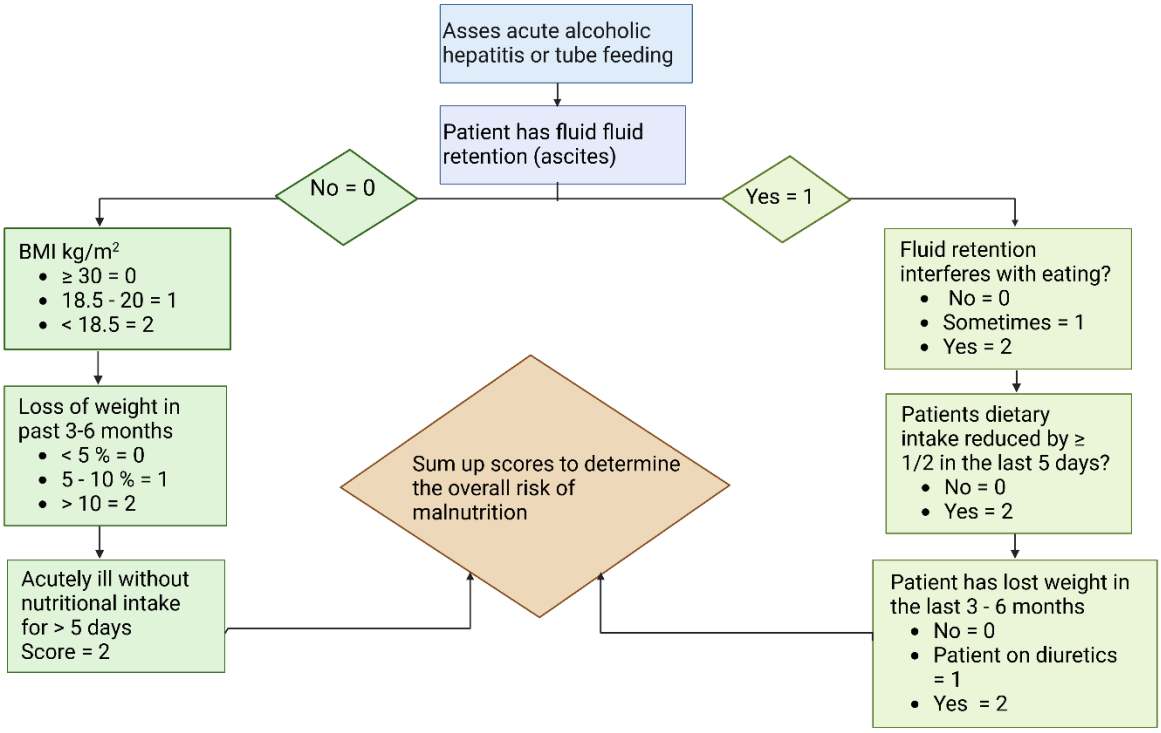

Figure 6. Flow chart of RFH-NPT factors and scores for determination of malnutrition in cirrhotic patients. It was created with BioRender.com.

Sampling procedure

Blood samples from the study participants were collected in in vacutainer tubes (BD, New Jersey, USA) at room temperature and subsequently centrifuged at 3000xg for 10 minutes at 4º C. 250µl of serum was aliquoted and stored at -80º C waiting for further analysis. Serum aliquots were received on dry ice and thawed on the day of sample analyses. Additionally, stool samples were provided by the study participants in a sterile dry screw-top container (Carl Roth, Karlsruhe, Germany). The stool samples were obtained and frozen at -80 ºC, awaiting further analysis. Urine samples provided by the patients in sterile urine containers (Carl Roth, Karlsruhe, Germany) were received and immediately stored at -20°C pending further investigations.

DNA extraction

Sequencing was performed at Institute of Clinical Molecular Biology, Christian-Albrechts-University of Kiel. The manufacturer's instructions were followed to extract DNA from the stool samples. Firstly, stool samples (0.25 g) were defrosted and homogenized in 500 µl of bacterial lysis buffer (Roche, Mannheim, Germany). Mechanical lysis was then performed on 250 µl of the homogenized stool samples using Magna Lyser green bead tubes prefilled with ceramic beads (1.4 mm) (Roche, Mannheim, Germany) by spinning the samples at a speed of 7500 x g for 45 seconds using Magna Lyser centrifuge (220 V, Roche Diagnostics, Basel, Switzerland). Next, the samples were incubated at 37 °C for 30 minutes in a preheated water bath. The total DNA was isolated from frozen stool samples using the MagnaPure LC DNA Isolation Kit III (Bacteria, Fungi) (Roche, Mannheim, Germany).

Enzymatic lysis was then carried out by adding 25 µl of proteinase K and 200 µl of buffer (without ethanol) to the mixture, which was vortexed for 30 seconds and incubated at 60 °C for 30 minutes in a heating block. Following this, 200 µl of ethanol (96-100%) was added to the samples and mixed by vortexing. The samples were then added to a spin column placed in a 2 ml microcentrifuge tube and spun at full speed (14000 rpm) for 3 minutes. The spin column was then placed in a new 2 ml microcentrifuge tube, and 500 µl of buffer was added before spinning again at a speed of 14000 rpm for 3 minutes. Finally, the spin column was placed in a new 2 ml microcentrifuge tube, and DNA was eluted by adding 200 µl of elution buffer, and the content was spun at a speed of 14000 rpm for 1 minute. The extracted DNA was stored at -20 °C for further analysis. The steps were based on the Magna Pure DNA protocol provided in the DNA extraction kit.

16s rRNA gene library preparations and sequencing

The NanoDrop 2000c spectrophotometer (Thermo Fischer Scientific, USA) was used to measure the extracted bacterial total DNA concentration. The bacterial DNA load present in the fecal samples was quantified by Real-Time PCR System (BioRad CFX 96, BioRad Laboratories, California, USA) using primer sets (Eurofins, Ebersberg, Germany) targeting 16 s RNA hypervariable V1-V2 regions (27F: AGAGTTTGATCCTGGCTCAG and 357R: CTGCTGCCTYCCGTA). The quantitative PCR was conducted using SYBR green in a 25.0 µl PCR reaction in triplicates containing 12.5 µl SYBR green master mix (Promega, Vienna, Austria),

1.0 µl of forward primer (27 F, 25 µM), 1.0 µl of reverse primer (357 R, 25 µM), 9.5 µl DNAse free water (Promega, Vienna, Austria), and 2.0 µl of DNA template (100 pg).

The DNA was denatured (95°C for 3 minutes), followed by 30 cycles of denaturation at 95°C for 45 seconds, annealing at 55°C for 45 seconds, extension for 72°C for 1 minute and a final extension of 72°C for 7 minutes. On a SequalPrep Normalization Plate (Life Technologies), 15 µl of the pooled PCR product from the three triplicates were normalized following the manufacturer's instructions before being tested on a 1% agarose gel. 15 µl of the normalized PCR product were used as a template for indexing PCR in a 50.0 µl single reaction to introduce barcode sequences to each sample as previously described (Kozich et al. 2013). Only 8 amplification cycles were used, with the cycling parameters remaining the same as for the targeted PCR.

After indexing, the unpurified library was put onto a 1% agarose gel and then purified using a Qiaquick gel extraction kit (Qiagen, Hilden, Germany) following the manufacturer's recommendations. According to the manufacturer's instructions, the pool was quantified using sequencing library size on the Promega Quantus instrument. The sequencing library size was validated using an Agilent 2100 Bioanalyzer (Agilent, California, USA) and a high-sensitivity DNA assay. The pool, including all samples, was run using version 3600 cycle chemistry (Illumina, Eindhoven, Netherlands) at 6 pM final concentration with 20 % PhiX control DNA (Illumina, Eindhoven, Netherlands) following the manufacturer's instructions. Batch effects were minimized by randomly distributing the samples into isolation and sequencing batches. In addition, negative controls were executed for DNA isolation, library preparation, and sequencing to evaluate and manage any contamination originating from reagents and potential cross-contamination throughout the process. The raw gut microbiome sequencing data (FASTQ) have been deposited at NCBI sequencing Read Archive (accession number, PRJNA933898, https://www.ncbi.nlm.nih.gov/sra/PRJNA933898).

ELISA

Ready-to-use solid-phase sandwiches on the market LBP (Hycult Biotechnology, Uden, Netherlands), sCD14 (R&D Systems, Abingdon, UK), IGF-1 (Immundiagnostik, Bensheim, Germany), myostatin (Immundiagnostik, Bensheim, Germany), FGF-21 (BioVendor, Brno, Czech Republic), irisin (BioVendor, Brno, Czech Republic), and DAO (Immundiagnostik, Bensheim, Germany) were all quantified in serum using ELISA kits. Furthermore, zonulin (Immundiagnostik, Bensheim, Germany) and calprotectin (Immundiagnostik, Bensheim, Germany) in the stool were

also measured using ELISA kits. The manufacturer's methodology was followed correctly throughout the analysis, and a summary of the ELISA kits used is shown in (Table 3).

Table 3. Summary of ELISA used to quantify gut permeability, bacterial translocation, and inflammation biomarkers.

Elisa Test	Supplier	Type of ELISA	Anti-bodies	Photometer
Serum LBP	Hycult Biotechnology, Uden, Netherlands	Sandwich	Biotinylated tracer antibody and Streptavidin-peroxidase conjugate antibody	Spectrostar Omega (BMG LABTECH)
Serum sCD14	R&D systems Abingdon, UK	Sandwich	Monoclonal anti-human CD14 antibody and polyclonal anti-human CD14 antibody conjugated to horseradish peroxidase	Spectrostar Omega (BMG LABTECH)
Serum IGF-1	BioVendor, Brno, Czech Republic)	Sandwich	Biotinylated labeled antibody and Streptavidin-peroxidase conjugate antibody	Spectrostar Omega (BMG LABTECH)
Serum FGF-21	BioVendor, Brno, Czech Republic)	Sandwich	Biotinylated labeled antibody and Streptavidin-peroxidase conjugate antibody	Spectrostar Omega (BMG LABTECH)
Serum myostatin	Immundiagnostik, Bensheim, Germany	Competitive	Polyclonal anti-myostatin and streptavidin-labeled - peroxidase antibody	Spectrostar Omega (BMG LABTECH)
Serum irisin	BioVendor, Brno, Czech Republic	Competitive	Detection antibody and horseradish peroxidase-conjugated anti-rabbit IgG	
Serum DAO	Immundiagnostik, Bensheim, Germany	Sandwich	Polyclonal rabbit anti-DAO antibody and biotinylated polyclonal anti-DAO antibody.	Spectrostar Omega (BMG LABTECH)
Stool zonulin	Immundiagnostik, Bensheim, Germany	Competitive	Polyclonal anti-ZFP antibody and peroxidase-labeled streptavidin	Spectrostar Omega (BMG LABTECH)

Stool calprotectin	Immundiagnostik Bensheim, Germany	Sandwich	Monoclonal anti-human calprotectin antibody and peroxidase-labeled conjugate	Spectrostar Omega (BMG LABTECH)

High-performance liquid chromatography-tandem mass spectrometry (HPLC-MS/MS) for analysis of serum and stool bile acids

Serum and stool bile acids were quantified using HPLC-MS/MS (Thermo Fisher Scientific, Massachusetts, USA). Organic solvents for precipitation were supplied by different vendors (Table 2). The mobile phase solvents were provided by (Sigma Aldrich Handels GesmbH, Vienna, Austria) and Merck (Germany), while bile acid controls (abnormal and normal) were provided by Trinity Biotech (Ref B6021 and B5021). Bile acid standards were purchased from different suppliers (Table 2). The bile acid internal standard was prepared by pipetting 100 µl of each bile standard into a 10 ml volumetric flask and topping up to 10 ml with methanol to achieve a final concentration of (2 nmol/100µl) as described (Table 3).

Different bile acid standards were weighed and placed in labeled tubes to make a calibration curve for serum and stool bile acids quantification (Table 3). Each standard was mixed with 10 ml methanol to make a stock solution of (2 mmol/l). After that, 50 µl of each bile acid standards stock solution was mixed with 250 µl methanol (100 nmol/ml). The mixtures were then serially diluted with 500 µl of methanol up to the 13th tube to achieve a concentrations range of (0.02-100 nmol/ml). Furthermore, the internal standard stock solution was diluted 1:10 with methanol to reach a final concentration of (0.2 nmol/100µl). For serum bile acid quantification, 10 µl of serum was deproteinized using 400 µl of acetonitrile mix by vortexing (IKA, Wilmington, USA). Supernatant from the samples and controls were transferred into fresh tubes. 100 µl internal standard (0.2 nmol/100 µl in methanol) was added to each sample, and the mixture was homogenized by vortexing. Samples and controls were centrifuged for 10 minutes at 4000g at 4º C. 100 µl supernatant of the samples and controls were transferred into a fresh tube and dried under a stream of nitrogen and re-dissolved in 100 µl of mobile phase solvent B (MeOH and ammonium hydroxide, 100:0.1; v/v) and transferred to auto-sampler vials. The HPLC-MS was conducted on 5 ml reversed-phase (Agilent, California, USA), using a methanol/water gradient. 10 µl was used as the injection volume of all samples and controls. The absolute concentrations of bile acids were calculated using calibration curves generated by internal standards.

The frozen stool samples were thawed, 10 mg of stool samples were homogenized in 2 ml of NaOH (0.1M). The mixture was incubated at 60°C for 1 hr. After that, stool samples were

homogenized in a sonicator water bath for 15 seconds. The stool homogenate was diluted with NaOH (1:100, 0.1M). After that, 100µl internal standard (2 nmol/100µl methanol) and 4 ml of deionized water were added to the diluted stool samples. The stool samples were homogenized in a sonicator water bath (Ultrasons-H, Barcelona, Spain) for 15 seconds. 4ml acetonitrile (80 % v/v) was added to the sonicated samples suspension. The sample suspensions were incubated at room temperature for 20 minutes and further centrifuged at 2500 rpm for 20 minutes at room temperature. The supernatant was then collected, placed in clean tubes, and dried overnight at under a stream of nitrogen in a speedVacs concentrator (SC250EXP Thermo Fisher Scientific, Massachusetts, USA). The overnight dried samples were later dissolved in 4ml of ammonium acetate (15mM, PH=5.3). In that order, a 10 ml reversed-phase cartridge C18 (Agilent, California USA) was preconditioned by adding 5 ml of deionized water, 5 ml of methanol, and 5 ml of deionized water. After that, sample suspensions were loaded into a preconditioned C18 cartridge. The washing step involved 6 ml of de-ionized water (HPLC high grade), 6 ml of hexane, and 6 ml of water (HPLC high-grade water) in that order. The C18 cartridge content was eluted into a clean tube marked with sample identification. The samples were eluted using 3ml methanol (HPLC gradient grade). The eluted samples were later dried overnight in a stream of nitrogen using a speedVacs centrifuge. After that, 100µl of mobile phase B was added to the stool sample in the tubes and 100µl pipetted into autosampler vials. The sealed samples were stored at -20°C awaiting further analysis. 10 µl was used as the injection volume for all samples and controls (normal and abnormal). The absolute concentrations of bile acids were calculated using calibration curves generated by internal standards. The methods used for bile acid extraction were adapted from (174, 175). Dr. Günther Fauler from the Clinical Institute for Medical and Chemical Laboratory Diagnosis kindly supported the bile acid analysis.

Table 4. Chemicals and reagents for serum and stool bile acids quantification.

Reagent	Supplier	Catalog No
Organic solvents		
Methanol	Merck, Vienna, Austria	1.0600.1011
Acetonitrile	Merck, Vienna, Austria	1.000302.2500
Chloroform	Merck, Vienna, Austria	C2432
Ammonium acetate	Merck, Vienna, Austria	1.01116.1000
Acetic acid	Merck, Vienna, Austria	1.00063.1011
Formic acid	Merck, Vienna, Austria	1.00264.1000
De-ionized water	Merck, Vienna, Austria	WAK-AQ-250-50L
Hexane	Sigma Aldrich, Vienna	110-54-3
Acetone	Carl Roth, Karlsruhe, Germany	9372.4
Sodium hydroxide	Sigma Aldrich, Vienna, Austria	S8045
LC-MS grade Water	Merck, Vienna, Austria	7732-18-5
Bile acid controls		
Normal	Trinity Biotech, USA	B6021
Abnormal	Trinity Biotech, USA	B5021
Bile acid standards		
Cholic acid	Sigma Aldrich, Vienna, Austria	C1129
Glycocholic acid	Sigma Aldrich, Vienna, Austria	G7132
Taurocholic acid	Sigma Aldrich, Vienna, Austria	D2510
Chenodeoxycholic acid	Sigma Aldrich, Vienna, Austria	C9377
Glycochenodeoxycholic acid	Sigma Aldrich, Vienna, Austria	G0759
Taurochenodeoxycholic acid	Sigma Aldrich, Vienna, Austria	T6260
Deoxycholic acid	Sigma Aldrich, Vienna, Austria	D2941
Glycodeoxycholic acid	Sigma Aldrich, Vienna, Austria	G6132
Taurodeoxycholic acid	Sigma Aldrich, Vienna, Austria	T287245
Lithocholic acid	Sigma Aldrich, Vienna, Austria	L6250
Glycolithocholic acid	Steraloid, Rhode Island, USA	G801
Taurolithocholic acid	Steraloid, Rhode Island, USA	H2555
Ursodeoxycholic acid	Sigma Aldrich, Vienna, Austria	U5127
Glycodeoxycholic acid	Sigma Aldrich, Vienna, Austria	H894
Taurodeoxycholic acid	Steraloid, Rhode Island, USA	L1655

Table 5. Bile acid standards weight for standard stock solutions preparation (2 mmol/ml).

Bile acid standards	Concentrations	Weight dissolved in methanol
Cholic acid	MG: 408.6 g/mol	8.17 mg to 10 ml make up with methanol
Glycocholic acid	MG: 487.2 g/mol	9.74 mg to 10 ml make up with methanol
Taurocholic acid	MG: 536.1 g/mol	10.72 mg to 10 ml make up with methanol
Deoxycholic acid	MG: 391.6 g/mol	7.83 mg to 10 ml make up with methanol
Glycodeoxycholic acid	MG: 471.6 g/mol	9.41 mg to 10 ml make up with methanol
Taurodeoxycholic acid	MG: 520.3 g/mol	10.41 mg to 10 ml make up with methanol
Chenodeoxycholic acid	MG: 392.2 g/mol	7.84 mg to 10 ml make up with methanol
Glycochenodeoxycholic Acid	MG: 471.2 g/mol	9.42 mg to 10 ml make up with methanol
Taurochenodeoxycholic Acid	MG: 521.7 g/mol	10.43 mg to 10 ml make up with methanol
Lithocholic acid	MG: 376.2 g/mol	7.52 mg to 10 ml make up with methanol
Glycolithocholic acid	MG: 455.2 g/mol	9.1 mg to 10 ml make up with methanol
Taurolithocholic acid	MG: 505.7 g/mol	10.11 mg to 10 ml make up with methanol
Ursodeoxycholic acid	MG: 392.2 g/mol	7.84 mg to 10 ml make up with methanol
Glycoursodeoxycholic acid	MG: 449.6 g/mol	8.99 mg to 10 ml make up with methanol
Tauroursodeoxycholic acid	MG: 521.3 g/mol	10.42 mg to 10 ml make up with methanol

Quantification of serum, stool, and urine metabolites using Nuclear Magnetic Resonance (NMR)

Stored serum, urine, and stool samples were received in dry ice, and samples were then thawed at room temperature and mixed by vortexing. To remove protein and to quench the enzymatic reaction, 200 µl of samples (serum, urine, or stool) were mixed with 400 µl of a buffer solution (15% D_2O, 3mM trimethylsilypropanoic acid (TMSP), and 0.9% NaCl). The mixtures were centrifuged at 12000g at 4 ºC for 10 min. After that, 500 µl of the supernatant was transferred into an mm NMR tube for further analysis (176). The samples (serum, urine, stool) metabolites were quantified using 310 K NMR spectroscopy (Bruker Avance 600 MHz) equipped with TXI probe head and processed as described. Furthermore, the 1D CPMG (Carr-Purcell-Meiboom-Gill); pulse sequence (cpmgpr1d, 512 scans, 73,728 points in F1,11,904.76 HZ spectral width, 512 transients, recycle delay 4 s) with water suppression using pre-saturation was used for ^{1}H 1D

NMR experiments. The experiments were conducted as previously described (176). Professor Tobias Mandl's lab group conducted the wet lab analysis of serum, urine, and stool metabolome.

Stool bile acids gene abundance quantification by qPCR

We measured the abundance of several stool bile acids genes, including bile salt hydrolase (BSH), bile acid inducer CD and E (BaiCD and E), three alpha-hydroxysteroid dehydrogenases (3-HSDH), three beta-hydroxysteroid dehydrogenases (3-HSDH), five alpha reductases (7-HSDH), seven beta-hydroxysteroid dehydrogenases (7-HSDH), and twelve alpha-hydroxysteroid dehydrogenases (12α-HSDH). Bioinformatics tool (Primer-Blast) was used to obtain the sequences of the primers. Further, it analyzed the designed primers against relevant databases to ensure specificity to the target bacterial genes and minimize potential off-target binding. A non-redundant database (Refseq mRNA) was chosen and predicted transcripts were excluded from the database search, among other stringent measures (21). Eurofins Genomics (Vienna, Austria) synthesized and supplied the primers (Table 4). The genomic DNA isolated from stool samples was used in the qPCR experiment to quantify bile acids gene abundance. The qPCR was performed in Bio-Rand (Roche Diagnostic, Mannheim, Germany). 25µl reaction volume was used containing: 12.5 µl SYBR green (SYBR, Promega, Madison, WI USA) and 5.5 µl of RNA/DNases free water (Promega, Madison, WI USA), 1.0µl of 10.0 µM for forward primer and 1.0µl of 10.0 µM reverse primer (Eurofins Genomics, Vienna, Austria), and 5.0 µl of template DNA. For the standard curve, 5.0 µl DNA from each sample was pooled. 7 µl of the pooled DNA was pipetted into a tube containing 14 µl of DNAse free water to achieve a dilution factor of (1:3); this process was serially repeated until the 7^{th} tube to achieve desired varied concentrations used for the standard curve. The qPCR thermocycling conditions included: 95 ºC for 2 min followed by 40 cycles of denaturation at 98 ºC for 10 sec, primer-specific annealing at 52 ºC for 20 sec, and elongation at 68 ºC for 1 min. The bile acids gene abundances were quantified relative to bacterial 16s rDNA gene abundances. The normalized bile acids gene abundance dataset was used for further statistical analysis. The method was adopted from previously published protocols (122).

Table 6. Primer sequence for stool bile acid genes abundances.

Gene label	F/R	Primer sequence	Enzyme	Product Length
BSH	F	TGGCTAGCCTGCTTTTCTTG	bile salt hydrolase	318 bp
	R	CCGTGGCAAAGTTATCAAGC		
3α-HSDH	F	AGAAGATCTACGCCGAAGCG	3α-hydroxysteroid dehydrogenase	159 bp
	R	CCATGTACACCTTGGCACCT		
3β-HSDH	F	CAGGCTACCGCCACATAGAC	3β-hydroxysteroid dehydrogenase	140 bp
	R	GGTGTCGTACCCTCTTTCCG		
5 AR	F	CCTAAGGAATCTCAGAAAACCAGG	5α- reductase	117 bp
	R	GCATAGCCACACCACTCCATGA		
BaiCD	F	CAGCCCRCAGATGTTCT TTG	7α-dehydroxylase	200 bp
	R	GCATGGAATTCHACTGCRTC		
BaiE	F	GCCCGAAGGAAGTTACCGAT	7-alpha dehydratase	93 bp
	R	TGTCAATGGTGATCTCCGGC		
7α-HSDH	F	CACGGGACAAACAATCGTCG	7α-hydroxysteroid dehydrogenase	209 bp
	R	CCACTCTTCCCCCTTTTCGAT		
7β-HSDH-F	F	TACGCGAGATCATCGAAGGC	7β-hydroxysteroid dehydrogenases	230 bp
	R	TTCCGGGTACGGGAAGTAGT		
12α- HSDH	F	GGCTTCTGCGTCGGGTATT	12α-hydroxysteroid dehydrogenase	192 bp
	R	GCATATGCACACTGACCGAAGT		
16s rRNA	F	GTGSTGCAYGGYTGTCGTCA		527 bp
	R	ACGTCRTCCMCACCTTCCTC		

2Note: Abbreviations: F, forward primer; R, reverse primer; BSH, bile salt hydrolase; BaiCD E bile acid inducer CD, and E; 3α-HSDH, 3 alpha-hydroxysteroid dehydrogenases; 3β-HSDH, 3 beta-hydroxysteroid dehydrogenases; 7α-HSDH, 7 alpha-hydroxysteroid dehydrogenases; 7β-HSDH, 7 beta-hydroxysteroid dehydrogenases; 12α-HSDH, 12 alpha-hydroxysteroid dehydrogenases

Statistical analysis

Data from cirrhotic patients with and without sarcopenia as well as controls with and without sarcopenia were evaluated and compared using descriptive and comparative statistics. Chi-square was used to calculate the significant differences between the two groups for categorical variables. Additionally, the student's t-test was employed to assess the significance of the differences between the two groups for continuous data. The Mann-Whitney U test was employed as an alternative to the Student's t-test when the assumptions of parametric testing were not satisfied. Multiple testing, especially in “wider than long” data sets, might inflate alpha and beta error and influence the perception of significant results. Minimizing both error types is a delicate trade-off. In our study, we preselected and grouped relevant features within each data pool to make the multiplicity control less restrictive and reduce the beta error. On the other hand, we set a relatively stringent false discovery rate of 5% within the Benjamini-Hochberg correction to select only the most robust results in each data pool and thereby reduce the alpha error. All p-values were adjusted for multiple testing according to the Benjamini-Hochberg method.

On a local Galaxy instance (https://galaxy.medunigraz.at), the pre-processing of sequence reads was implemented for Quantitative Insights into Microbial Ecology 2 (QIIME 2). Divisive amplicon denoising algorithm 2 (DADA2) was used to perform denoising (deleting primers, quality filtering, fixing faults in marginal sequences, removing chimeric sequences, removing singletons, combining paired-ended reads, and dereplication). A Nave Bayes classifier was used to assign taxonomies based on the Silva V132 database release at 99% operational taxonomic unit level. After pre-processing, the raw sequence data were rarefied, and an average of 17.105 sequence reads (with a possible range of 3.525 to 34.816) were obtained for each sample. The amplicon sequence variants (ASV) table in biom format and metadata of the study participants were uploaded into Calypso 8.84 (http://cgenome.net/wiki/index.php/Calypso) for further processing and analysis as previously established (177). Cyanobacteria and chloroplasts, samples with fewer than 1000 sequence reads, and taxa with less than 0.01 relative abundance across all samples were all excluded from the ASV table after it had been filtered and normalized. To quantify alpha and beta diversity, principal coordinates analysis (PCoA) and Chao1 identified the richness of the gut microbiome community. To determine ASV linked to sarcopenia in cirrhosis and to evaluate the significance of the variations in ASV abundances between the groups, linear discriminant analysis (LDA), effect size (LEfSe), and analysis of the composition of the microbiome (ANCOM) were performed, respectively. Furthermore, R software 4.0.2 (http://www.R-project.org) packages (readxl, tidyverse, phyloseq, metagMisc, viridis, ggpubr, lme4, lmerTest, jtools, writexl, ggplotify,

vegan, ggConvexHull, pldist, ggh4x, cowplot, Maaslin, and splancs were used to study the gut microbiota. MicrobiomeAnalyst 2.0 (https://www.microbiomeanalyst.ca/) received an ASV abundance table with a valid taxonomy identifier, representative sequence table, and metadata for further processing, which included filtering, rarefaction normalization, and sample inferencing. The SILVA reference database served as the basis for assigning the taxonomy. The anticipated function profiles of cirrhotic patients with and without sarcopenia and non-cirrhotic controls with and without sarcopenia were determined using Tax4Fun 2. The data processing workflow has been previously described (178, 179).

R software 4.0.2 (http://www.R-project.org) was used to implement regularized logistic least absolute shrinkage (LASSO) regression; packages used included (glmnet, dplyr, tidyr, rsample, ggplot2, ModelMetrics, ggplot2, glmnet, ncvreg, coefplot, pROC, readxl, mice, corrplot, foreign, RColorBrewer, wesanderson, foreign). LASSO regression is prone to overfitting and underfitting like any other supervised or unsupervised machine learning algorithm. When using LASSO regression to build prediction models, we employed strategies to overcome overfitting or underfitting and lambda selection problems. One strategy was cross-validation. This technique is crucial in preventing overfitting and selecting the lambda value. Using cross-validation, we aimed to find the optimum lambda value that strikes the right balance between fitting the data and avoiding excessive complexity. This approach also helps to ensure that our model's performance remains consistent even when faced with different data subsets. In our study, we adopted a 10-fold cross-validation setup. This means that we divided our dataset into ten parts: seven parts were used for training, and the remaining three were used for testing. Through this process, we repeatedly trained and evaluated the LASSO regression model using different subsets of the data. Ultimately, the optimal lambda value emerged after parameter regularization. This optimal lambda value was determined by evaluating the performance metric across all ten folds of the cross-validation. By choosing the lambda value that led to the best overall performance, we identified the setting that yielded the lowest average error or the highest average R-squared, indicators of the model's predictive capability.

Another challenge we faced was the presence of multicollinearity among the variables. To address this issue, we pooled related variables into a single dataset. The purpose of this consolidation was to reduce the multicollinearity among the variables. By doing so, we aimed to mitigate a significant issue using the LASSO regression model. The LASSO model, used for feature selection and regularization in regression analysis, can be heavily influenced by correlated variables. We hoped to minimize adverse effects on the LASSO model's performance by reducing

multicollinearity. The process of lowering multicollinearity through variable pooling had a simplifying effect on the model. We made the model less susceptible to capturing random fluctuations in the data (noise). This is crucial because an overly complex model that captures noise can lead to inaccurate predictions when applied to new data. Notably, we introduced the combined datasets into the model in parallel. This approach allowed us to manage the complexity of the model and ensure that the variables' interrelationships were appropriately considered.

Through this approach, we wanted to ensure that our model leveraged the most relevant and meaningful information for making predictions. By reducing multicollinearity and simplifying the model's structure, we aimed to enhance its ability to identify proper relationships between variables and the outcome. This way, our model would be more robust and reliable in its predictions. Furthermore, we aimed to balance fitting the training data well and maintaining the model's ability to make accurate predictions on new data. To investigate the influence of covariates in sarcopenia prediction, the LASSO calculated coefficients were employed. Additionally, models that independently predicted sarcopenia even after adjusting for potential confounders were created using multivariate logistic regression.

Nuclear Magnetic Resonance (NMR) spectra processing procedures were conducted using Bruker Topspin software version 4.0.2. Signal deconvolution, Fourier transformation of the Free Induction Decay (FID), automatic phasing, and baseline correction were performed within this software. Subsequently, a MATLAB script compatible with version 2014b was employed to import the spectra. Signal integration of normalized spectra was used for the quantification of metabolites. A distinctive, non-overlapping peak for each metabolite was identified, and integration boundaries were set around that peak. An R script, executed in RStudio 2023 with R version 4.1.3, was utilized to integrate the areas of all peaks across all samples and metabolites. The resulting values were expressed in arbitrary units , reflecting proportional concentrations of the respective analytes. An explorative multivariate analysis was conducted. The serum, stool, and urine metabolites were measured using NMR spectroscopy to assess the differences in their concentration between cirrhotic patients with and without sarcopenia, as well as non-cirrhotic controls with and without sarcopenia. The resulting clusters were visualized with orthogonal projection latent structure discriminant analysis (O-PLS-DA), a supervised modeling method used for dimension reduction. The model underwent cross-validation, outliers were removed, and testing was done after 100 permutations. The O-PLS-DA analysis showed that serum, stool, and urine metabolome could discriminate between cirrhotic and control groups. Furthermore, the student’s t-test or Mann-Whitney U test was used to determine significant differences in the

concentration of these metabolites between groups. All p-values were adjusted for multiple testing according to the Benjamini-Hochberg method. The metabolite set enrichment analysis (MSEA) and pathway analysis were carried out using the MetaboAnalyst 5.0 (https://www.metaboanalyst.ca), which made it possible to identify substantially different metabolite sets and pathways that reveal physiologically important patterns between comparison groups. The metabolite abundances from the serum (45), urine (50), and stool (43) metabolomics data were uploaded to MetaboAnalyst 5.0. To assure its reliability and comparability, the data was standardized. Chemical names were used to identify metabolites, and the human metabolome database (HMDB) and Kyoto Encyclopedia of Genes and Genomes (KEGG) metabolite set library were used to annotate them. The correlation of differentially important clinical parameters, BAs, metabolomes, and ASV was carried out using Spearman's approach. SPSS version 25 (IBM Corporation, Armonk, USA), R software 4.0.2 (http://www.R-project.org), and MetaboAnalyst 5.0 (180, 181) were used for the analysis.

RESULTS

Some results are reported in (1).

Clinical and demographic characteristics of the study participants

The study involved 175 participants, consisting of 116 liver cirrhotic patients (with sarcopenia, n=78 and without sarcopenia, n=38) and 59 controls (with sarcopenia, n=39 and without sarcopenia, n=20). Baseline characteristics for each group are provided in (Tables 7, 8, and Figure 7). In the cirrhotic group, males were found to be 1.5 times more likely to develop sarcopenia than females ($p = 0.005$), with significantly more males (82.1%) than females (17.9%) being sarcopenic. GMS and RFH-NPT showed that 16 % and 22.1 % of cirrhotic patients with sarcopenia were at risk of malnutrition, while 4 % of cirrhotic patients without sarcopenia were at risk of malnutrition. However, there was no significant difference in the prevalence of malnutrition among patients with cirrhosis who had sarcopenia and those who did not ($p > 0.05$). Additionally, cirrhotic patients with sarcopenia showed significantly lower values for BMI, muscle mass, mid-arm muscle circumference (MAMC), hematocrit (Hct), and alanine aminotransferase (ALT) levels compared to cirrhotic patients without sarcopenia ($p = 0.0001$, $p = 0.0001$, $p = 0.0001$, $p = 0.044$, and $p = 0.041$, respectively). Furthermore, non-cirrhotic controls with sarcopenia had significantly lower BMI, muscle mass, and MAMC compared to their non-sarcopenic counterparts ($p = 0.001$, $p = 0.001$, and $p = 0.01$, respectively). However, when comparing non-cirrhotic controls with and without sarcopenia, hematocrit and ALT levels were found to be comparable ($p > 0.05$). Interestingly, albumin levels were significantly lower in non-cirrhotic controls with sarcopenia compared to those without ($p = 0.015$).

When we conducted separate analyses for male and female patients, we observed that BMI, muscle mass, and MAMC were significantly lower in cirrhotic patients with sarcopenia compared to those without, and this difference was consistent for both sex. Additionally, male cirrhotic patients, but not females, showed a significant difference in hematocrit when comparing those with and without sarcopenia. However, regardless of sex, cirrhotic patients with or without sarcopenia had similar ALT and albumin levels in their serum. In control group, both male and female, BMI, muscle mass, and MAMC were significantly lower in patients with sarcopenia compared to those without. On the other hand, ALT and hematocrit levels in controls with and without sarcopenia were similar for both sexes. Even after considering factors such as sex and

the severity of liver disease, our multivariate regression analysis revealed that BMI, muscle mass, and MAMC were independently associated with sarcopenia.

These findings suggest that while hematocrit and ALT levels are related to sarcopenia in the context of cirrhosis, BMI, muscle mass, and MAMC are indicators of sarcopenia irrespective of the presence of cirrhosis. Moreover, albumin levels are associated with sarcopenia regardless of cirrhosis. Surprisingly, various biomarkers, including zonulin, calprotectin, DAO, LBP, sCD14, IGF-1, myostatin, FGF-21, and irisin, did not exhibit significant differences between cirrhotic patients with and without sarcopenia, as well as between non-cirrhotic controls with and without sarcopenia ($p > 0.05$), contrary to our expectations. However, zonulin and calprotectin levels in stool and serum CRP were notably elevated in cirrhotic patients with sarcopenia when compared to non-cirrhotic controls with sarcopenia ($p = 0.04$, $p = 0.005$, and $p = 0.001$, respectively, as shown in Fig 7). Furthermore, irisin and IGF-1 levels in serum were significantly reduced in cirrhotic patients with sarcopenia compared to non-cirrhotic controls with and without sarcopenia ($p = 0.001$, $p = 0.03$, $p = 0.001$, and $p = 0.001$, respectively, as illustrated in Fig 7). These results indicate that alterations in zonulin, calprotectin, CRP, irisin, and IGF-1 are associated with cirrhosis, independent of the presence of sarcopenia. Notably, there were no sex-specific differences observed in gut permeability, bacterial translocation, or muscle biomarkers.

Table 7. Demographic characteristics and clinical parameters of cirrhotic patients with and without sarcopenia. This table has been reproduced from (1).

	Cirrhosis sarcopenia (n=78)	**Cirrhosis no sarcopenia (n=38)**	**P-values**
Gender (n/%)	Male 64 (82.1%) female 14 (17.9%)	Male 22 (57.9%) female 16 (42.1%)	p = 0.007
Age (years)	64 (61;68)	62 (60;67)	Ns
Body mass index (kg/m^2)	25.7 (24.2;27.1)	29.5 (27.4;31.2)	p < 0.0001
Charlson comorbidity index	5 (5;6)	5 (4;6)	Ns
	Muscle mass and function		
Muscle mass (cm^2/m^2)	39.80(37.58;41.17)	55.58 (49.70;58.63)	p < 0.0001
HGS (kg)	29.15 (27.00;31.00)	30.33 (26.33;33.60)	Ns
MAMC (cm)	23.6 (23.1;24.6)	27.4 (25.7;28.1)	p < 0.0001
Gait speed (m/sec)	0.92 (0.84;1.00)	1.02 (0.91;1.07)	Ns

Chair rise (sec)	17.95 (16.41;19.60)	14.68 (14.02;19.28)	Ns
	Malnutrition assessment		
GMS Scores (No risk/ High risk)	65 (84.0 %)/ 13 (16.0%)	34 (89.5 %)/ 4 (10.5 %)	Ns
RFH-NPT (No risk/ High risk)	60 (77.9 %)/ 17 (22.1 %)	34 (89.5 %)/ 4 (10.5 %)	Ns
TSFT (mm)	12.15 (11.00;13.60)	12.10 (10.20;14.40)	Ns
	Liver functions		
MELD score	11 (10;14)	11 (9;12)	Ns
Bilirubin (mg/dL)	0.70 (0.55;0.96)	0.38 (0.30;0.57)	Ns
Albumin (g/dL)	3.5 (3.4;3.7)	3.6 (3.4;3.9)	Ns
Total protein (g/dL)	7.2 (7.7;7.5)	7.2 (6.9;7.4)	Ns
Prothrombin time (INR)	1.23 (1.16;1.32)	1.21 (1.15;1.28)	Ns
AST (U/L)	46 (43;52)	52 (47;89)	Ns
ALT (U/L)	28 (26;35)	40 (34;59)	p = 0.041
GGT(U/L)	131 (96;156)	113 (92;164)	Ns
	Other routine laboratory parameters		
CRP (mg/dL)	5.5 (3.4;9.5)	6.1 (2.8;7.8)	Ns
Hematocrit (%)	33.2 (31.2;35.6)	36.5 (34.4;39.4)	p = 0.044
Creatinine (mg/dL)	0,89 (0.81;99)	0.91 (0.84;1.02)	Ns
Urea (mg/dl)	40.0 (35.0;47.0)	32.0 (30.0;44.0)	Ns
	Gut permeability, bacterial translocation, and inflammation		
Zonulin (ng/mL)	98.1 (80.8;110.3)	113.4 (92.4;162.0)	Ns
DAO (U/ml)	19.50 (16.23;25.40)	17.37 (14.09;20.77)	Ns
Calprotectin (µg/g)	101.1 (75.4;126.7)	58.4 (40.8;116.0)	Ns
LBP (µgml)	19.21 (17.71;22.30)	17.73 (16.74;22.02)	Ns
sCD14 (µgml)	1.75 (1.67;1.87)	1.76 (1.70;1.84)	Ns
	Muscle biomarkers		
Myostatin (ng/ml)	36.45 (34.01;40.47)	43.27 (36.08;47.36)	Ns
Irisin (µg/ml)	1.48 (1.33;1.88)	1.81 (1.41;2.13)	Ns
FGF21 (ng/ml)	0.36 (0.25;0.48)	0.27 (0.15;0.37)	Ns
IGF-1 (ng/ml)	55.89 (44.37;65.70)	51.74 (43.36;76.35)	Ns

1Note: The data shown are absolute numbers and percentages, or median and 95% confidence interval (lower; upper). P<0.05 values were obtained from the student's t-test or Mann-Whitney U test.

Abbreviations: MELD, model of end-stage liver disease; INR, international normalized ratios; AST, aspartate aminotransferase; ALT, alanine aminotransferase; GGT, gamma-glutamyl-transferase; CRP, C-reactive protein; DAO, diamino-oxidase; LBP, lipopolysaccharide; sCD14, soluble CD14; FGF-21, fibroblast growth factor 21; IGF-1, insulin-like growth factor 1.

Table 8. Demographic characteristics and clinical parameters of non-cirrhotic patients with and without sarcopenia. This table has been reproduced from (1).

	Control sarcopenia (n=39)	**Control no sarcopenia (n=20)**	**P-values**
Gender (n/%)	Male 20 (51.3%); female 19 (48.7%)	Male 13 (65.0%); female 7 (35.0%)	Ns
Age (years)	59 (56;66)	59 (53;67)	Ns
Body mass index (kg/m^2)	23.9 (21.5;25.2)	28.2 (26.0;29.7)	p < 0.0001
Charlson comorbidity index	0 (0;0)	1 (0;6)	Ns
	Muscle mass and function		
Muscle mass (cm^2/m^2)	35.99 (33.36;42.88)	54.48 (50.00;56.12)	p < 0.0001
Handgrip strength (kg)	27.30 (23.30;36.00)	39.39 (29.00;45.30)	Ns
Mid-arm muscle circumference (cm)	24.49 (22.70;25.09)	26.48 (25.11;28.90)	p = 0.003
Triceps Skinfold Thickness (mm)	11.70 (9.50;16.00)	15.00 (11.40;19.00)	Ns
Gait speed (m/sec)	1.04 (0.93;1.11)	1.02 (0.98;1.19)	Ns
Chair rise (sec)	16.69 (14.72;19.37)	15.54 (13.43;17.09)	Ns
	Liver functions		
Bilirubin (mg/dL)	0.19 (0.16;0.24)	0.18 (0.15;0.27)	Ns
Albumin (g/dL)	4.4 (4.4;4.6)	4.6 (4.4;4.8)	p = 0.015
Total protein (g/dL)	7.3 (7.2;7.5)	7.6 (7.4-7.7)	Ns
Prothrombin time (INR)	0.92 (0.88;0.96)	0.94 (0.89;0.98)	Ns
AST (U/L)	22 (20;26)	22 (19;28)	Ns
ALT (U/L)	21 (20;33)	26 (18;34)	Ns
GGT(U/L)	32 (24;52)	31 (22;55)	Ns
CRP (mg/dL)	2.0 (1.0;3.9)	4.2 (3.2;9.0)	Ns

Hematocrit (%)	40.2 (38.5;41.2)	42.8 (38.3;44.7)	Ns
Creatinine (mg/dL)	0.81 (0.77;0.93)	0.97 (0.81;1.01)	Ns
Urea	29.5 (25.0;33.0)	33.0 (31.0;35.0)	Ns
Gut permeability, bacterial translocation, and inflammation			
Zonulin (ng/mL)	62.8 (47.5;96.2)	50.0 (33.5;133.7)	Ns
DAO (U/ml)	18.74 (16.93;21.59)	13.45 (7.78;21.60)	Ns
Calprotectin (µg/g)	30.2 (19.2;57.1)	27.5 (17.0;57.1)	Ns
LBP (µgml)	16.04 (15.29;19.53)	18.58 (16.08;21.16)	Ns
CD14 (µgml)	1.66 (1.54;1.85)	1.65 (1.56;1.87)	Ns
Muscle biomarkers			
Myostatin (ng/ml)	38.59 (36.91;40;82)	44.25 (36.21;50.08)	Ns
Irisin (µg/ml)	2.58 (2.08;3.49)	2.24 (1.85;2.98)	Ns
FGF21 (ng/ml)	0.33 (0.25;0.42)	0.26 (0.19;0.43)	Ns
IGF-1 (ng/ml)	138.49 (126.64;167.24)	116.43 (101.44;165.61)	Ns

1Note: The data shown are absolute numbers and percentages, or median and 95% confidence interval (lower; upper). P<0.05 values were obtained from the student's t-test or Mann-Whitney U test.

Abbreviations: MELD, model of end-stage liver disease; INR, international normalized ratios; AST, aspartate aminotransferase; ALT, alanine aminotransferase; GGT, gamma-glutamyl-transferase; CRP, C-reactive protein; DAO, diamino-oxidase; LBP, lipopolysaccharide; sCD14, soluble CD14; FGF-21, fibroblast growth factor 21; IGF-1, insulin-like growth factor 1.

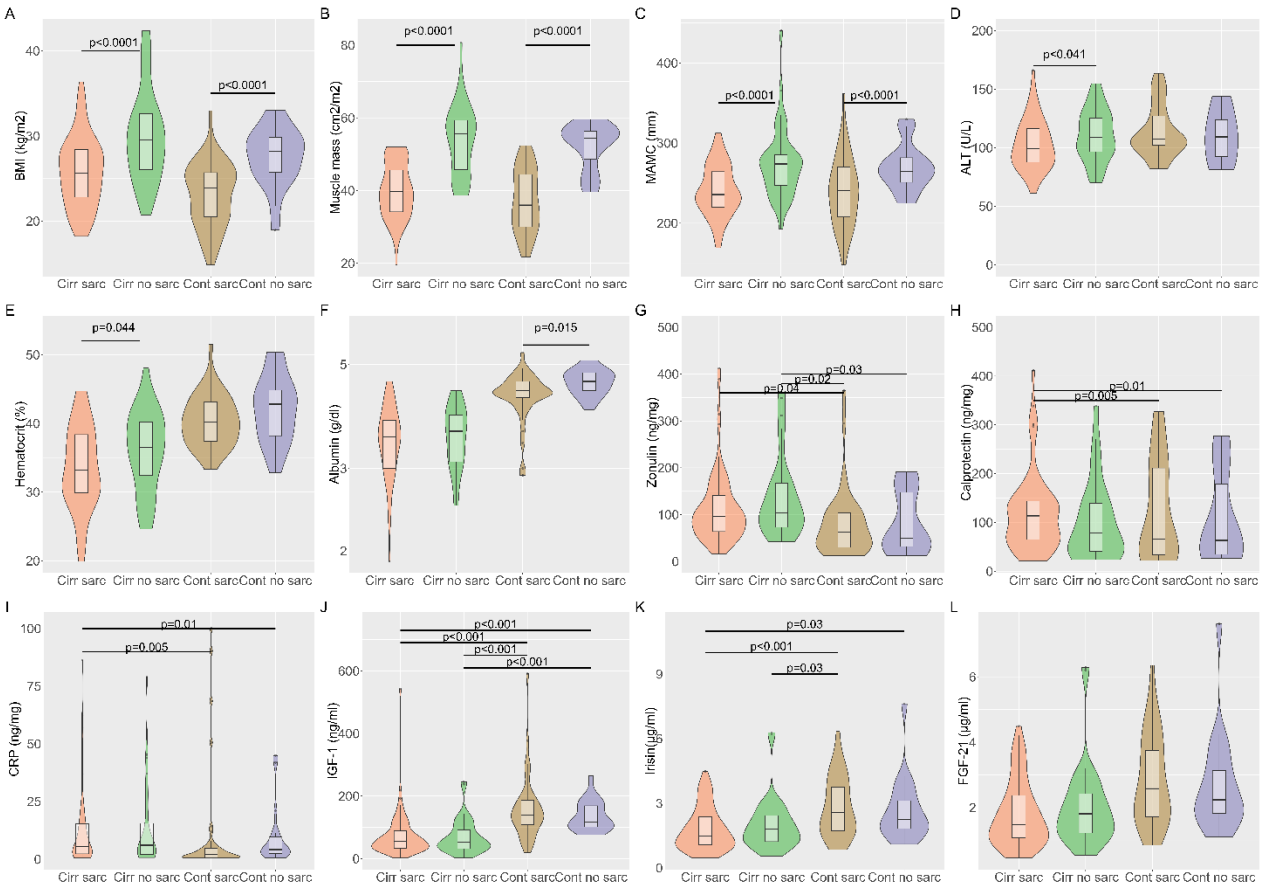

Figure 7. Differences in anthropometric measurements and muscle mass biomarkers (A and B-C, respectively) among cirrhotic patients with and without sarcopenia and controls with and without sarcopenia. Differences in laboratory parameters (D-F) between cirrhotic patients with and without sarcopenia.

Altered gut microbiome composition in sarcopenia in cirrhosis and controls

Stool 16s rRNA gene sequencing was conducted to investigate changes in the taxonomic composition of the gut microbiome composition between cirrhotic patients with and without sarcopenia, as well as between non-cirrhotic controls with and without sarcopenia. According to our findings, cirrhotic patients with and without sarcopenia had comparable alpha diversity (Chao1 index) and beta diversity (PCoA) ($p > 0.05$, Fig. 8 A-B). However, LEfSe showed that some bacterial taxa were connected to sarcopenia in patients with cirrhosis. Notably, cirrhotic patients who had sarcopenia were associated with *Bacteroides fragilis, Blautia marseille, Sutterella* spp., and *Veillonella parvula*. At the same time, cirrhotic patients with sarcopenia were associated with *Bacteroides ovatus* (Fig. 8 C). Furthermore, *Bacteroides ovatus* was significantly more abundant

in cirrhotic patients without sarcopenia than in cirrhotic patients with sarcopenia, according to ANCOM analysis (Fig. 8 D).

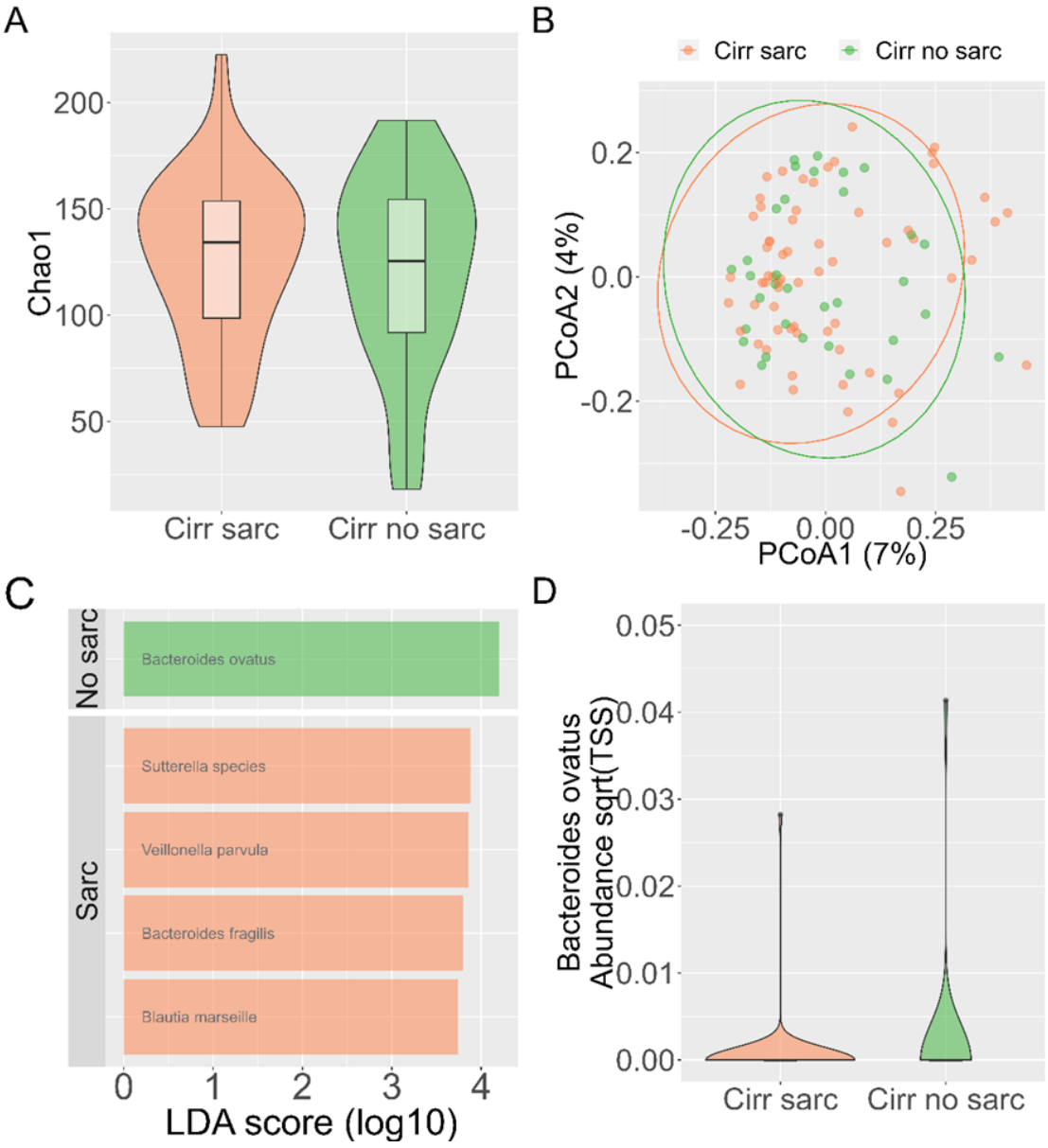

Figure 8. Figure 8. In the comparison of cirrhotic patients with and without sarcopenia, we utilized several analyses: (A) We employed the Chao1 index as a measure of alpha diversity. (B) The Bray-Curtis measure was used to determine beta-diversity. (C) To identify the bacterial species associated with cirrhotic patients with and without sarcopenia, we applied the Regularized Logistic Least Absolute Shrinkage and Selection Operator (LEfSe) method. (D) Notably, cirrhotic patients with and without sarcopenia showed differences in the abundance of *Bacteroides ovatus*.. This figure has been adapted from (1).

Furthermore, non-cirrhotic controls with sarcopenia showed significantly reduced alpha and beta diversity compared to non-cirrhotic controls without sarcopenia (Chao1, p = 0.03 and PCoA,

respectively, Fig 9 A-B). Furthermore, LEfSe analysis showed that *Alistipes putredinis*, *Alistipes onderdonkii* subspp *vulgaris*, *Ruminococcaceae*, *Bacteroides coccae*, and *Eubacterium coprostanoligenes* were associated with non-cirrhotic controls without sarcopenia, and ANCOM confirmed *Alistipes putredinis* to be significantly more abundant in non-cirrhotic controls without sarcopenia compared to non-cirrhotic controls with sarcopenia. These findings suggest that sarcopenia may have different impacts on the gut microbiome of cirrhotic and non-cirrhotic patients. However, cirrhotic patients with sarcopenia showed significantly reduced beta diversity but not alpha diversity when compared to cirrhotic patients without sarcopenia and controls with and without sarcopenia (p = 0.001). LEfSe showed that *Veillonella parvula* was associated with cirrhotic patients with sarcopenia, while *Alistipes putredinis* and *Eubacterium coprostanoligenes* were associated with non-cirrhotic control without sarcopenia. ANCOM further confirmed that *Veillonella parvula* is significantly more abundant in cirrhotic patients with sarcopenia than in cirrhotic patients without sarcopenia and controls with and without sarcopenia.

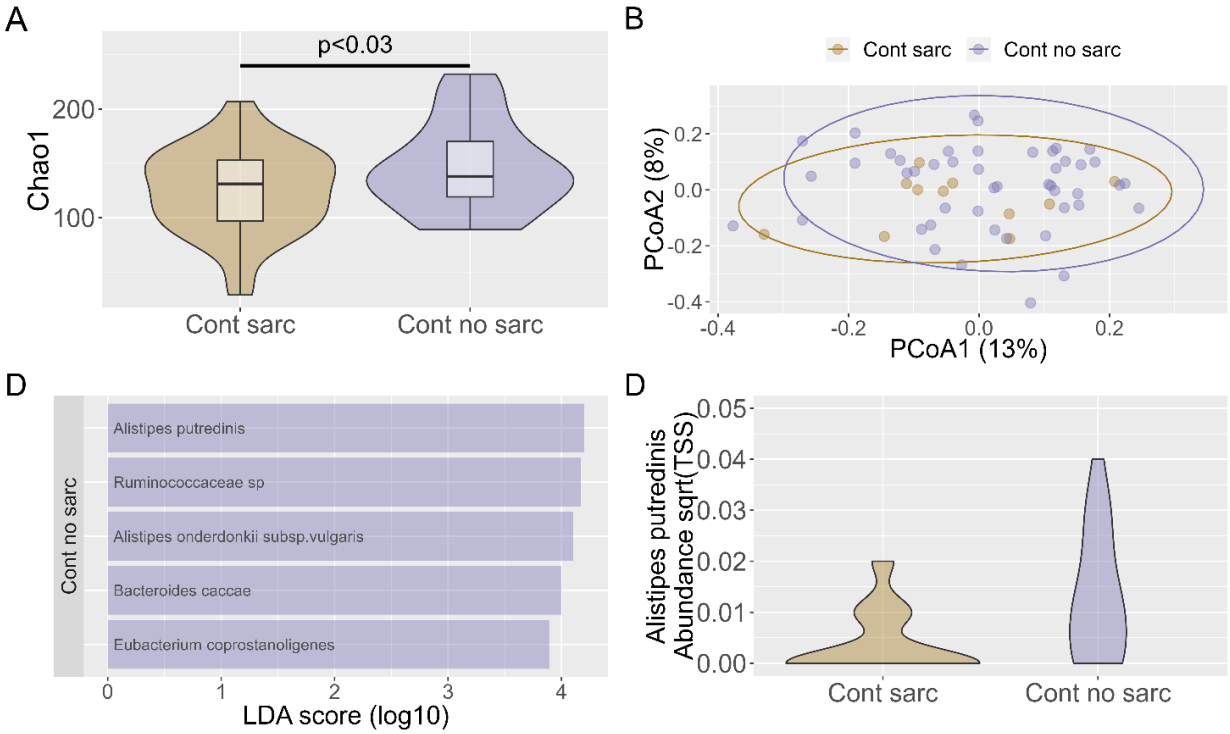

Figure 9. (A) Alpha diversity, represented by the Chao1 index, was assessed to compare patients with and without sarcopenia. (B) We used the Bray-Curtis measure to evaluate beta-diversity among non-cirrhotic patients with and without sarcopenia. (C) To identify specific bacterial species associated with non-cirrhotic patients in these two groups, we applied the Regularized Logistic Least Absolute Shrinkage and Selection Operator (LEfSe) method. (D) Notably, changes in the abundance of *Alistipes putredinis* were observed between non-cirrhotic patients with and without sarcopenia.

There were no sex-specific differences in alpha and beta diversity. The LEfSe results showed that *Bacteroides fragilis* was associated with male cirrhotic patients with sarcopenia, whereas *Bacteroides ovatus* was associated with male cirrhotic patients without sarcopenia. Additionally, ANCOM analysis showed that male cirrhotic patients with sarcopenia had significantly more abundant *Bacteroides ovatus* than those without. *Veillonella parvula* was associated with female cirrhotic patients with sarcopenia. Even after controlling for drug use, multivariate regression analysis revealed that *Bacteroides ovatus* continued to be independently associated with sarcopenia in male cirrhotic patients. These findings suggest that whereas sex may have an impact on taxonomic composition, it had no effect on alpha or beta diversity.

To be able to explore the changes in the gut microbiome associated with functional and metabolic alterations in different study populations, including cirrhotic patients with and without sarcopenia and non-cirrhotic controls with and without sarcopenia, we performed a functional prediction analysis. We identified significant differences in the functional profiles between these groups using Tax4Fun (Fig. 10). The functional profiles in cirrhotic patients with sarcopenia were predominantly associated with the hypermetabolic pathways, transporter systems, and bacterial LPS O-antigen production pathway. We specifically noticed alterations in the pathways 4-carboxymuconolactone decarboxylase, undecaprenyl-phosphate galactose phosphotransferase, pyruvate decarboxylase subunit B, and aminobezoyl-glutamate utilization protein A. On the other hand, cirrhotic individuals without sarcopenia displayed an association with the functional profile of the 3-oxoacyl-[acyl-carrier-protein] synthase involved in fatty acid production.

Similarly, non-cirrhotic controls with sarcopenia demonstrated functional profiles associated with DNA transpose mechanisms (Transposase) and transporters (permease protein of the iron complex transport systems). In contrast, functional profiles related to metabolism, processing of genetic information, and cell division were associated with non-cirrhotic controls without sarcopenia (alpha-arabinofuranosidase, rhamnogalacturonyl hydrolase, phosphoserine phosphatase, phenylacetate-CoA ligase, fructokinase). Overall, these findings indicate that sarcopenia is associated with decreased fatty acid biosynthesis, changes in genetic information processing, and changed cell division pathways, regardless of the existence of cirrhosis. The examination of gut microbiome functional profiles of each sex individually failed to identify any significant characteristic associated with sarcopenia in cirrhosis or the control group.

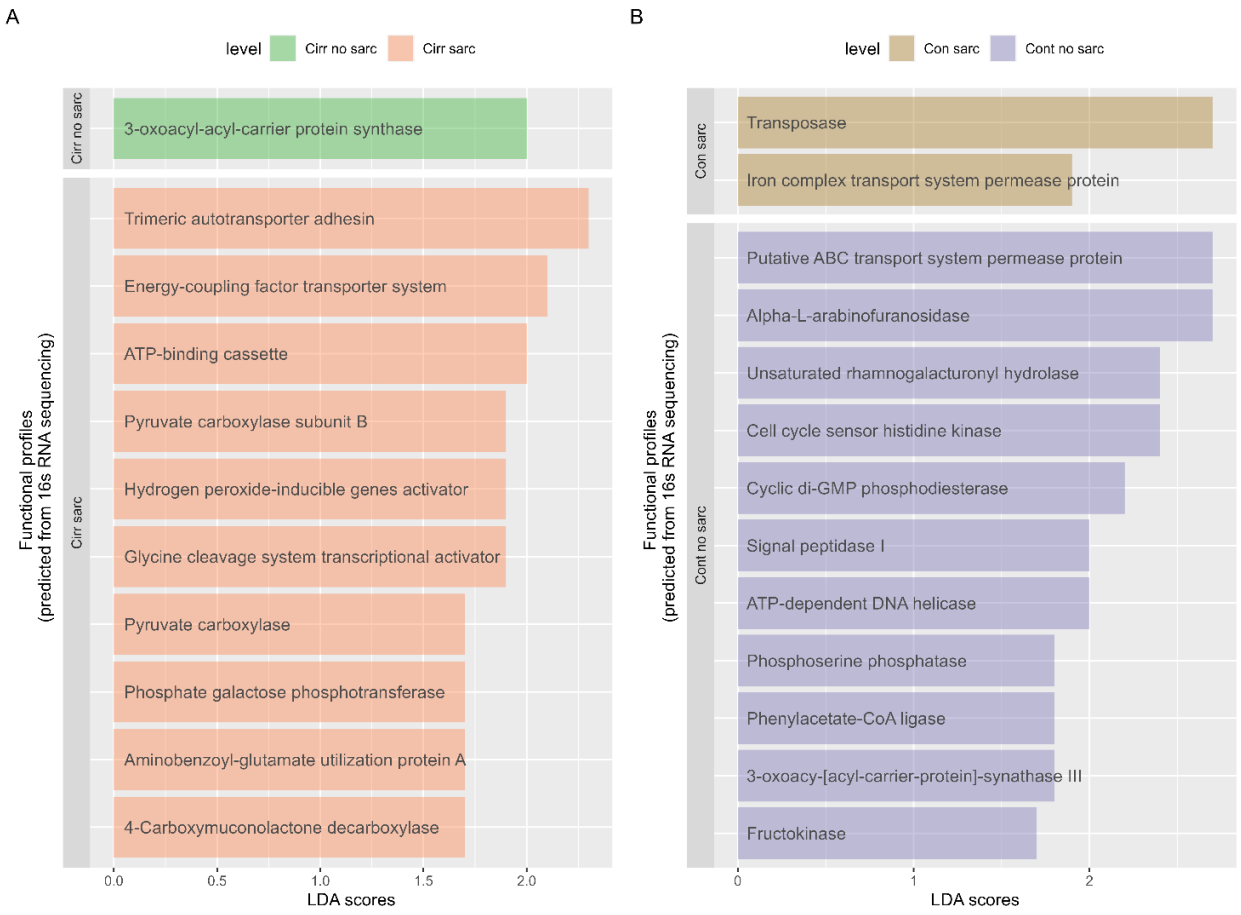

Figure 10. We compared the predicted functional profiles of two groups: cirrhotic patients with and without sarcopenia (A) and controls with and without sarcopenia (B) using the Tax4Fun method. This figure has been adapted from (1).

To further understand whether changes in the gut microbiome could be used to predict sarcopenia in cirrhosis, we conducted a multivariate logistic regression. A multivariate logistic regression model was used to predict sarcopenia, including *Bacteroides ovatus*, MELD, and PPI as independent variables, using the formula (sarcopenia ~ *Bacteroides ovatus* + MELD + PPI). The severity of liver disease and PPI use can influence the gut microbiome composition; hence, this model controls them. The model's intercept, corresponding to *Bacteroides ovatus* = 0, MELD = 0, and PPI, was at 1.19 (95% CI (-0.08, 2.49)). In this model, the effect of *Bacteroides ovatus* was statistically significant and negative, with a beta of -1.51 (95% CI (-3.08, -0.45), p = 0.019; Std. beta = -2.09, 95% CI (-4.27, -0.63)). Conversely, the effect of MELD was not statistically significant and negative (beta = -7.30e-03, 95% CI (-0.10, 0.09), p = 0.873; Std. beta = -0.04, 95% CI (-0.48, 0.43)). Similarly, the effect of PPI was not statistically significant and negative, with a beta of -0.38 (95% CI (-1.32, 0.53), p = 0.420; Std. beta = -0.38, 95% CI (-1.32, 0.53)). The results for

other ASV are summarized in the table (Table 9). These findings suggest that *Bacteroides ovatus* is an independent predictor for sarcopenia in liver cirrhosis even after controlling for the severity of liver disease and drug use, with a lower abundance of *Bacteroides ovatus* being associated with an increased risk of sarcopenia. These results suggest that *Bacteroides ovatus* could predict sarcopenia in liver cirrhosis.

Table 9. Models for predicting sarcopenia in liver cirrhosis adjusted for the severity of liver disease and drug use. All values were reported as coefficients and odds ratios (95% CI).

Predictors	Coefficients	Odds ratios (95% CI)	Adjusted P-values
		Model 1	
Bacteroides ovatus	-1.510	12.76 (168.14;2.18)	p = 0.01
MELD	-0.02	1.00 (1.00;0.99)	Ns
PPI	-0.47	0.63 (0.24;1.61)	Ns
β-blocker	0.21	1.24 (0.47;0.32)	Ns
Diuretics	0.77	2.17 (0.87;5.60)	Ns
		Model 2	
Bacteroides fragilis	0.50	28 (1.01;1.92)	Ns
MELD	0.01	1.00 (0.99;1.01)	Ns
PPI	-0.10	0.90 (0.37;2.20)	Ns
β-blocker	0.20	1.22 (0.49;3.04)	Ns
Diuretics	0.76	2.14 (0.87;5.34)	Ns
		Model 3	
Blautia marseille	3.27	43.00 (3.25;420)	Ns
MELD	0.01	1.00 (0.99;1.01	Ns
PPI	-0.02	0.98 (0.40;2.40)	Ns
β-blocker	0.2 3	1.25 (0.50;3.13)	Ns
Diuretics	0.55	0.73 (0.70;4.33)	Ns
		Model 4	
Sutterella	1.11	3.42 (1.12;97.4)	Ns
MELD	0.02	1.00 (0.99;1.02)	Ns
PPI	-0.19	0.83 (0.33; 2.04)	Ns
β-blocker	0.15	1.17 (0.46;2.94)	Ns
Diuretics	0.67	1.95 (0.80;4.87)	Ns
		Model 5	

Veillonella parvula	0.14	1.18 (0.85;1.90)	Ns
MELD	0.01	1.00 (0.99;1.01)	Ns
PPI	-0.15	0.86 (0.34;2.12)	Ns
β-blocker	0.19	1.21 (0.49;3.00)	Ns
Diuretics	0.68	1.98 (0.82;4.88)	Ns

*p-values obtained by multivariate logistic regression and adjusted for drug use.

Changes in the composition of bile acids, bile acids gene abundances between cirrhotic patients with and without sarcopenia as well as non-cirrhotic controls with and without sarcopenia

In order to examine the composition of BA in cirrhotic patients with and without sarcopenia as well as non-cirrhotic controls with and without sarcopenia, the amounts of BA in serum and stool were determined using high-performance liquid chromatography-tandem mass spectrometry (HPLC-MS/MS). Additionally, qPCR was used to quantify the abundances of BAs genes in stools.

As compared to cirrhotic patients without sarcopenia, cirrhotic patients with sarcopenia had significantly higher levels of secondary bile acids (total DCA, p = 0.04, total LCA, p = 0.03, DCA, p = 0.01, and LCA, p = 0.02) and stool total LCA (p = 0.02). In contrast, cirrhotic patients with sarcopenia had significantly lower stool CA (p = 0.02, Table 11 and Fig. 11 C) and, as a result, an elevated stool ratio of cholic acid to chenodeoxycholic acid (CA: CDCA), indicating that bile acid synthesis may have shifted from the classical to the alternative pathway (p = 0.03, Table 11 and Fig. 11 D). Additionally, the ratios of serum deoxycholic acid to cholic acid (DCA: CA, p = 0.04), serum lithocholic acid to chenodeoxycholic acid (LCA: CDCA, p = 0.03), stool deoxycholic acid to cholic acid (DCA: CA, p = 0.01), and stool lithocholic acid to chenodeoxycholic acid (LCA: CDCA, p = 0.04) were significantly elevated in cirrhotic patients with sarcopenia compared to cirrhotic patients without sarcopenia (Table 10 and Table 11 and Fig 11 E-H), suggesting a potential change in the gut microbiome taxonomic composition marked by an increase in the abundance of 7α-dehydroxylase producing bacteria.

The ratio of serum total ursodeoxycholic acid to total secondary bile acids (T-UDCA: total-sec-BAs), which serves as an indicator of the hydrophilicity status of the BAs pool, was significantly reduced in cirrhotic patients with sarcopenia compared to cirrhotic patients without sarcopenia (p = 0.03, Table 10, and Fig. 11 I). Furthermore, when compared to cirrhotic patients without sarcopenia, cirrhotic patients with sarcopenia demonstrated a significantly higher serum ratio of 12 hydroxylated to non-12 hydroxylated bile acids (12 OH (CA and DCA): non-12 OH BAs (CDCA

and LCA), p = 0.049, Table 10 and Fig. 11 J), which suggests increased 12 hydroxylated bile acid metabolisms as demonstrated by increased CA and DCA. When compared to controls without sarcopenia, the stool ratio of 12 OH: non-12 OH BAs was significantly reduced (p = 0.01, Table 11).

Contrary to what we expected, secondary BAs conjugation as measured by the ratios of taurolithocholic acid to lithocholic acid (TLCA: LCA), glycodeoxycholic acid to lithocholic acid (GDCA: DCA), and glycolithocholic acid to lithocholic acid (GLCA: LCA) in serum and stool were comparable between cirrhotic patients with and without sarcopenia (p > 0.05, Table 10).. However, cirrhotic patients with sarcopenia had a significantly elevated ratio of GDCA: DCA and TDCA: DCA in serum compared to non-cirrhotic controls with and without sarcopenia (p < 0.001). Furthermore, GDCA, GDCA: DCA, and GLCA: LCA in serum as an indicator of increased glycine conjugation were significantly elevated in non-cirrhotic controls with sarcopenia compared to non-cirrhotic controls without sarcopenia (p = 0.04 p=0.03, p= 0.02, and, respectively, Table 12). These findings demonstrate that although there were no alterations in taurine or glycine conjugation in cirrhotic patients with and without sarcopenia, in non-cirrhotic controls with sarcopenia, there was increased glycine conjugation of secondary bile acids. However, total DCA, total LCA, DCA, LCA, DCA: CA, LCA: CDCA, 12 α-OH: non-12 α-OH BAs, and T-UDCA: total-sec-BAs in serum and stool were comparable between non-cirrhotic controls with and without sarcopenia (p > 0.05, Table 12 and Table 13). These results indicate that the observed changes in BAs profile are features linked to sarcopenia in liver cirrhosis.

We identified significantly elevated levels of serum DCA, LCA, and LCA:CDCA in male cirrhotic patients with sarcopenia compared to those without sarcopenia (p = 0.04, p = 0.03, and p = 0.02, respectively) when we looked at male and female patients separately. Serum DCA, LCA, and LCA:CDCA levels were comparable between female cirrhotic patients with and without sarcopenia (p > 0.05). Notably, when we separately examined male and female cirrhotic patients, we observed that total DCA, total LCA in serum, stool LCA, stool CA: CDCA, serum DCA: CA, serum LCA, stool DCA: CA, stool LCA: CDCA, T-UDCA: total-sec-BAs, and 12 OH: non-12 OH BAs were comparable between those with and without sarcopenia. . The same pattern emerged when we compared these BAs profiles in control groups with and without sarcopenia in both sexes (p > 0.05). These results indicate that DCA, LCA, and LCA: CDCA are features of sarcopenia in males with cirrhosis, but this association is not observed in female cirrhotic patients. However, the small sample size of female cirrhotic patients may have contributed to these results. Even after adjusting for sex and MELD scores, our multivariate regression analysis showed that T-

UDCA: total-sec-BAs, 12 OH: non-12 OH BAs, and GLCA: CDCA levels in serum, along with Stool CA: CDCA, continued to be independently associated with sarcopenia in cirrhosis (p = 0.04, p = 0.03, p = 0.03, and p = 0.04, Table 4). The relevance of T-UDCA: total-sec-BAs, 12OH: non-12OH BAs, GLCA: CDCA in blood, and Stool CA: CDCA as predictors of sarcopenia in cirrhosis is demonstrated by these findings, independent of sex.

To assess the potential of the gut microbiome to transform bile acids, we measured the gene abundance of BAs transforming genes, BSH, BaiCD and E, 3 α-HSDH, 3 β-HSDH, 5-alpha reductase, 7α-HSDH), and 12-HSDH. Although we observed changes in the serum and stool BAs composition, there were no significant changes in the abundances of the BAs genes (BSH, BaiCDE, 3α-HSDH, 3 β-HSDH, 7α-HSDH, and 12-HSDH) between cirrhotic patients with and without sarcopenia (p >0.05, Table 14). However, non-cirrhotic controls with sarcopenia showed significantly elevated 7α-HSDH compared to non-cirrhotic controls without sarcopenia (p = 0.04, Table 15). This result indicates that 7α-HSDH producing bacteria may be more abundant in non-cirrhotic controls with sarcopenia.

Table 10. Serum BAs and BAs ratios concentration between cirrhotic patients with and without sarcopenia. All values are reported as median (95% CI). The table has been reproduced from (1).

Bile Acids profiles	**Cirrhosis sarcopenia (n=78)**	**Cirrhosis no sarcopenia (n=38)**	**Adjusted P-values**
Total UDCA (µmol/l)	0.39 (0.27;0.63)	0.68 (0.30;2.31)	Ns
GUDCA (µmol/l)	0.28 (0.17;0.40)	0.39 (0.15;1.15)	Ns
TUDCA (µmol/l)	0.05 (0.01;0.08)	0.12 (0.01;0.47)	Ns
UDCA (µmol/l)	0.09 (0.06;0.14)	0.14 (0.11;0.17)	Ns
Total DCA (µmol/l)	1.58 (1.19;2.45)	1.01 (0.45;1.74)	p = 0.04
GDCA (µmol/l)	0.81 (0.59;1.15)	0.42 (0.14;0.95)	Ns
TDCA (µmol/l)	0.33 (0.18;0.59)	0.20 (0.05;0.49)	Ns
DCA (µmol/l)	0.27 (0.21;0.40)	0.07 (0.04;0.27)	p = 0.01
Total LCA (µmol/l)	0.14 (0.10;0.19)	0.06 (0.03;0.09)	p = 0.03
GLCA (µmol/l)	0.02 (0.01;0.04)	0.00 (0.00;0.00)	Ns
TLCA (µmol/l)	0.00 (0.00;0.00)	0.00 (0.00;0.00)	Ns
LCA	0.09 (0.06;0.10)	0.04 (0.03;0.06)	p = 0.02
Total CA(µmol/l)	7.89 (4.98;15.22)	8.86 (5.48;12.42)	Ns
GCA (µmol/l)	4.48 (2.70;6.63)	3.65 (2.79;7.66)	Ns

TCA (µmol/l)	2.25 (1.19;4.51)	2.06 (0.92;4.93)	Ns
CA (µmol/l)	0.29 (0.24;0.38)	0.32 (0.26;0.53)	Ns
Total CDCA	15.88 (9.84;24.51)	21.13 (9.04;32.61)	Ns
TCDCA (µmol/l)	3.34 (2.29;9.14)	7.97 (1.64;13.49)	Ns
GCDCA (µmol/l)	8.30 (6.24;14.16)	11.68 (5.33;16.97)	Ns
CDCA (µmol/l)	0.34 (0.24;0.50)	0.40 (0.26;0.57)	Ns
Shift from the classical to the alternative pathway			
CA: CDCA	1.28 (0.96;1.88)	0.94 (0.70;1.34)	Ns
Gut microbial modification			
DCA: CA	0.73 (0.34;1.38)	0.14 (0.6;0.84)	p = 0.04
LCA: CDCA	0.25 (0.13;0.46)	0.09 (0.04;0.13)	p = 0.03
UDCA: CDCA	0.26 (0.16;0.34)	0.33 (0.14;0.62)	Ns
Conjugation of bile acids			
TDCA: DCA	1.17 (0.53;2.17)	1.09 (0.25;2.67)	Ns
GDCA: DCA	2.52 (1.82;3.91)	3.04 (1.86;4.04)	Ns
GLCA: LCA	0.17 (0.08;0.36)	0.00 (0.00;0.00)	Ns
TLCA: LCA	0.00 (0.00;0.00)	0.00 (0.00;0.00)	Ns
Other bile acids			
T-UDCA: total-Sec BAs	0.19 (0.14;0.26)	0.35 (0.24;0.65)	p = 0.03
12α-OH: non 12α-OH Bas	0.72 (0.64;0,85)	0.62 (0.38;0.73)	p = 0.04
GLCA: CDCA	0.05 (0.00;0.14)	0.00 (0.00;0.00)	p = 0.014
GDCA: CA	2.27 (1.39;4.03)	0.91 (0.50;2.22)	Ns
TDCA: CA	0.75 (0.40;1.42)	0.34 (0.17;2.04)	Ns
TLCA: CDCA	0.00 (0.00;0.01)	0.00(0.00;0.01)	Ns

2Note: The data shown are absolute numbers and percentages, or median and 95% confidence interval (lower; upper). P<0.05 values were obtained from the student's t-test or Mann-Whitney U test.

Abbreviations: UDCA, ursodeoxycholic acid; TUDCA, tauroursodeoxycholic acid; GUDCA, glycodeoxycholic acid; DCA, deoxycholic acid; GDCA, glycodeoxycholic acid; TDCA, taurodeoxycholic acid; LCA, lithocholic acid; GLCA, glycolithocholic acid; TLCA, taurolithocholic acid; CA, cholic acid; TCA, taurocholic acid; GCA, glycocholic acid; CDCA, chenodeoxycholic acid; TCDCA, taurochenodeoxycholic acid; GCDCA, glycochenodeoxycholic acid; CA: CDCA, cholic acid to chenodeoxycholic acid; DCA: CA, deoxycholic acid to cholic acid; LCA: CDCA, lithocholic acid to chenodeoxycholic acid; UDCA: CDCA, ursodeoxycholic acid to chenodeoxycholic acid; TDCA: DCA, taurodeoxycholic acid to deoxycholic acid; GDCA: DCA; glycodeoxycholic acid to deoxycholic acid; TLCA: LCA, taurolithocholic acid to lithocholic acid; GLCA: LCA, glycolithocholic acid to lithocholic acid; 12-α OH Bas: non 12-α-OH Bas, 12 alpha-

hydroxylated to non-12 alpha-hydroxylated BAs; T-UDCA: total-sec Bas, total ursodeoxycholic acid to total secondary BAs.

Table 11. Stool BAs and BAs ratios concentration between cirrhotic patients with and without sarcopenia. All values are reported as median (95% CI.) The table has been reproduced from (1).

Bile Acids profiles	Cirrhosis sarcopenia (n=78)	Cirrhosis no Sarcopenia (n=38)	Adjusted P-values
Total UDCA (µmol/l)	18.41 (15.06;30.80)	27.28 (14.90;74.60)	Ns
GUDCA (µmol/l)	2.35 (1.80;3.00)	1.65 (1.30;3.50)	Ns
TUDCA (µmol/l)	0.81 (0.70;1.41)	1.00 (0.80;1.37)	Ns
UDCA (µmol/l)	13.96 (10.10;23.00)	15.80 (11.41;56.90)	Ns
Total DCA (µmol/l)	650.10 (418.30;946.10)	364 (133.40;691.60)	Ns
GDCA (µmol/l)	9.05 (6.90;11.70)	4.00 (1.70;13.10)	Ns
TDCA (µmol/l)	3.40 (2.40;5.50)	1.400 (0.90;7.24)	Ns
DCA (µmol/l)	628.58 (402.80;931.90)	323.70 (122.10;684.80)	Ns
Total LCA (µmol/l)	1221.20 (646.60;1461.00)	430.91 (88.10;1095.00)	p = 0.01
GLCA (µmol/l)	0.90 (0.70;1.10)	0.87 (0.70;1.80)	Ns
TLCA (µmol/l)	0.70 (0.50;1.00)	0.52 (0.23;0.61)	Ns
LCA	838.05 (493.10;1217.60)	427.80 (103.90;903.39)	Ns
Total CA (µmol/l)	80.65 (59.00;97.00)	121.47 (82.20;250.75)	Ns
GCA (µmol/l)	10.30 (8.58;17.50)	10.60 (5.50;27,20)	Ns
TCA (µmol/l)	8.20 (6.00;14.40)	8.00 (5.00;12.70)	Ns
CA (µmol/l)	50.25 (34.30;62.00)	98.30 (64.70;148.30)	p = 0.02
Total CDCA (µmol/l)	118.65 (78.70;138.70)	123.19 (80.30;240.29)	Ns
GCDCA (µmol/l)	33.25 (22.10;52.70)	26.30 (21.31;47.70)	Ns
TCDCA (µmol/l)	13.60 (7.80;19.70)	12.30 (8.70;19.20)	Ns
CDCA (µmol/l)	46.80 (40.30;65.20)	81.10 (50.30;124.32)	Ns
	Shift from the classical to the alternative pathway		
CA: CDCA	0.84 (0.75;1.11)	1.29 (1.04;2.09)	p = 0.028
	Gut microbiome modification		
DCA: CA	15.96 (9.35;18.13)	2.58 (0.86;13.91)	p = 0.014
LCA: CDCA	15.47 (12.67;20.93)	4.65 (1.49;21.31)	p = 0.042

UDCA: CDCA	0.31 (0.24;0.44)	0.29 (0.20;0.56)	Ns
	Conjugation of secondary bile acids		
TDCA: DCA	0.01 (0.00;0.01)	0.01 (0.01;0.01)	Ns
GDCA: DCA	0.01 (0.01;0.02)	0.01(0.01;0.03)	Ns
TLCA: LCA	0.00 (0.00;0.00)	0.00 (0.00;0.00)	Ns
GLCA: LCA	0.00 (0.00;0.00)	0.00 (0.00;0.00)	Ns
	Other bile acid modification		
T-UDCA: total-sec BAs	0.01 (0.01;0.02)	0.03 (0.01;0.06)	Ns
12α-OH: non-12α-OH Bas	0.94 (0.70;1,11)	1.05 (0.79;1.63)	Ns
GLCA: CDCA	0,02 (0.02;0.03)	0.01 (0.01;0.03)	Ns
GDCA: CA	0.20 (0.16;0.28)	0.06 (0.03;0.14)	Ns
TDCA: CA	0.08 (0.06;0.11)	0.04 (0.02;0.08)	Ns
TLCA: CDCA	0.01 (0.01;0.02)	0.01 (0.00;0.03)	Ns

3Note: The data shown are absolute numbers and percentages, or median and 95% confidence interval (lower; upper).

P<0.05 values were obtained from the student's t-test or Mann-Whitney U test.

Abbreviations: UDCA, ursodeoxycholic acid; TUDCA, tauroursodeoxycholic acid; GUDCA, glycodeoxycholic acid; DCA, deoxycholic acid; GDCA, glycodeoxycholic acid; TDCA, taurodeoxycholic acid; LCA, lithocholic acid; GLCA, glycolithocholic acid; TLCA, taurolithocholic acid; CA, cholic acid; TCA, taurocholic acid; GCA, glycocholic acid; CDCA, chenodeoxycholic acid; TCDCA, taurochenodeoxycholic acid; GCDCA, glycochenodeoxycholic acid; CA: CDCA, cholic acid to chenodeoxycholic acid; DCA: CA, deoxycholic acid to cholic acid; LCA: CDCA, lithocholic acid to chenodeoxycholic acid; UDCA: CDCA, ursodeoxycholic acid to chenodeoxycholic acid; TDCA: DCA, taurodeoxycholic acid to deoxycholic acid; GDCA: DCA; glycodeoxycholic acid to deoxycholic acid; TLCA: LCA; taurolithocholic acid to lithocholic acid; GLCA: LCA, glycolithocholic acid to lithocholic acid; T-UDCA: total-sec Bas, total ursodeoxycholic acid to total secondary BAs; 12-α OH Bas : non 12-α-OH Bas, 12 alpha-hydroxylated to non-12 alpha-hydroxylated BAs.

Table 12. Serum BAs and BAs ratios concentration between non-cirrhotic control with and without sarcopenia. All values are reported as median (95% CI). The table has been reproduced from (1).

Bile Acids profiles	**Control sarcopenia (n=39)**	**Control no sarcopenia (n=20)**	**Adjusted P-values**
Total UDCA (µmol/l)	0.14 (0.10;0.27)	0.09 (0.07;0.20)	Ns
GUDCA (µmol/l)	0.08 (0.04;0.10)	0.03 (0.02;0.06)	Ns
TUDCA (µmol/l)	0.00 (0.00;0.01)	0.00(0.00;0.01)	Ns
UDCA (µmol/l)	0.07 (0.05;0.13)	0.06 (0.04;0.10)	Ns
Total DCA (µmol/l)	0.64 (0.49;0.95)	0.45 (0.33;0.86)	Ns

GDCA (µmol/l)	0.25 (0.18;0.40)	0.13 (0.05;0.22)	p = 0.04
TDCA (µmol/l)	0.00 (0.00;0.01)	0.00 (0.00;0.01)	Ns
DCA (µmol/l)	0.35 (0.31;0.45)	0.29 (0.22;0.55)	Ns
Total LCA (µmol/l)	0.03 (0.03;0.06)	0.03 (0.02;0.05)	Ns
GLCA (µmol/l)	0.00 (0.00;0.01)	0.00 (0.00;0.01)	Ns
TLCA (µmol/l)	0.00 (0.00;0.01)	0.00 (0.00;0.01)	Ns
LCA	0.03 (0.02;0.04)	0.03 (0.02;0.05)	Ns
Total CA(µmol/l)	0.42 (0.27;0.71)	0.54 (0.32;1.06)	Ns
GCA (µmol/l)	0.17 (0.10;0.26)	0.15 (0.06;0.29)	Ns
TCA (µmol/l)	0.00 (0.00;0.03)	0.00 (0.00;0.01)	Ns
CA (µmol/l)	0.24 (0.17;0.34)	0.34 (0.21;0.74)	Ns
Total CDCA	1.05 (0.76;1.24)	1.08 (0.46;2.58)	Ns
TCDCA (µmol/l)	0.03 (0,02;0.08)	0.03 (0.01;0.08)	Ns
GCDCA (µmol/l)	0.72 (0.58;1.02)	0.63 (0.44;1.39)	Ns
CDCA (µmol/l)	0.12 (0.07;0.15)	0.27 (0.03;0.90)	Ns
Shift from the classical to the alternative pathway			
CA: CDCA	1.99 (1.07;2.32)	1.20 (0.64;1.75)	Ns
Gut microbial modification			
DCA: CA	1.26 (1.10;2.18)	1.31 (0.47;1.68)	Ns
LCA: CDCA	0.26 (0.07;0.45)	0.10 (0.01;0.31)	Ns
UDCA: CDCA	0.60 (0.35;0.97)	0.13 (0.10;0.36)	Ns
Conjugation of bile acids			
TDCA: DCA	0.00 (0.00;0.01)	0.00 (0.00;0.01)	Ns
GDCA: DCA	0.67 (0.49;0.84)	0.29 (0.11;0.76)	p = 0.03
GLCA: LCA	0.03 (0.00;0.22)	0.00 (0.00;0.00)	p = 0.02
TLCA: LCA	0.00 (0.00;0.00)	0.00 (0.00;0.00)	Ns
Other bile acids			
T-UDCA: total-Sec BAs	0.16 (0.12;0.27)	0.11 (0.08;0.19)	Ns
12α-OH: non 12α-OH Bas	0.92 (0.76;1.21)	1.13 (0.67;1.83)	Ns

2*Note*: The data shown are absolute numbers and percentages, or median and 95% confidence interval (lower; upper).

P<0.05 values were obtained from the student's t-test or Mann-Whitney U test.

Table 13. Stool BAs and BAs ratios concentration between non-cirrhotic control with and without sarcopenia. All values are reported as median (95% CI). The table has been reproduced from (1).

Bile Acids profiles	Control sarcopenia (n=39)	Control no sarcopenia (n=20)	Adjusted P-values
Total UDCA (µmol/l)	33.16 (21.90;103.50)	32.90 (20.40;336.80)	Ns
GUDCA (µmol/l)	4.45 (2.88;9.60)	3.85 (2.30;7.87)	Ns
TUDCA (µmol/l)	1.05 (0.80;1.60)	0.80 (0.70;2.90)	Ns
UDCA (µmol/l)	24.80 (17.00;70.60)	25.80 (9.49;67.60)	Ns
Total DCA (µmol/l)	1770.43 (753.30;2518.80)	1383.79 (711.80;3354.90)	Ns
GDCA (µmol/l)	22.26 (14.30;35.20)	17.15 (6.20;42.80)	Ns
TDCA (µmol/l)	4.60 (2.20;8.00)	6.26 (3.20;10.85)	Ns
DCA (µmol/l)	1693.45 (714.70;2464.60)	1367.25 (706.60;3334.70)	Ns
Total LCA (µmol/l)	1585.40 (1006.20;3126.90)	1141.80 (657.50;3885.70)	Ns
GLCA (µmol/l)	1.70 (1.31;2.90)	1.25 (0.70;1.71)	Ns
TLCA (µmol/l)	1.30 (0.96;3.60)	2.30 (1.45;4.00)	Ns
LCA	1388.63 (526.40;1940.60)	1034.39 (556.29;1816.60)	Ns
Total CA(µmol/l)	98.35 (52.70;192.00)	122.1 (42.4;218.6)	Ns
GCA (µmol/l)	11.90 (8.10;25.10)	11.91 (8.80;18.60)	Ns
TCA (µmol/l)	5.65 (4.00;8.00)	5.50 (2.86;10.20)	Ns
CA (µmol/l)	57.30 (31.40;128.76)	98.95 (27.80;162,90)	Ns
Total CDCA	173 0(131.0;197.0)	119.54 (85.20;243.40)	Ns
GCDCA (µmol/l)	57.40 (32.60;69.20)	32.25 (20.00;54.20)	Ns
TCDCA (µmol/l)	15.56 (7.80;19.60)	14.05 (6.70;18.60)	Ns
CDCA (µmol/l)	90.30 (65.13;109.90)	60.15 (25.20;193.80)	Ns
Shift from the classical to the alternative pathway			
CA: CDCA	0.83 (0.63;1.14)	0.70 (0.58;2.49)	Ns
Gut microbial modification			
DCA: CA	28.15 (16.00;76.20)	35.81 (8.12;70.91)	Ns
LCA: CDCA	19.60 (12.56;30.31)	17.69 (8.97;26.06)	Ns

UDCA: CDCA	0.38 (0.27;0.64)	0.26 (0.17;0.69)	Ns
	Conjugation of bile acids		
TDCA: DCA	0.00 (0.00;0.001)	0.00 (0.00;0.001)	Ns
GDCA: DCA	0.01 (0.01;0.03)	0.01 (0.01;0.02)	Ns
GLCA: LCA	0.03 (0.00;0.22)	0.00 (0.00;0.00)	Ns
TLCA: LCA	0.00 (0.00;0.00)	0.00 (0.00;0.00)	Ns
	Other bile acids		
T-UDCA: total-Sec BAs	0.01 (0.00;0.02)	0.01 (0.00;0.02)	Ns
12α-OH: non 12α-OH Bas	1.07 (0.92;1.26)	1.65 (1.24;2.13)	p = 0.01

2*Note*: The data shown are absolute numbers and percentages, or median and 95% confidence interval (lower; upper).

P<0.05, values were obtained from the student's t-test or Mann-Whitney U test.

Table 14. Bile acid gene abundance distribution between cirrhotic patients with and without groups. Median (95% CI).

Genes	Cirrhosis Sarcopenia (n=78)	Cirrhosis no sarcopenia (n=38)	Adjusted P-values
BSH	1.05 (0.38;1.65)	0.63(0.44;1.14)	Ns
3α-HSDH	0.35(0.23;0.96)	0.40(0.18;1.04)	Ns
3β-HSDH	0.30(0.22;0.41)	0.33(0.28;0.43)	N
5α-reductase	0.21(0.12;0.28)	0.24(0.15;0.41)	Ns
7α-HSDH	0.67(0.50;0.87)	0.83(0.41;1.04)	Ns
7β-HSDH	0.30(0.22;0.46)	0.39(0.20;0.57)	Ns
12α-HSDH	0.11(0.06;0.21)	0.50(0.11;1.22)	Ns
BaiCD	0.98(0.65;1.35)	0.91(0.65;1.37)	Ns
BaiE	0.20(0.12;0.28)	0.24(0.15;0.41)	Ns

P<0.05, values were obtained from the student's t-test or Mann-Whitney U test.

Table 15. Bile acid gene abundance distribution between non-cirrhotic control patients with and without groups. Median (95% CI).

Genes	Control sarcopenia (n=39)	Control no sarcopenia (n=20)	Adjusted P-values
BSH	0.71 (0.29;1.51)	0.38 (0.05;0.82)	Ns
3α-HSDH	0.34 (0.29;0.66)	0.41 (0.09;1.23)	Ns

3β-HSDH	0.57 (0.31;1.19)	0.38 (0.24;0.70)	Ns
5α-reductase	0.54 (0.36;0.81)	0.30 (0.19;1.00)	Ns
7α-HSDH	0.72 (0.53;1.08)	0.27 (0.11;0.76)	p = 0.04
7β-HSDH	0.38 (0.27;0.77)	0.50 (0.36;0.84)	Ns
12α-HSDH	0.23 (0.13;0.46)	1.37 (0.05;2.51)	Ns
BaiCD	0.99 (0.52;1.22)	0.115 (0.47;2.53)	Ns
BaiE	0.82 (0.36;1.05)	1.18 (0.33;1.93)	Ns

P<0.05, values were obtained from the student's t-test or Mann-Whitney U test.

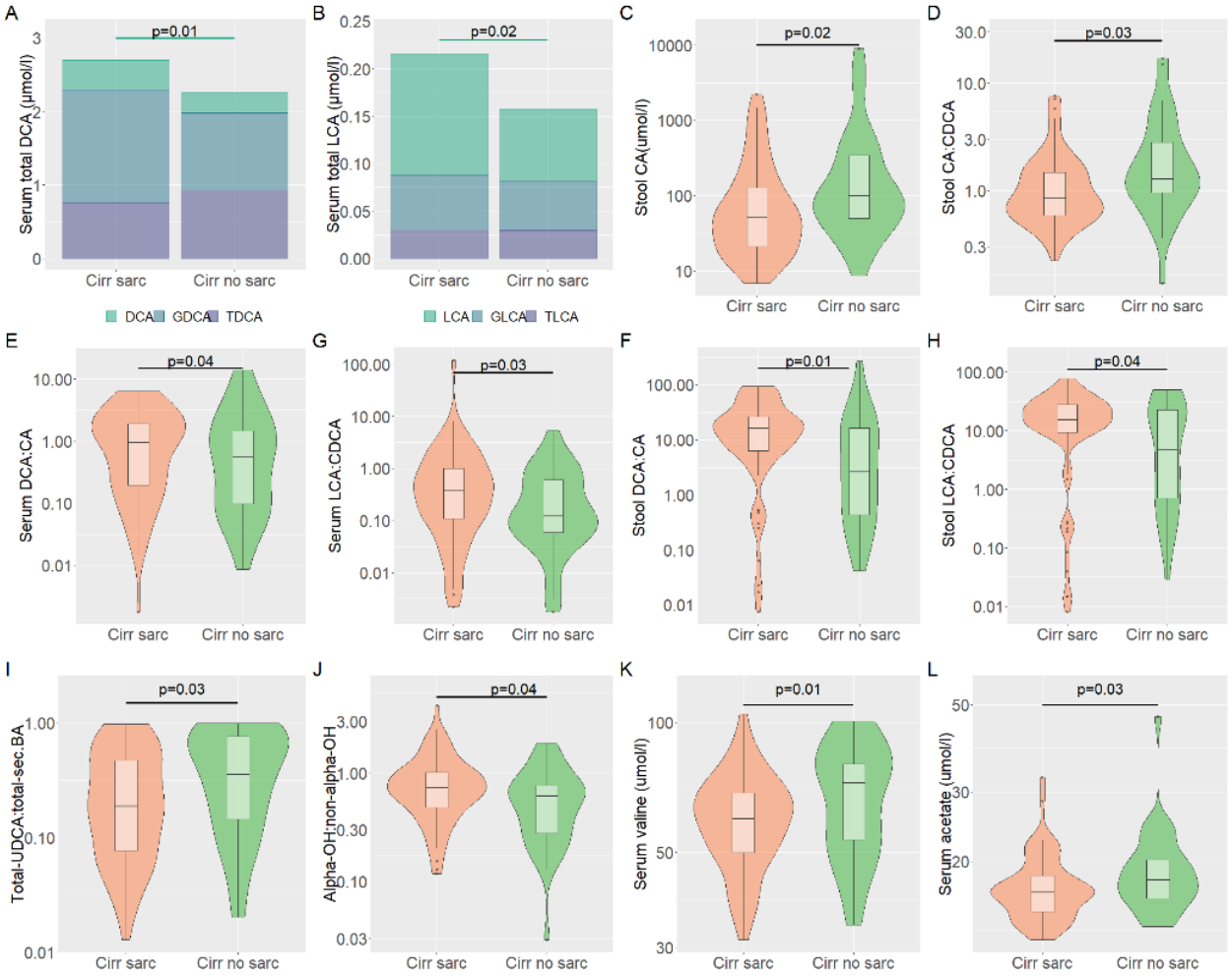

Figure 11. Differences in bile acid profiles were observed between two groups: cirrhotic patients with and without sarcopenia (A-C). There was a noticeable shift between the classical and alternative pathways in cirrhotic patients with and without sarcopenia (D). Bile acid biotransformation transitioned from primary to secondary bile acids in cirrhotic patients with and without sarcopenia (E-H). The hydrophilicity status of the bile acid pool was altered in cirrhotic patients with and without sarcopenia (I). Moreover, changes in 12-alpha-hydroxylation were observed between these two groups (J). Additionally, there were variations in the levels of valine and acetate in the serum of cirrhotic patients with and without sarcopenia (K-L). This figure has been adapted from (1).

Changes in the composition of metabolome and pathways between cirrhotic patients with and without sarcopenia as well as non-cirrhotic controls with and without sarcopenia

An explorative multivariate analysis was conducted. The serum, stool, and urine metabolites were measured using NMR spectroscopy to assess the differences in their concentration between cirrhotic patients with and without sarcopenia, as well as non-cirrhotic controls with and without sarcopenia. The resulting clusters were visualized with orthogonal projection latent structure discriminant analysis (O-PLS-DA), a supervised modeling method used for dimension reduction. The model underwent cross-validation, outliers were removed, and testing was done after 100 permutations. The O-PLS-DA analysis showed that serum, stool, and urine metabolome could distinguish between cirrhotic and control groups (Fig 12-17).

Furthermore, cirrhotic patients with sarcopenia showed significantly lower serum valine, serum acetate, and urine acetone levels than cirrhotic patients without sarcopenia ($p = 0.01$, $p = 0.03$, $p = 0.02$, respectively, refer to Table 16). On the other hand, non-cirrhotic controls with sarcopenia had significantly higher levels of serum acetone, serum ethanol, and urine acetone, as well as lower levels of phenylalanine in serum, when compared to non-cirrhotic controls without sarcopenia ($p = 0.01$, $p = 0.02$, $p = 0.03$, and $p = 0.04$, respectively, Table 17). We did not find significant changes in other serum, urine, and stool metabolites between cirrhotic patients with and without sarcopenia, as well as non-cirrhotic controls with and without sarcopenia ($p > 0.05$, Tables 16 and 17). These results suggest that altered serum valine and acetate are sarcopenia features in liver cirrhosis. In contrast, altered acetone in urine is a feature of sarcopenia, irrespective of liver cirrhosis. Furthermore, changes in ethanol and phenylalanine are sarcopenia-linked features unrelated to liver cirrhosis. When examining both sexes separately, only the valine level in the serum showed a significant difference between male cirrhotic patients with and without sarcopenia. Additionally, multivariate regression analysis revealed that the serum valine level was independently associated with sarcopenia in liver cirrhosis, even after adjusting for sex and MELD scores.

Metabolic pathways associated with sarcopenia in liver cirrhosis

As part of an exploratory analysis aimed at determining the metabolic pathways associated with sarcopenia in liver cirrhosis, Metabolites set enrichment (MSEA) and pathway analysis were conducted. The top 20 pathways with a $p < 0.05$ were considered significant (Fig 18 and Fig 19). Our results showed that ubiquinone biosynthesis, phenylalanine, tyrosine, tryptophan, and BCAAs (valine, leucine, and isoleucine) degradation were the top pathways associated with sarcopenia in cirrhosis ($p = 0.04$, $p = 0.04$, and $p = 0.03$, respectively, Table 18). Conversely, selenocompound metabolism was associated with cirrhotic patients without sarcopenia ($p = 0.05$).

Moreover, non-cirrhotic controls with sarcopenia were associated with BCAAs (valine, leucine, and isoleucine) degradation (p = 0.02, Table 19 A). In contrast, non-cirrhotic controls without sarcopenia were associated with BCAAs (valine, leucine, and isoleucine) biosynthesis (p = 0.04, Table 19 A). These findings suggest that BCAA degradation is a characteristic of sarcopenia regardless of cirrhosis. BCAA (valine, isoleucine, alanine) degradation and the selenocompound pathways stayed associated with sarcopenia in both cirrhotic and controls when both sexes were analyzed separately. These results indicate that sex did not influence the BCAAs pathway degradation.

Table 16. Serum, stool, and urine metabolite concentrations between cirrhotic patients with and without sarcopenia. All values are reported as median (95% CI). The table has been reproduced from (1).

Metabolites	**Cirrhosis sarcopenia (n=78)**	**Cirrhosis no sarcopenia (n=38)**	**Adjusted p-values**
	Serum		
Valine (µmol/l)	59.7 (57.0;65.6)	72.2 (56.0;79.3)	p = 0.01
Lactate (µmol/l)	680.3 (639.7;707.3)	687.5 (592.6;775.5)	Ns
Alanine (µmol/l)	99.2 (92.1;107.4)	108.7 (99.3;123.6)	Ns
Acetate (µmol/l)	16.7 (16.4;17.4)	17.9 (17.0;19.8)	p = 0.03
Acetone (µmol/l)	31.6 (30.7;32.8)	31.6 (31.1;33.0)	Ns
Ethanol (µmol/l)	427.9 (415.9;447.2)	427.1 (407.1;444.9)	Ns
Succinate (µmol/l)	9.1 (8.5;9.3)	9.1 (8.6;10.1)	Ns
3-HB (µmol/l)	11.4 (7.8;17.6)	11.8 (8.9;19.0)	Ns
Phenylalanine (µmol/l)	73.4 (70.4; 75.8)	77.5 (73.4;82.0)	Ns
Glucose (µmol/l)	187.9 (167.0;202.0)	185.2 (167.4;220.3)	Ns
Hippurate (µmol/l)	1.4 (1.3; 1.6)	1.5 (1.3;2.0)	Ns
Glutamine (µmol/l)	32.40 (31.10;36.00)	33.60 (30.00;38,30)	Ns
	Stool		
Valine (µmol/l)	68.5 (54.3;80.6)	68.3 (56.7;77.4)	Ns
Lactate (µmol/l)	68.1 (65.5;76.4)	64.8 (60.8;70.2)	Ns
Alanine (µmol/l)	109.8 (93.9;130.3)	113.9 (96.2;134.4)	Ns
Glycine (µmol/l)	34.3 (31.5;44.8)	32.1 (30.0;39.5)	Ns
Acetate (µmol/l)	818.4 (703.5;865.2)	764.0 (555.6;896.3)	Ns
Succinate (µmol/l)	31.0 (25.78;43.1)	29.9 (27.9;43.6)	Ns
Phenylalanine (µmol/l)	78.7 (69.3;95.8)	80.8 (71.8;90.9)	Ns

Glucose (µmol/l)	10.9 (8.5;13.1)	10.5 (8.5;14.9)	Ns
Acetone (µmol/l)	18.9 (17.7;21.8)	20.8 (17.5;23.3)	Ns
Tyrosine (µmol/l)	15.1 (13.3;17.4)	17.4 (14.2;20.2)	Ns
Isoleucine (µmol/l)	47.1 (41.0;56.4)	50.0 (44.3;57.6)	Ns
Leucine (µmol/l)	165.4 (148.9;191.8)	177.6 (149.8;210.6)	Ns
	Urine		
Lactate (µmol/l)	37.9 (33.7;43.4)	34.2 (30.8;38.4)	Ns
Alanine (µmol/l)	25.8 (24.1;27.8)	26.2 (22.2;30.9)	Ns
Acetate (µmol/l)	22.9 (21.5;27.4)	26.0 (22.9;28.0)	Ns
Acetoacetate (µmol/l)	15.8 (14.0;19.0)	16.4 (14.8;18.5)	Ns
Acetone (µmol/l)	8.1 (7.62;8.5)	8.6 (8.2;11.9)	p = 0.02
Succinate (µmol/l)	26.2 (24.7;28.0)	25.6 (23.5;28.4)	Ns
Hippurate (µmol/l)	56.4 (43.9;88.4)	59.3 (40.2;78.3)	Ns
Phenylalanine (µmol/l)	55.6 (49.0;70.1)	70.0 (55.9;90.0)	Ns
Glucose (µmol/l)	14.4 (13.7;17.0)	15.0 (13.3;20.2	Ns

P-values were obtained from the student's t-test or Mann-Whitney U test.

Table 17. Serum, stool, and urine metabolite concentrations between non-cirrhotic controls with and without sarcopenia. All values were reported as median (95% CI).

Metabolite	**Controls sarcopenia (39)**	**Control no sarcopenia (20)**	**Adjusted P-values**
	Serum		
Valine (µmol/l)	74.39 (63.02;79.48)	73.66 (69.72;98.61)	Ns
Lactate (µmol/l)	623.42 (558.80;708.13)	590.86 (542.98;1340.89)	Ns
Alanine (µmol/l)	107.28 (102.93;115.51)	111.52 (87.82;203.52)	Ns
Acetate (µmol/l)	17.24 (15.50;18.28)	16.17 (15.43;18.79)	Ns
Acetone (µmol/l)	30.19 (29.86;32.10)	26.43 (24.33;32.26)	p = 0.017
Ethanol (µmol/l)	436.65 (431.60;454.61)	388.74 (381.34;458.30)	p = 0.021
Succinate (µmol/l)	9.34 (8.82;9.69)	9.67 (8.62;12.74)	Ns
3-HB (µmol/l)	8.23 (6.56;19.28)	13.95 (9.46;28.61)	Ns

Phenylalanine (µmol/l)	66.51 (63.71;69.53)	78.42 (65.25;84.88)	p = 0.048
Glucose (µmol/l)	161.56 (154.49;165.98)	155.83 (145.10;247.11)	Ns
Hippurate (µmol/l)	1.51 (1.41;1.93)	1.44 (1.10;4.56)	Ns
Glutamine (µmol/l)	39.55 (36.90;42.50)	39.05 (36.10;42.70)	Ns
	Stool		
Valine (µmol/l)	62.84 (48.83;96.87)	51.56 (40.87;72.97)	Ns
Lactate (µmol/l)	62.52 (57.16;74.72)	68.08 (60.03;138.56)	Ns
Alanine (µmol/l)	115.29 (78.26;132.01)	98.58 (84.12;131.79)	Ns
Glycine (µmol/l)	29.62 (23.83;34.02)	29.83 (23.55;62.17)	Ns
Acetate (µmol/l)	759.95 (589.10;1189.57)	949.90 (765.76;1119.30)	Ns
Succinate (µmol/l)	27.20 (22.88;36.06)	43.56 (22.61;62.82)	Ns
Phenylalanine (µmol/l)	77.89 (70.73;90.22)	80.64 (72.39;98.42)	Ns
Glucose (µmol/l)	6.71 (5.02;10.03)	5.94 (4.42;33.96)	Ns
Acetone (µmol/l)	19.21 (15.66;25.63)	14.84 (13.62;20.92)	Ns
Tyrosine (µmol/l)	13.23 (10.79;21.32)	15.33 (10.99;21.66)	Ns
Isoleucine (µmol/l)	46.75 (34.41;63.10)	44.13 (35.92;61.23)	Ns
Leucine (µmol/l)	171.07 (135.86;238.09)	167.68 (107.52;211.13)	Ns
	Urine		
Lactate (µmol/l)	36.29 (32.00;44.50)	32.92 (30.39;49.00)	Ns
Alanine (µmol/l)	24.26 (21.82;31.42)	22.71 (22.25;43.32)	Ns
Acetate (µmol/l)	23.80 (21.94;28.87)	20.85 (20.78;24.02)	Ns
Aceto-acetate (µmol/l)	15.47 (13.26;19.89)	15.35 (14.78;17.60)	Ns
Acetone (µmol/l)	8.77 (8.04;9.51)	8.17 (8.00;8.55)	p = 0.037
Succinate (µmol/l)	27.43 (25.94;28.74)	24.71 (24.51;28.16)	Ns
Hippurate (µmol/l)	84.22 (58.63;121.31)	80.47 (57.59;228.90)	Ns

Phenylalanine (µmol/l)	63.78 (44.54;95.90)	41.14 (35.44;77.05)	Ns
Glucose (µmol/l)	13.31 (11.48;17.64)	13.28 (12.40;16.54)	Ns

*P<0.05, values were obtained from the Student's t-test or Mann-Whitney U test

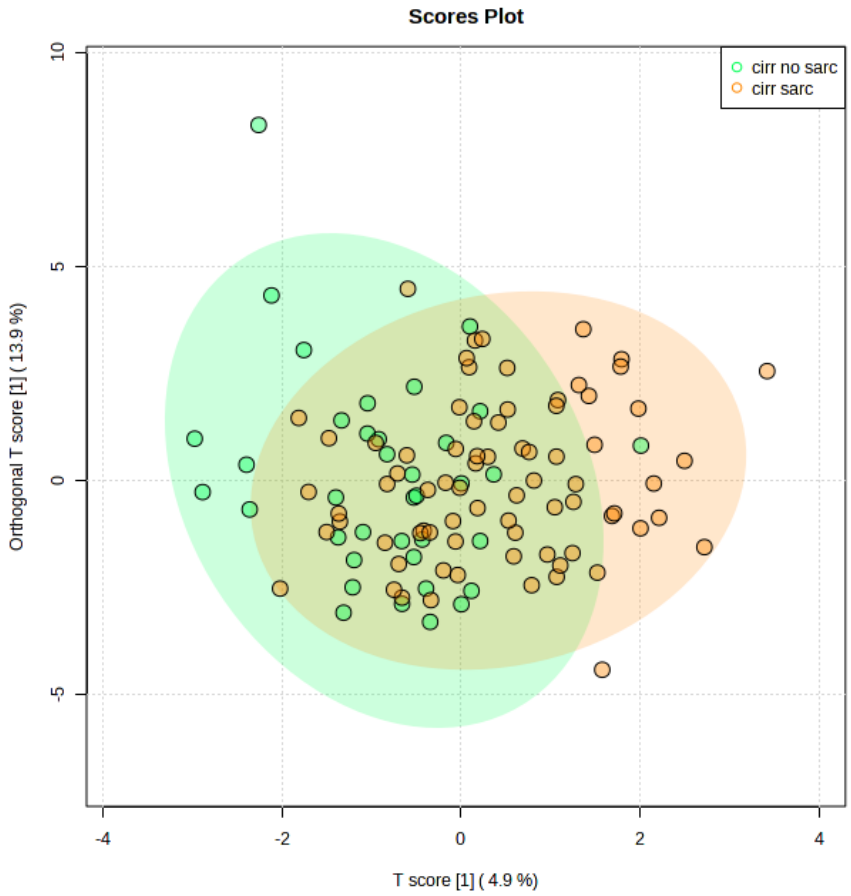

Figure 12. Grouping of cirrhotic patients, both those with and without sarcopenia, was illustrated through the utilization of a score plot derived from orthogonal-PLS-DA analysis, which considered serum metabolite patterns.

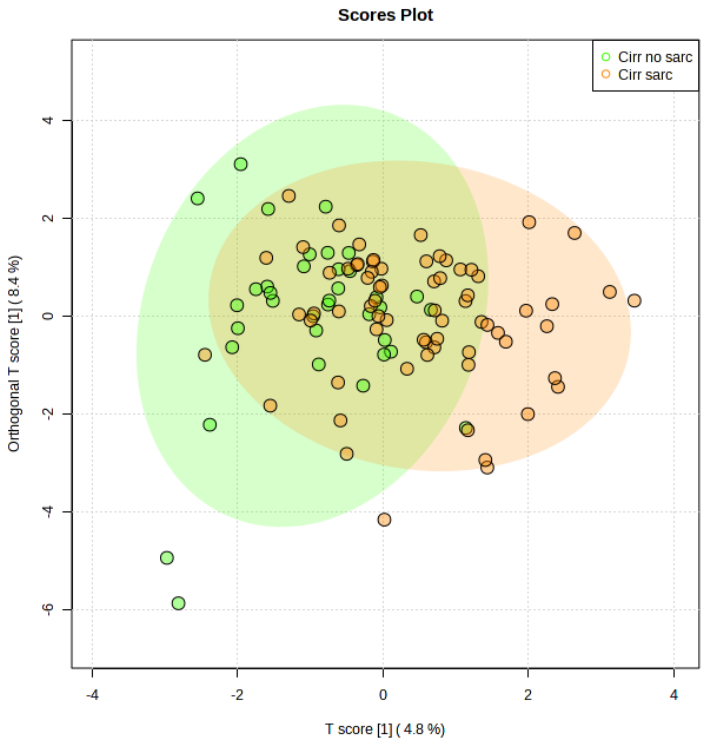

Figure 13. Grouping of cirrhotic patients, both those with and without sarcopenia, was illustrated through the utilization of a score plot derived from orthogonal-PLS-DA analysis, which considered urine metabolite patterns.

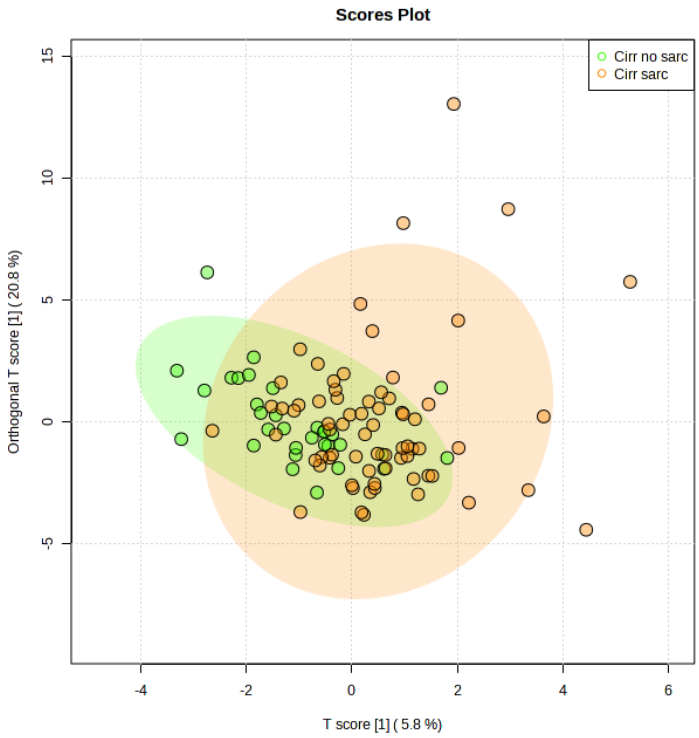

Figure 14. Grouping of cirrhotic patients, both those with and without sarcopenia, was illustrated through the utilization of a score plot derived from orthogonal-PLS-DA analysis, which considered stool metabolite patterns.

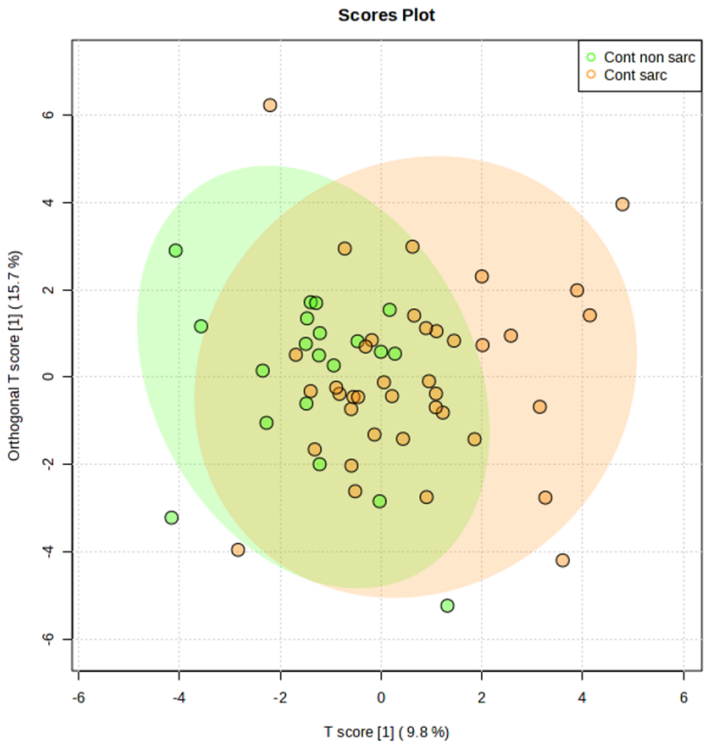

Figure 15. Grouping of non-cirrhotic patients, both those with and without sarcopenia, was illustrated through the utilization of a score plot derived from orthogonal-PLS-DA analysis, which considered serum metabolite patterns.

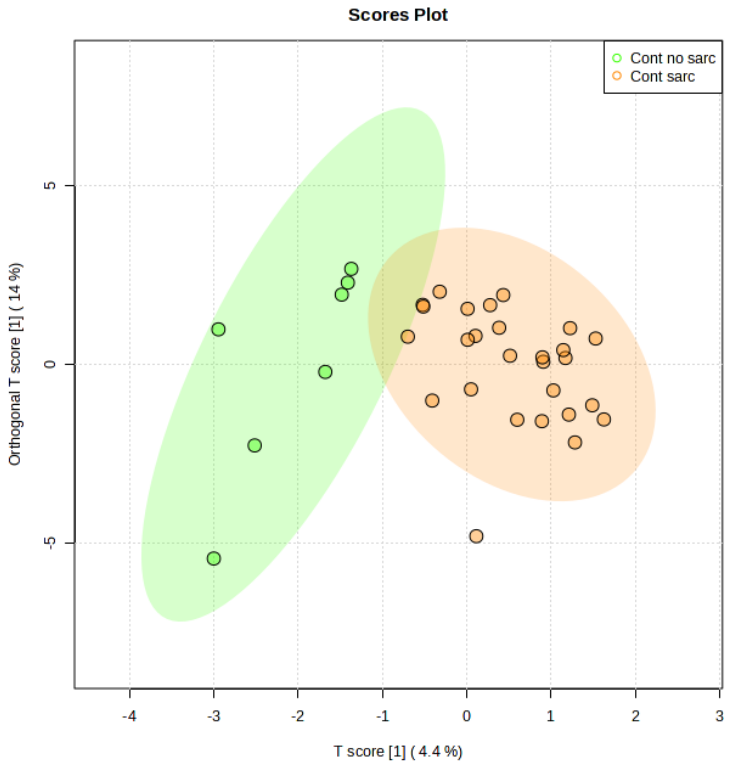

Figure 16. Grouping of non-cirrhotic patients, both those with and without sarcopenia, was illustrated through the utilization of a score plot derived from orthogonal-PLS-DA analysis, which considered urine metabolite patterns.

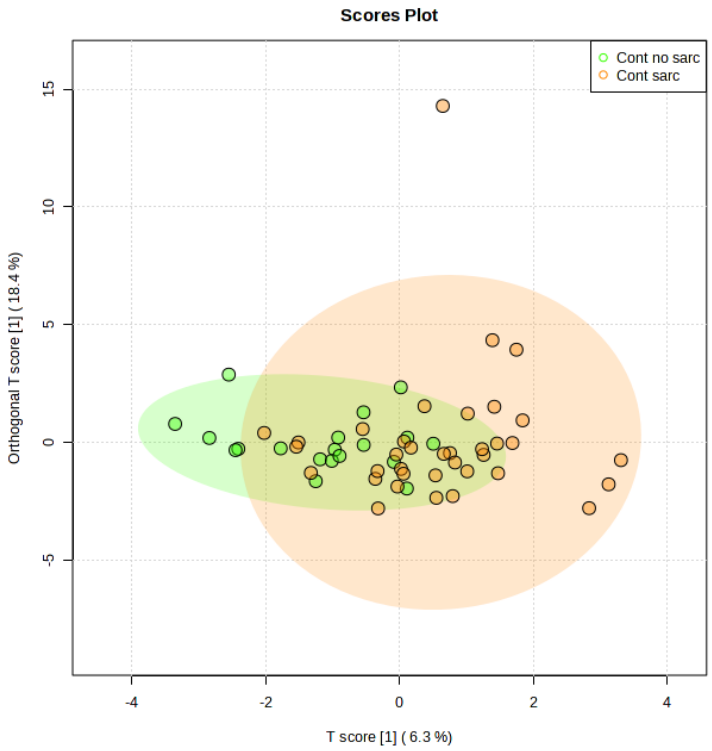

Figure 17. Grouping of non-cirrhotic patients, both those with and without sarcopenia, was illustrated through the utilization of a score plot derived from orthogonal-PLS-DA analysis, which considered stool metabolite patterns.

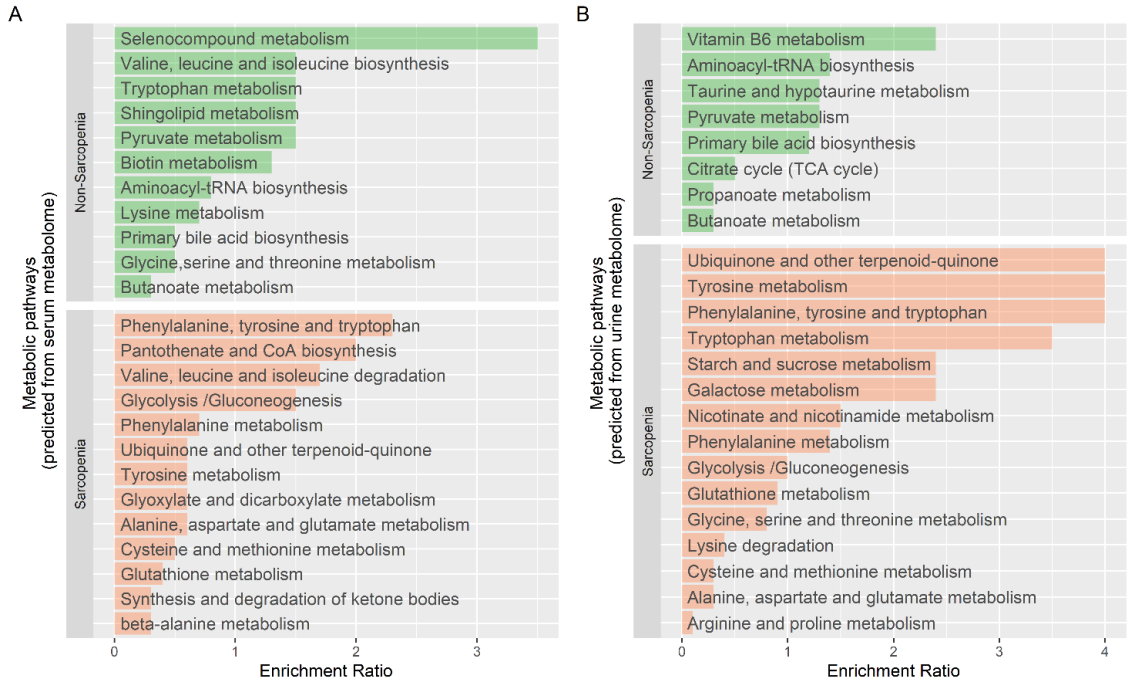

Figure 18. Alterations in the sets of serum and urine metabolites, as well as the related pathways (A and B, respectively), between cirrhotic individuals with and without sarcopenia. This figure has been adapted from (1).

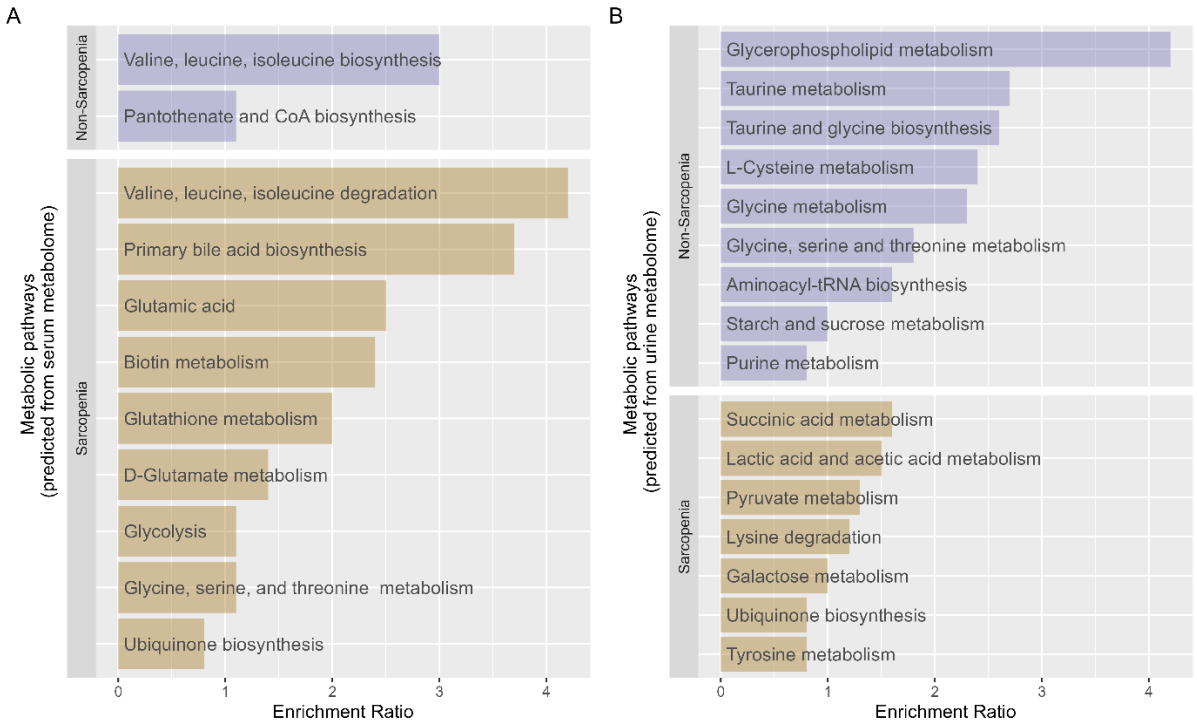

Figure 19. Alterations in the sets of serum and urine metabolites, as well as the related pathways (A and B, respectively), between non-cirrhotic patients with and without sarcopenia.

Systems biology analysis

We determined gut microbiome features, BAs profiles, and metabolomes associated with sarcopenia in liver cirrhosis using LASSO and multivariate logistic regression.

LASSO regression models

We found many features associated with sarcopenia in cirrhosis using LASSO regression (Fig. 20). BMI, MAMC, albumin, irisin, creatinine, hematocrit, myostatin, CRP, FGF-21, sCD14, DAO, bilirubin, ALT, APPT, and hematocrit were among these features. Bile acid profiles and metabolome including CDCA: CDCA, GDCA: DCA, TDCA: DCA, GLCA: LCA, TLCA: LCA, CA: CDCA, T-UDCA: total-sec BAs, 12 α-OH: non-12 α OH BAs, Serum valine, serum phenylalanine, serum alanine, and serum acetate were also identified.

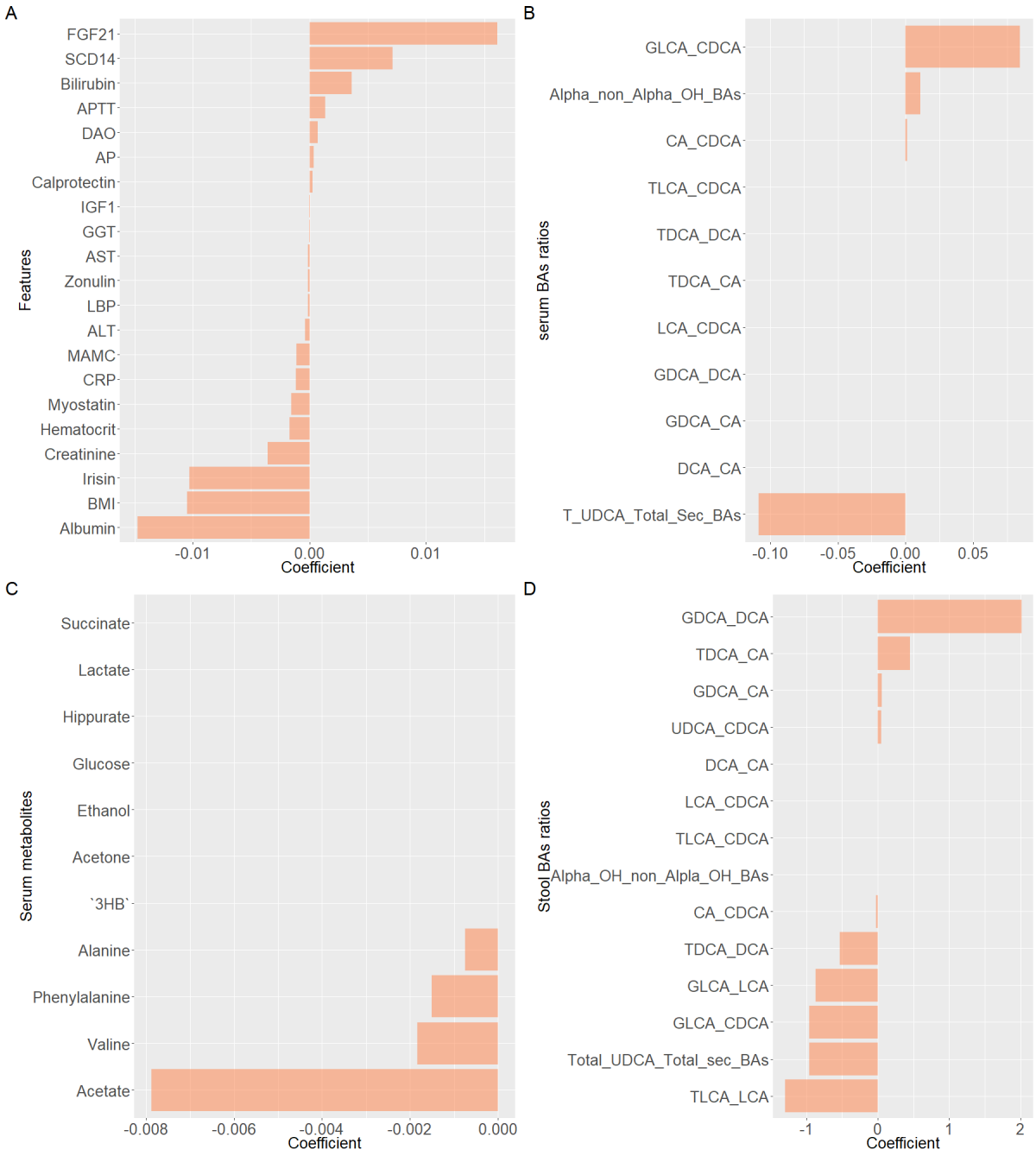

Figure 20. Features identified by LASSO regression as predictors of sarcopenia in liver cirrhosis. The figure has been reproduced from (1).

Multivariate logistic regression analysis

Multivariate logistic regression was used to determine the clinical parameters, bile acids, and metabolome factors associated with sarcopenia in liver cirrhosis while controlling for confounding factors such as the severity of liver disease and drug use. The results of the multivariate are reported in (Table 18 and Fig. 21). The results of the multivariate logistic regression analysis showed that MAMC (p = 0.001), BMI (p = 0.001), CA: CDCA (p = 0.03), 12-α OH: non-12-α-OH BAs (p = 0.03), T-UDCA: total-sec BAs (p = 0.01), and serum valine (p = 0.04) were independently associated with sarcopenia in cirrhosis, even when corrected for the severity of the liver disease and drug use. These findings suggest that bile acids and valine may play a role in mediating sarcopenia in liver cirrhosis.

BMI independently predicted sarcopenia in liver cirrhosis

We used a multivariate logistic regression model to predict sarcopenia in liver cirrhosis. BMI, MELD, PPI, beta-blocker, and diuretic were used as independent variables (formula: sarcopenia ~ BMI + MELD + PPI + beta-blocker + diuretic). The model had an explanatory power of R^2 = 0.20, and the intercept for the model (BMI = 0, MELD = 0, PPI, beta-blocker, and diuretic) was found to be 5.89 (95% CI: 2.99, 9.28; p < .001).

Within the model, the effect of BMI was statistically significant and negative (beta = -0.21, 95% CI: -0.32, -0.11; p < .001; Std. beta = -1.03, 95% CI: -1.58, -0.56), indicating that a decrease in BMI was associated with an increased risk of sarcopenia in liver cirrhosis. On the other hand, the effects of MELD (beta = -6.20e-03, 95% CI: -0.09, 0.08; p = 0.889; Std. beta = -0.03, 95% CI: -0.48, 0.42), PPI (beta = -3.19e-03, 95% CI: -0.90, 0.89; p = 0.994; Std. beta = -3.19e-03, 95% CI: -0.90, 0.89), beta-blocker (beta = 0.36, 95% CI: -0.56, 1.28; p = 0.442; Std. beta = 0.36, 95% CI: -0.56, 1.28), and diuretic (beta = 0.90, 95% CI: -8.82e-03, 1.86; p = 0.056; Std. beta = 0.90, 95% CI: -8.82e-03, 1.86) were not statistically significant.

These findings suggest that BMI is an independent predictor for sarcopenia in liver cirrhosis even after controlling for the severity of liver disease and drug use. A lower BMI is associated with an increased risk of sarcopenia. However, the other factors tested in the model, including MELD, PPI, beta-blocker, and diuretics, did not show significant associations with sarcopenia.

Muscle mass independently predicted sarcopenia in liver cirrhosis

A multiple logistic regression model was conducted to predict sarcopenia using muscle mass, MELD, PPI, beta-blocker, and diuretic as predictors, with the formula (Sarcopenia ~ muscle mass + MELD + PPI +beta-blocker + diuretic). The model showed substantial explanatory power with an R-squared value of 0.43. The model's intercept, when muscle mass = 0, MELD = 0, PPI, beta-blocker, and diuretic were at 10.92 (95% CI (6.84, 16.08), p < .001).

The effect of muscle mass was statistically significant and negative within this model (beta = -0.21, 95% CI (-0.30, -0.14), p < .001; Std. beta = -2.16, 95% CI (-3.10, -1.42)). In contrast, the effects of MELD (beta = -0.06, 95% CI (-0.17, 0.05), p = 0.283; Std. beta = -0.31, 95% CI (-0.87, 0.26)), PPI (beta = -0.37, 95% CI (-1.47, 0.68), p = 0.495; Std. beta = -0.37, 95% CI (-1.47, 0.68)), beta-blocker (beta = 0.06, 95% CI (-1.05, 1.15), p = 0.918; Std. beta = 0.06, 95% CI (-1.05, 1.15)), and diuretic (beta = 0.71, 95% CI (-0.37, 1.83), p = 0.200; Std. beta = 0.71, 95% CI (-0.37, 1.83)) were not statistically significant.

These findings suggest that muscle mass is an independent predictor for sarcopenia in liver cirrhosis, even after controlling for the severity of liver disease and drug use. A lower muscle mass is associated with an increased risk of sarcopenia.

MAMC independently predicted sarcopenia in liver cirrhosis

A multiple logistic regression model was used to predict sarcopenia in liver cirrhosis by incorporating several variables, including MAMC, MELD, PPI, beta-blocker, and diuretics. The formula for this model was Sarcopenia ~ MAMC + MELD + PPI + Betablocker + Diuretic. The model’s explanatory power was moderate, as indicated by R2 = 0.18. The intercept of the model, corresponding to MAMC = 0, MELD = 0, PPI, beta-blocker, and diuretic, was 7.09, with a 95% confidence interval of (3.38, 11.50), and p < .001.

The standardized beta value was -1.01, with a 95% confidence interval of (-1.60, -0.50). Within this model, the effect of MAMC was statistically significant and negative, with a beta value of -0.03 and a 95% confidence interval of (-0.04, -0.01), and p < .001. On the other hand, the effects of MELD, PPI, beta-blocker, and diuretics were not statistically significant.

These findings suggest that MAMC is an independent predictor for sarcopenia in liver cirrhosis even after controlling for the severity of liver disease and drug use. A lower MAMC is associated

with an increased risk of sarcopenia. These results suggest that MAMC could potentially predict sarcopenia in liver cirrhosis.

The ratio of CA to CDCA independently predicted sarcopenia in liver cirrhosis

A multivariate logistic regression model predicted sarcopenia in liver cirrhosis patients. The model included several variables, such as the stool ratio of CA: CDCA, MELD, PPI, beta-blocker, and diuretic, and was represented by the formula (Sarcopenia ~ Stool ratio of CA: CDCA + MELD + PPI +beta-blocker + diuretic).

The model had an $R^2 = 0.11$, and the intercept was 0.37 (95% CI: -1.03, 1.79; p = 0.599) when all variables were set to 0. Among the variables, only the stool ratio of CA: CDCA had a statistically significant and negative effect on sarcopenia (beta = -0.25, 95% CI: -0.51, -0.05; p = 0.034; Std. beta = -0.64, 95% CI: -1.32, -0.13). MELD had a statistically non-significant and positive effect (beta = 9.08e-03, 95% CI: -0.08, 0.10; p = 0.848; Std. beta = 0.05, 95% CI: -0.42, 0.53), as did PPI (beta = 0.36, 95% CI: -0.55, 1.30; p = 0.438; Std. beta = 0.36, 95% CI: -0.55, 1.30), beta-blocker (beta = 0.20, 95% CI: -0.76, 1.14; p = 0.683; Std. beta = 0.20, 95% CI: -0.76, 1.14), and diuretic (beta = 0.76, 95% CI: -0.17, 1.72; p = 0.113; Std. beta = 0.76, 95% CI: -0.17, 1.72).

These results suggest that the stool ratio of CA: CDCA could potentially predict sarcopenia in liver cirrhosis.

The ratio of 12 alpha to non-12 alpha OH BAs and sarcopenia independently predicted sarcopenia in liver cirrhosis

A multiple logistic regression model was used to predict sarcopenia in liver cirrhosis using the ratio of 12 alpha to non-12 alpha OH BAs, MELD, PPI, beta-blocker, and diuretic as predictors (formula: sarcopenia ~ ratio of serum 12 alpha to non-12 alpha OH BAs + MELD + PPI +beta-blocker + diuretic).

The model had an explanatory power of $R^2 = 0.08$. The model's intercept, corresponding to 12 alpha to non-12 alpha OH BAs = 0, MELD = 0, PPI, beta-blocker, and diuretic, was -0.80 (95% CI (-2.31, 0.65), p = 0.288). Within this model, the effect of 12 alpha to non-12 alpha OH BAs was statistically significant and positive (beta = 1.00, 95% CI (0.14, 2.06), p = 0.042; Std. beta = 0.59, 95% CI (0.08, 1.22)), while the effects of MELD (beta = 0.02, 95% CI (-0.06, 0.11), p = 0.566; Std. beta = 0.12, 95% CI (-0.29, 0.55)), PPI (beta = 0.07, 95% CI (-0.77, 0.91), p = 0.867; Std. beta =

0.07, 95% CI (-0.77, 0.91)), betablocker (beta = 0.20, 95% CI (-0.67, 1.07), p = 0.643; Std. beta = 0.20, 95% CI (-0.67, 1.07)), and diuretic (beta = 0.70, 95% CI (-0.15, 1.56), p = 0.110; Std. beta = 0.70, 95% CI (-0.15, 1.56)) were not significant. These results suggest that the ratio of serum 12 alpha to non-12 alpha OH BAs has the potential as a predictor for sarcopenia in cirrhosis.

The ratio of total UDCA to total secondary BAs independently predicted sarcopenia in liver cirrhosis

A multiple logistic regression model was utilized to predict sarcopenia in liver cirrhosis by considering the variables, including the ratio of serum T-UDCA: total sec BAs, MELD, PPI, beta-blocker, and diuretic (formula: sarcopenia ~ T-UDCA: total sec BAs + MELD + PPI + Betablocker + Diuretic). The model's explanatory power was determined to be (R^2 = 0.09). The model's intercept, corresponding to T-UDCA: total sec BAs = 0, MELD = 0, PPI, and diuretic, was found to be 0.58 (95% CI (-0.70, 1.89), p = 0.372).

Within this model, the effect of the ratio of serum T-UDCA: total sec BAs was statistically significant and negative (beta = -1.75, 95% CI (-3.19, -0.38), p = 0.014; Std. beta = -0.53, 95% CI (-0.96, -0.11)). On the other hand, the effect of MELD (beta = 0.02, 95% CI (-0.06, 0.11), p = 0.639; Std. beta = 0.10, 95% CI (-0.32, 0.54)), the effect of PPI (beta = 0.11, 95% CI (-0.73, 0.97), p = 0.798; Std. beta = 0.11, 95% CI (-0.73, 0.97)), the effect of beta-blocker (beta = 0.42, 95% CI (-0.48, 1.32), p = 0.363; Std. beta = 0.42, 95% CI (-0.48, 1.32)), and the effect of diuretic (beta = 0.52, 95% CI (-0.36, 1.40), p = 0.246; Std. beta = 0.52, 95% CI (-0.36, 1.40)) were not significant. These results indicate that the ratio of serum T-UDCA: total sec BAs could be a predictor for sarcopenia in cirrhosis.

Serum valine independently predicted sarcopenia in liver cirrhosis

A multivariate logistic regression model was used to predict sarcopenia, with serum valine, MELD, PPI, beta-blocker, and diuretic as predictors. The model was found to have a statistically significant (R^2 = 0.09, F(3, 91) = 3.06, p = 0.032, adj. R2 = 0.06). The model's intercept was found to be 1.65 (95% CI (0.91, 2.38), t(91) = 4.47, p < .001) when serum valine equals 0.

The effect of serum valine within the model was found to be statistically significant and negative (beta = -7.54e-03, 95% CI (-0.01, -9.22e-04), t(91) = -2.26, p = 0.026; Std. beta = -0.27, 95% CI (-0.50, -0.03)). In contrast, the effects of MELD (beta = -0.01, 95% CI (-0.03, 0.01), t(91) = -1.07,

p = 0.289; Std. beta = -0.13, 95% CI (-0.36, 0.11)), PPI (beta = -0.18, 95% CI (-1.11, 0.74), p = 0.706; Std. beta = -0.18, 95% CI (-1.11, 0.74)), beta-blocker (beta = 0.40, 95% CI (-0.56, 1.34), p = 0.410; Std. beta = 0.40, 95% CI (-0.56, 1.34)), and diuretic (beta = 0.44, 95% CI (-0.59, 1.47), p = 0.394; Std. beta = 0.44, 95% CI (-0.59, 1.47)) were not found to be statistically significant.

These findings suggest that serum valine is an independent predictor for sarcopenia in liver cirrhosis, even after controlling for the severity of liver disease and drug use. A lower serum valine is associated with an increased risk of sarcopenia.

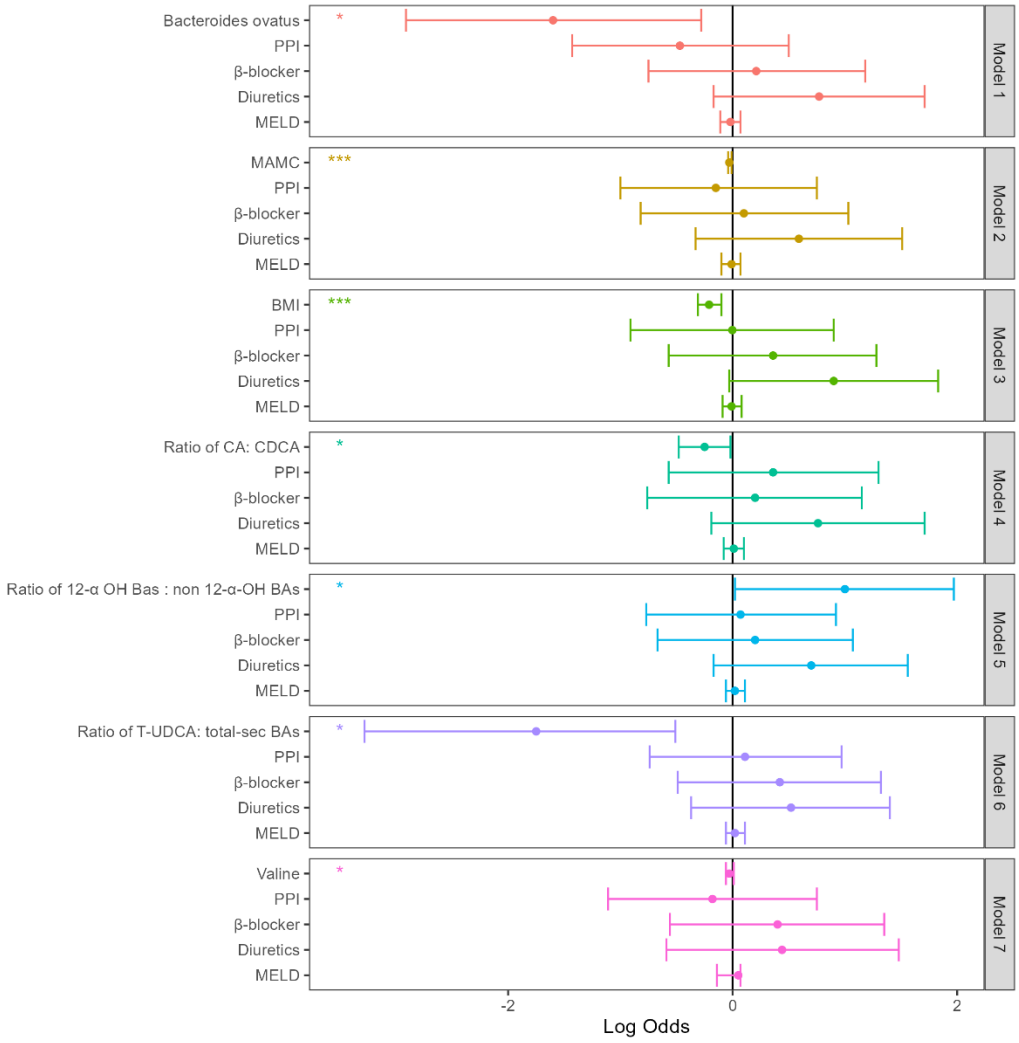

Figure 21. Models for predicting sarcopenia in liver cirrhosis adjusted for the severity of liver disease and drug use. Values were reported as log odds.

Table 18. Models for predicting sarcopenia in cirrhosis adjusted for the severity of liver disease and drug use. All values were reported as coefficients and odds ratios (95% CI). This table has been reproduced from (1).

LASSO predictors	Log odds	Odd ratios (95% CI)	Adjusted P-values
		Model s	
MAMC	-0.03	1.00 (1.01;1.00)	p < 0.001
MELD	-0.01	1.00 (1.00;0.99)	Ns
PPI	-0.15	0.87 (0.35;2.08)	Ns
β-blocker	0.10	1.10 (0.43;2.75)	Ns
Diuretics	0.59	1.80 (0.72;0.45)	Ns
		Model 2	
BMI	-0.21	1.04 (1.07;1.02)	p < 0.001
MELD	-0.01	1.00 (1.01;1.00)	Ns
PPI	-0.003	0.99 (0.41;2.45)	Ns
β-blocker	0.36	1.43 (0.57;3.60)	Ns
Diuretics	0.90	2.47 (0.99;6.41)	Ns
		Model 3	
CA: CDCA	-0.25	1.64 (1.14;1.01)	p = 0.03
MELD	0.01	1.00 (1.01;0.99)	Ns
PPI	0.36	1.44 (0.58;3.67)	Ns
β-blocker	0.20	1.22 (0.48;3.13)	Ns
Diuretics	0.76	2.14 (0.84;5.60)	Ns
		Model 4	
12-α OH Bas: non 12-α-OH Bas	1.00	2.71 (1.15;7.82)	p = 0.04
MELD	0.02	1.00 (0.99;1.02)	Ns
PPI	0.07	1.07 (0.46;2.50)	Ns
β-blocker	0.20	1.23 (0.51;2.91)	Ns
Diuretics	0.70	2.01 (0.86;4.78)	Ns
		Model 5	
T-UDCA: total-sec BAs	-1.75	21.38 (264.28;1.94)	p = 0.01
MELD	0.02	1.00 (0.99;1.02)	Ns
PPI	0.11	1.12 (0.48;2.63)	Ns
β-blocker	0.42	1.51 (0.62;3.74)	Ns

Diuretics	0.52	1.68 (0.70;4.06)	Ns
		Model 6	
Valine	-0.03	1.00 (1.02;1.00)	p = 0.04
MELD	0.05	1.00 (0.99;1.00)	Ns
PPI	-0.18	0.84 (0.33;2.09)	Ns
β-blocker	0.40	1.49 (0.57;3.83)	Ns
Diuretics	0.44	1.56 (0.57;4.34)	Ns

4Note. p-values obtained through multivariate logistic regression and adjusted for the severity of liver disease and drug use. Abbreviations: MAMC, mid-arm muscle circumference; MELD, model of end-stage liver disease; BMI, body mass index; PPI, proton pump inhibitor; CA: CDCA, the ratio of cholic acid to chenodeoxycholic acid; 12-α OH BAs: non 12-α-OH Bas, 12 alpha-hydroxylated to non-12 alpha-hydroxylated BAs; T-UDCA: total-sec Bas, total ursodeoxycholic acid to total secondary BAs.

Hierarchical clustering and correlational analysis of features associated with sarcopenia

We identified four hierarchical categories by correlational analysis, which were represented by a dendrogram in four different colors (Fig. 22). The first group included the cirrhosis-associated bacteria *Bacteroides fragilis, Blautia marseille*, and *Sutterella* spp. BMI, muscle mass, and MAMC were shown to be negatively correlated with these bacteria, but secondary bile acids including DCA, LCA, total DCA, and total LCA, as well as bile acid ratios like DCA: CA, LCA: CDCA, and 12 OH: non-12 OH-BA, were positively correlated with these bacteria. These findings imply that *Bacteroides fragilis*, *Blautia marseille*, and *Sutterella* spp. may all be engaged, either separately or together, in the biotransformation of primary bile acids into secondary bile acids.

Veillonella parvula, which is also associated with cirrhosis with sarcopenia, was shown to cluster differently but to be negatively correlated with BMI, muscle mass, and MAMC. *Bacteroides ovatus*, which is associated with cirrhosis without sarcopenia, on the other hand, exhibited a positive correlation with BMI, muscle mass, valine, and acetate. Additionally, a negative association was found between BMI, muscle mass, and MAMC and the following variables: DCA, LCA, total DCA, total LCA, DCA: CA, LCA: CDCA, and 12-OH to non-12-OH-BAs. These findings suggest that secondary BAs (DCA and LCA) may have a negative impact on the health of skeletal muscles.

Bacteroides fragilis, Blautia marseille, and *Sutterella* spp consistently formed a single cluster when both sexes were examined independently. The BMI, muscle mass, and MAMC all consistently showed a negative correlation with this cluster. Additionally, this cluster showed a

positive correlation with secondary BAs (DCA, LCA) and BAs ratios (DCA: CA and 12-OH: non-12-OH-BAs). These results suggest that these biomarkers are associated with sarcopenia regardless of sex.

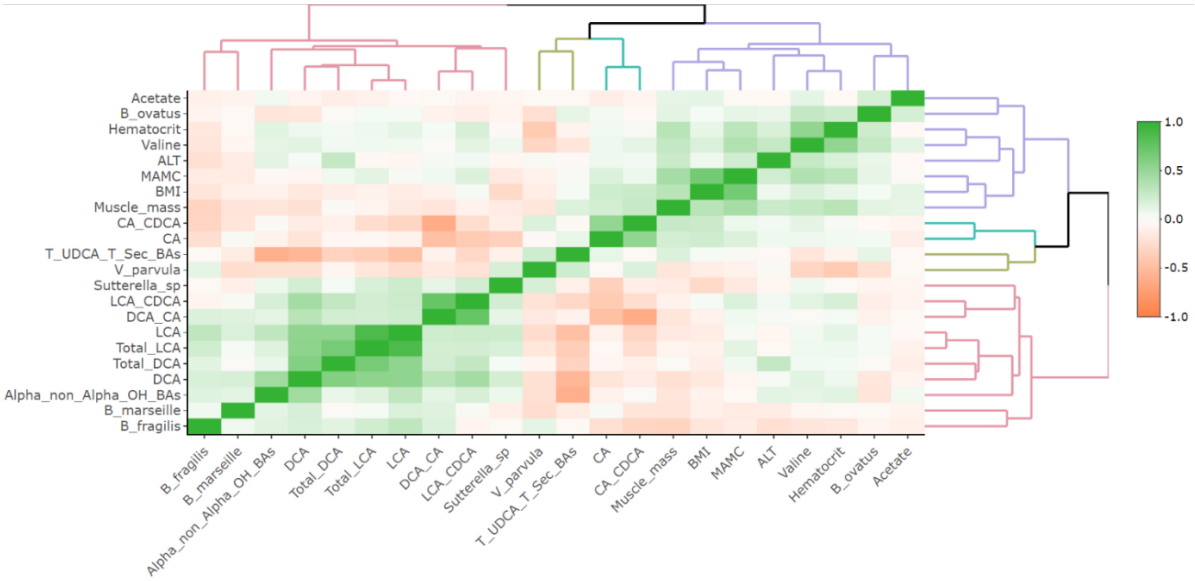

Figure 22. Correlation between clinical parameters, bacterial ASV, BAs, and metabolites. Green and Indian red indicate positive and negative correlations, respectively. This figure has been adapted from (1).

DISCUSSION

Some parts of the discussion are also part of the published paper (Aliwa et al., 2023).

Sarcopenia is a common complication of liver cirrhosis, characterized by a progressive and generalized loss of muscle mass and function that predisposes to fragility, worsened quality of life, and increased mortality risk (2, 3, 8, 21). Liver cirrhosis is a chronic end-stage progressive liver disease that impairs liver functions (19). The liver plays a crucial role in metabolizing bioactive metabolites, including bile acids and amino acids (44, 114). Therefore, liver dysfunction can lead to metabolic disorders, protein synthesis and degradation imbalances, hyperammonemia, and hormonal and nutritional status alterations. These factors may mediate the decline of skeletal muscle cell growth and differentiation, contributing to the development of sarcopenia in liver cirrhosis (2, 3, 151). Additionally, altered gut microbiome composition and inflammation have been associated with liver cirrhosis and may contribute to the development of sarcopenia (2, 3, 34, 48).

A prospective cohort study was conducted to elucidate the possible association between changes in the composition of the gut microbiome, bile acids, metabolome, and sarcopenia status in cirrhosis. In liver cirrhosis, the gut microbiome composition is characterized by an increased abundance of pathogenic and less abundant beneficial bacterial species (34, 42, 43). Furthermore, altered gut microbiome composition has been associated with increased gut permeability, bacterial translocation, inflammation, and accumulation of cytotoxic metabolites, including bile acids. These factors may contribute to losing muscle mass and function in liver cirrhosis (2, 34, 140). Despite these observations, little is known about the molecular mechanisms underlying the etiology of sarcopenia in liver cirrhosis, and there are currently no effective therapeutic interventions. Therefore, this study aimed to determine changes in the gut microbiome, bile acids, and metabolome composition that may mediate the development of sarcopenia in liver cirrhosis. Identifying potential molecules mediating the mechanisms underlying the gut-liver-muscle axis may lead to discovering novel therapeutic targets to treat cirrhosis-related sarcopenia.

Our results demonstrated that BMI, muscle mass, and MAMC significantly reduced in cirrhotic patients with sarcopenia compared to cirrhotic patients without sarcopenia. Moreover, BMI, muscle mass, and MAMC independently predicted sarcopenia in liver cirrhosis, even after controlling for the severity of the liver disease. Similarly, BMI, muscle mass, MAMC, and albumin were significantly reduced in non-cirrhotic controls with sarcopenia compared to those without sarcopenia. These results suggest that BMI and MAMC may be potential biomarkers for sarcopenia, regardless of cirrhosis. To support this point, MAMC and albumin have been associated with sarcopenia in liver cirrhosis (170). Furthermore, MAMC is an independent predictor of mortality in cirrhotic patients undergoing liver transplants (170). In liver cirrhosis, the increased systemic circulation of pro-inflammatory mediators and oxidative status has been associated with structural and functional changes in albumin (182). Albumin has numerous functions, including maintenance of oncogenic pressure, detoxification, immune system modulation, and antioxidants in cirrhotic patients (182, 183). The function of albumin is based on its distribution and molecular concentrations in plasma. In particular, the negative charge of albumin and high intravascular concentrations facilitates its role as an oncogenic pressure regulator (184). Indeed albumin has been used as an adjunct to diuretics to improve diuretic response in cirrhotic patients (183). Additionally, albumin has been shown to bind a range of toxic metabolites, inflammatory mediators, and ROS (182, 184). Interestingly, incubation with albumin prevented induced neutrophil dysfunction in cirrhotic patients (185). However, the role of albumin in the pathophysiology of sarcopenia in liver cirrhosis has yet to be fully understood, and the

association between albumin and sarcopenia is inconclusive (186-188). Hypothetically, reduced serum albumin indicates a dysfunctional protein metabolism and increased protein loss in cirrhotic patients with sarcopenia.

This study found no significant differences in the biomarkers for gut permeability, bacterial translocation, inflammation, or altered hormonal/myokine status between cirrhotic patients with and without sarcopenia. These findings are consistent with a previous study that found comparable gut permeability and inflammatory markers in cirrhotic patients with and without sarcopenia. (189). In contrast, cirrhotic patients with sarcopenia showed significantly elevated levels of zonulin, calprotectin in stool, and serum CRP, while IGF-1 and irisin levels in serum were significantly lower when compared to non-cirrhotic patients with and without sarcopenia. Elevated levels of zonulin and calprotectin in stool and serum CRP indicate increased gut barrier impairment and intestinal inflammation, common in cirrhotic patients (190, 191). Furthermore, zonulin and calprotectin have been identified as potential biomarkers for predicting risk-related mortality in liver cirrhosis (190, 192). Studies have also shown that alcoholic liver disease and non-alcoholic fatty liver disease patients have increased zonulin levels, indicating gut-barrier dysfunction. (190, 192, 193). Moreover, zonulin has been found to negatively correlate with sarcopenia assessment parameters, including HGS indexes and gait speed in cirrhotic patients. (194). In liver cirrhosis, reduced satellite cell differentiation and proliferation have been associated with low levels of IGF-1 (195). IGF-1 can activate the protein kinase B (Akt)-mTOR pathway leading to the growth and differentiation of satellite cells, which are essential for muscle growth and repair (74). Similarly, skeletal muscle protein synthesis is positively regulated by protein kinase B (Akt)-mTOR pathway-dependent mechanism (195). Additionally, skeletal muscle secretes irisin, which has been shown to protect against muscle loss and regulate skeletal muscle energy expenditure and oxidative stress (84, 88). In differentiated skeletal muscle cells, irisin mediates glucose uptake through an AMP-activated protein kinase (AMPK)-dependent pathway coupled with increased GLUT 4 translation (196). Indeed, reduced levels of IGF-1 and irisin in serum have been associated with sarcopenia in cirrhosis and the elderly population (70, 88, 89, 195).

In this study, we further investigated the impact of sarcopenia on the diversity and composition of the gut microbiome in liver cirrhotic and non-cirrhotic control patients. Interestingly, our results demonstrated that alpha and beta diversity were comparable between liver cirrhotic patients with and without sarcopenia. However, when we analyzed the differential microbial abundances, we found an alteration in the gut microbiome taxonomic composition between cirrhotic patients with

and without sarcopenia. We showed that *Bacteroides fragilis*, *Blautia marseille*, *Sutterella* spp, and *Veillonella parvula* were more abundant and associated with liver cirrhotic patients with sarcopenia. Conversely, sarcopenia affected the alpha and beta diversity in non-cirrhotic control patients, where alpha and beta diversity were significantly altered in non-cirrhotic control patients with sarcopenia compared to non-cirrhotic controls without sarcopenia. Our functional prediction results further demonstrated that non-cirrhotic controls without sarcopenia had enriched functional profiles associated with genetic information processing and cell division, which may explain observed differences in richness and diversity of the gut microbiome between non-cirrhotic controls with and without sarcopenia. Furthermore, *Alistipes putredinis*, *Alistipes onderdonkii*, *Ruminococcaceae* spp, and *Eubacterium coprostanoligenes* were more abundant and associated with non-cirrhotic controls without sarcopenia. We further demonstrated that cirrhotic patients with sarcopenia had altered beta-diversity but not alpha-diversity compared to cirrhotic patients without sarcopenia and non-cirrhotic controls with and without sarcopenia. Moreover, *Veillonella parvula* was significantly more abundant and associated with cirrhotic patients with sarcopenia. We also showed that certain bacterial species were associated with potential muscle biomarkers, including muscle mass and MAMC. In cirrhotic sarcopenic patients, *Bacteroides fragilis*, *Blautia marseille*, *Veillonella parvula*, and *Sutterella* spp were inversely correlated with potential muscle biomarkers, including muscle mass and MAMC. Previous studies have reported conflicting findings regarding the impact of sarcopenia on alpha and beta diversity. Recently, one study showed that alpha and beta diversity were significantly altered between cirrhotic patients with and without sarcopenia and controls with and without sarcopenia. Furthermore, they found that sarcopenia did not impact alpha diversity in non-cirrhotic controls but affected gut microbiome taxonomic composition (189). In contrast to our study, they showed that Klebsiella and Streptococcus were more abundant at the genus levels. At the same time, *Veillonellaceae, Methanobacteriaceae, Ruminococcus*, and *Dialister* were reduced and associated with cirrhotic patients with sarcopenia. The differences in the inclusion and exclusion criteria for the study population may partly explain the contradictory findings. Our findings suggest that changes in the gut microbiome may play a role in the decline of skeletal muscle mass and strength or function in liver cirrhosis, as previously suggested (34, 189). Through functional prediction analysis, we demonstrated that the gut microbiome associated with cirrhotic patients with sarcopenia showed an enriched LPS antigen biogenesis pathway, which may explain the increase in the abundance of the potential LPS-producing bacterial species in cirrhotic patients with sarcopenia. Specifically, *Bacteroides fragilis*, *Blautia marseille*, *Veillonella parvula*, and *Sutterella* spp have been shown to produce LPS that may induce inflammatory responses,

potentially mediating the loss of muscle mass and function in humans and animal models. (35-37, 149, 190, 197). Additionally, age-related sarcopenia has been associated with an increased abundance of *Bacteroides fragilis* and *Sutterella* spp (37, 198).

Conversely, *Bacteroides ovatus* was more abundant and associated with cirrhotic patients without sarcopenia. Furthermore, *Bacteroides ovatus* correlated positively with muscle mass, MAMC, serum valine, and serum acetate. Again, *Bacteroides ovatus* predicted sarcopenia in liver cirrhosis even after controlling liver disease severity and drug use. *Bacteroides ovatus* has been shown to modulate immunoregulatory cytokines, including IL-10, or by recovering T regulatory/ T helper balance (149, 199). Furthermore, *Bacteroides ovatus* has been considered a potential next-generation probiotic considering its ability to inhibit LPS-mediated inflammatory responses (149, 200). Thus, these results suggest that *Bacteroides ovatus* may positively influence skeletal muscle health. However, further studies are required to understand the mechanistic interplay between *Bacteroides ovatus* and skeletal muscle. Similarly, *Alistipes* spp has been shown to have a protective role and a potential marker for dysbiosis in cirrhosis (201). Furthermore, a reduced abundance of *Alistipes onderdonkii* has been demonstrated in older people with sarcopenia (198). These findings suggest that the gut microbiome may regulate skeletal muscle mass and function by producing LPS capable of stimulating downstream inflammatory responses or modulation of anti-inflammatory cytokines. However, it is essential to note that the mechanistic interplay between the gut microbiome and skeletal muscle still needs to be studied and fully understood. Most of the studies are based on animal models. Hence generalization of these findings to humans comes with challenges and limitations. (202, 203).

The gut microbiome has inflammatory and metabolic functions (34, 203). One such metabolic function is the deconjugation and dehydroxylation of primary bile acids (CA and CDCA) into secondary bile acids (DCA and LCA), respectively, which are important processes in bile acid metabolism. (44, 55, 121, 131). The bacterial species from the genus *Lactobacilli, Bifidobacterium, Clostridium*, and *Bacteroides* have been shown to produce bile salt hydrolase (BSH) key to bile acid deconjugation. In contrast, a few bacterial species from *Clostridium, Eubacterium, Ruminococcus*, and *Blautia*, can produce 7 alpha dehydroxylase that catalyzes the 7 α-dehydroxylation of primary bile acids to secondary bile acids (55, 123, 125, 131, 132). Changes in bile acid profiles have been associated with altered gut microbiome taxonomic composition in chronic liver disease (57). Therefore, considering observed changes in the gut microbiome taxonomic composition between cirrhotic patients with and without sarcopenia, there was a need to investigate the possible gut microbiome-associated alteration of bile acid profiles

in the study population. Furthermore, the alteration of bile acid ratios was assessed to understand the potential shift in bile acid metabolism that could be linked to the alteration of gut microbiome taxonomic composition. This study revealed that cirrhotic patients with sarcopenia had significantly reduced primary bile acid CA in stool, higher levels of secondary bile acids (LCA and DCA) in serum, and thus changes in serum bile acid ration (DCA: CA, and LCA: CDCA) compared to cirrhotic patients without sarcopenia. Altogether these results point to a possible shift in the bile acid transformation linked to altered gut microbiota composition, indicated by elevated DCA and LCA in serum and enhanced 7α-dehydroxylation activity in cirrhotic patients with sarcopenia. We further demonstrated that DCA and LCA were positively associated with sarcopenia-in liver cirrhosis-linked bacteria, including *Bacteroides fragilis*, *Blautia marseille*, and *Sutterella* spp. Increased DCA and the ratio of LCA: CDCA in serum have been associated with increased relative abundances of *Blautia* spp, *Lactococcus*, and *Ruminococcus* in rats suggesting that these bacteria may be significantly involved in the 7 α-dehydroxylation of primary bile acid to secondary bile acids (44, 204). Therefore, hypothetically the individual or communal interaction between *Bacteroides fragilis, Blautia marseille,* and *Sutterella* spp. with bile acid may explain the changes in bile acids profiles between cirrhotic patients with and without sarcopenia.

Furthermore, DCA and LCA showed a negative correlation with skeletal muscle mass biomarkers muscle mass and MAMC indicating that these bile acids may mediate a decline in muscle mass and function in the cirrhotic cohort. Indeed, the secondary bile acids DCA and LCA are hydrophobic, cytotoxic, and potent agonists for the bile acid receptor TGR5 (99, 103). Activating bile acid receptors is necessary for any potential interaction between bile acids and skeletal muscle (103, 140). TGR5 activation by DCA, LCA, and CA has been shown to mediate skeletal muscle protein degradation, loss of muscle mass, and skeletal muscle mitochondrial dysfunction in mice models (99, 103, 140). Similarly, increased serum DCA has been associated with reduced skeletal muscle volume in non-alcoholic fatty liver disease (205). However, another study demonstrated that serum LCA was associated with skeletal muscle hypertrophy in liver cirrhotic patients and rat models (206). The differences in the ethnic background and selection criteria for the study population may explain the apparent contradicting results.

The gut microbiome not only metabolizes hydrophobic and cytotoxic bile acids, including secondary bile acids DCA and LCA but is also critical to the metabolism of hydrophilic and less cytotoxic secondary bile acid UDCA (207). However, the ability to metabolize UDCA from CDCA is only conserved in a small number of bacteria from the genera *Clostridium, Eubacterium,* and *Ruminococcus*, which can produce 7 β-hydroxysteroid dehydrogenases. (207). Our study

demonstrated that liver cirrhotic patients without sarcopenia showed a significantly elevated ratio of T-UDCA: total-sec BAs compared to cirrhotic patients with sarcopenia. Furthermore, even after adjusting for the severity of the liver disease and drug use, T-UDCA: total-sec BAs independently predicted sarcopenia in liver cirrhosis (207). The pathophysiological relevance of this finding cannot be answered by this thesis. The effect of UDCA on skeletal muscle is still unclear since conflicting data have been reported. T-UDCA treatment ameliorated skeletal muscle atrophic conditions in mice models (121). Conversely, in another study, UDCA did not improve muscle atrophic condition in cancer cachexic mice (208). Even though the same cancer cachexia C26 mice model was used in the two studies, different bile acid species that could explain the demonstrated contradicting results were used.

In contrast to our expectations, there were no significant differences in the abundance of bile acid genes, including bile salt hydrolase, bile acid inducer operon (CDE), 3 alpha-hydroxysteroid dehydrogenases, 3 beta-hydroxysteroid dehydrogenases, 5-alpha reductase, 7-alpha-hydroxysteroid dehydrogenases, 7-beta-hydroxysteroid dehydrogenases, and 12 alpha-hydroxysteroid dehydrogenases between liver cirrhotic patients with and without sarcopenia in the current study. However, since gene abundance does not necessarily translate to gene expression, these bile acid gene abundance results may not be definitive and restrict our understanding of bile acid metabolism. Moreover, there was no difference in the bile acid profiles between the non-cirrhotic controls with and without sarcopenia, suggesting that the observed differences in the bile acids profile are the cirrhotic-associated hallmark of sarcopenia. Based on these findings, we hypothesize that secondary bile acids (DCA and LCA) and UDCA may have opposing effects on skeletal muscle health. However, further in vitro studies employing human skeletal muscle cell lines are necessary to clarify potential mechanistic interactions between DCA, LCA, UDCA, and human skeletal muscle.

Furthermore, there were no significant differences in bile acid conjugation between cirrhotic patients with and without sarcopenia and non-cirrhotic controls with and without sarcopenia. However, cirrhotic patients with sarcopenia showed a significantly elevated ratio of GDCA: DCA and TDCA: DCA in serum compared to non-cirrhotic controls with and without sarcopenia. One reason for the increased bile acid conjugation may be attributed to increased expression and functional bile acid conjugation enzyme bile acid acyl-COA synthase transferase (BAAT). Another potential reason for the increased bile acid conjugation in cirrhotic patients with sarcopenia may be due to altered gut microbiome composition in the cirrhotic cohort indicated by reduced abundance in bile salt hydrolase-producing bacterial species. However, we can only speculate

since, in this current study, the gene expression of BAAT was not determined. Furthermore, it is worth noting that there was no significant difference in the BSH gene abundance between the study populations.

In addition to regulating bile acid metabolism, the gut microbiome has been shown to affect the metabolism and bioavailability of bioactive metabolites, including amino acids and short-chain fatty acids (SCFAs) (58, 203, 209). Branched-chain amino acids are the preferred energy source for skeletal muscle, and reduced plasma levels of BCAAs have been linked to sarcopenia in liver cirrhosis (203). A significantly lower serum ratio of BCAA to aromatic amino acid (AAAs) has been observed in cirrhotic patients compared to healthy controls indicating a metabolic shift to meet the demand for gluconeogenesis and ammonia detoxification (210). Our study revealed significantly reduced BCAA (valine) levels in the serum of cirrhotic patients with sarcopenia compared to cirrhotic patients without sarcopenia. Serum valine correlated positively with muscle biomarkers, including muscle mass, MAMC, and the cirrhotic without sarcopenia-associated bacteria *Bacteroides ovatus*. Furthermore, multivariate logistic regression, adjusted for the severity of liver disease and drug use, revealed serum valine to be an independent predictor of sarcopenia in liver cirrhosis. Increased abundance of *Bacteroides ovatus* has been associated with valine synthesis in an in vitro gut model (58).

Additionally, metabolic pathway analysis showed that BCAA (leucine, isoleucine, valine) degradation was enriched and associated with sarcopenia in liver cirrhosis and non-cirrhotic controls with sarcopenia. These results suggest that BCAAs degradation may be associated with sarcopenia irrespective of liver cirrhosis. Leucine, isoleucine, and alanine in serum and enriched amino acid biosynthesis pathway are significantly reduced in cirrhotic patients with sarcopenia (34). The skeletal muscle protein status results from tight regulation between protein synthesis and degradation (96). BCAA can mediate skeletal muscle protein synthesis and energy homeostasis (211, 212). BCAA supplementation has been shown to improve skeletal muscle volume and strength in liver cirrhotic patients (94). *Alistipes* spp and *Eubacterium coprostanoligenes* have been linked to elevated BCAAs and alanine in serum (201).

Apart from bile acid and BCAAs, short-chain fatty acids (SCFAs) are crucial in bridging the interaction between the gut microbiome and skeletal muscle (59). The gut microbiome ferments complex carbohydrates and, to a lesser extent, amino acids, producing SCFAs, including acetate, butyrate, and propionate (58, 59, 213, 214). Skeletal muscles have been found to express the short-chain fatty acid receptors, G-coupled protein receptor 41 (GPR41) (59). Previous studies have demonstrated that SCFAs can influence skeletal muscle protein synthesis, energy

expenditure, and glucose uptake both in vitro and in vivo (59, 198, 203, 214). A reduction in the abundance of SCFAs producing bacteria species has been shown to result in the downregulation of SCFA receptors expression in the intestine, affecting protein and glucose metabolism in skeletal muscle and potentially impacting muscle mass and function (39, 59). Additionally, SCFAs enhance insulin sensitivity, preserve skeletal muscle mass, and maintain oxidative status (59). They also modulate metabolism, immune response, and intestinal barrier function by selectively increasing tight junction proteins, thereby improving gut permeability (199-201). These effects of SCFAs on skeletal muscle are believed to be mediated by the activation of peroxisome proliferator-activated receptors and AMPK (59). Studies have demonstrated that prolonged butyrate treatment can protect against muscle atrophy, improve mitochondrial biogenesis, and decrease reactive oxygen species production and apoptosis in aged mice (213).

Similarly, administering a mixture of SCFAs has been shown to increase the weight of one muscle out of four, the strength of the hindlimb grasp, and decrease Atrogin-1 muscle expression (203). Our study found that the level of acetate in the serum was significantly reduced in cirrhotic patients with sarcopenia compared to cirrhotic patients without sarcopenia. Interestingly, *Bacteroides ovatus*, a bacterial species linked to cirrhosis patients without sarcopenia, correlated positively with serum acetate. Notably, *Bacteroides ovatus* can ferment dietary protein, associated with increased production of SCFAs such as acetate, propionate, and butyrate (58, 215, 216). Additionally, the level of acetate in the serum was comparable between non-cirrhotic controls with and without sarcopenia. The results of this study indicate that *Bacteroides ovatus* could play a significant role in the production and bioavailability of acetate. Additionally, the study suggests that serum acetate may be a promising biomarker for sarcopenia in patients with liver cirrhosis.

In liver cirrhosis, a condition marked by increased reactive oxygen species production, oxidative stress may occur (217). Our results on pathway analysis linked ubiquinone biosynthesis (Coenzyme, CoQ10) to cirrhotic patients with sarcopenia. Ubiquinone is an oxidative product of ubiquinol during oxidative stress (218-220). The ubiquinol to ubiquinone ratio has been proposed as a potential biomarker of oxidative stress, as it plays a significant role in mitochondrial and membrane processes (219, 221). Mitochondrial dysfunction-associated oxidative stress has been suggested as a possible cause of age-related sarcopenia (140). Exposure to ROS for an extended period is linked to oxidized skeletal muscle heavy chains, which impair skeletal muscle functions (222). On the other hand, selenocompound metabolism was associated with cirrhotic patients without sarcopenia Selenoproteins are antioxidants regulating oxidative stress and inflammatory responses (223). These results indicate that ubiquinone and selenoproteins pathways may be

necessary for understanding the involvement of mitochondrial oxidative stress in the pathogenesis of sarcopenia in liver cirrhosis.

Males are more likely to develop liver cirrhosis than females, and males with the condition are likewise more likely to develop sarcopenia (168). So, sex plays a significant role as a confounder in our analyses. In our sex-specific sensitivity analysis, we showed that the changes in microbiome composition showed sex specificity, although BMI, muscle mass, and MAMC maintained an association with sarcopenia in both cirrhotic patients and controls in both sexes.. Additionally, secondary bile acids DCA and LCA as well as serum valine were only significantly different in male cirrhotic patients with and without sarcopenia, which was also seen in other disease cohorts, males had significantly higher secondary bile acid levels than females in colorectal cancer patients (224). The observed lack of significance for several parameters in separate sex-specific analyses may be due to sample size limitations, which would reduce the statistical power to identify significant effects in either sex group. The observed sex differences may also be caused by sex-specific variables including hormonal influences or differences in body composition. (225). Consequently, when extrapolating our findings to both sexes collectively, interpretation of the data should be done with care. Future research is therefore required to better understand the potential sex-specific factors that may contribute to the development of sarcopenia in female cirrhotics and to identify its predictors. These studies should focus on female cirrhotic patients with and without sarcopenia.

The diversity and composition of the gut microbiome can vary depending on several factors, including ethnicity, region, and diet, as noted in previous research (226, 227). Our study has some limitations. Firstly, it's important to note that all our study participants were of Caucasian ethnicity, which may limit the generalizability of our findings to other ethnic groups. Notably, the sex disparity within our study population arises due to the inherent nature of the disease cohort under investigation. Cirrhosis, as a disease, predominantly affects males (168), and this disparity could introduce bias that might impact our results. To mitigate any potential drawbacks for the less represented group (in this instance, female participants), conducting sex-specific analysis and interpretation of results is imperative. Moreover, a cautious approach is necessary when interpreting our findings. We reported some regression models with low R^2. Furthermore, the associations we observed do not provide sufficient evidence to establish a causal relationship. To reach such a conclusion, further in-depth mechanistic studies are required. It is essential to note

that our conclusions are drawn from gene abundance data rather than gene expression information. This limitation curtails our comprehensive understanding of gene functionalities.

In conclusion, our study showed gut microbiome-host associations with altered BA profiles, reduced serum valine, and altered gut microbiome composition in cirrhotic patients who were sarcopenic, suggesting a potential cirrhosis-specific mechanistic interplay in understanding sarcopenia pathogenesis in cirrhosis. Our understanding of sex-specific associations provides the path for future studies to create focused strategies for treating sarcopenia in cirrhotic patients while also taking into account sex-specific oddities.

Bibliography

1. Aliwa B, Horvath A, Traub J, Feldbacher N, Habisch H, Fauler G, et al. Altered gut microbiome, bile acid composition and metabolome in sarcopenia in liver cirrhosis. J Cachexia Sarcopenia Muscle. 2023.
2. Ebadi M, Bhanji RA, Mazurak VC, Montano-Loza AJ. Sarcopenia in cirrhosis: from pathogenesis to interventions. J Gastroenterol. 2019;54(10):845-59.
3. Dasarathy S, Merli M. Sarcopenia from mechanism to diagnosis and treatment in liver disease. J Hepatol. 2016;65(6):1232-44.
4. Marzetti E. Musculoskeletal Aging and Sarcopenia in the Elderly. Int J Mol Sci. 2022;23(5).
5. Sayer AA, Syddall HE, Gilbody HJ, Dennison EM, Cooper C. Does sarcopenia originate in early life? Findings from the Hertfordshire cohort study. J Gerontol A Biol Sci Med Sci. 2004;59(9):M930-4.
6. Yuan S, Larsson SC. Epidemiology of sarcopenia: Prevalence, risk factors, and consequences. Metabolism. 2023:155533.
7. Morley JE, Baumgartner RN, Roubenoff R, Mayer J, Nair KS. Sarcopenia. J Lab Clin Med. 2001;137(4):231-43.
8. Janssen I, Heymsfield SB, Ross R. Low relative skeletal muscle mass (sarcopenia) in older persons is associated with functional impairment and physical disability. J Am Geriatr Soc. 2002;50(5):889-96.
9. Keller K, Engelhardt M. Strength and muscle mass loss with aging process. Age and strength loss. Muscles Ligaments Tendons J. 2013;3(4):346-50.
10. Bauer J, Morley JE, Schols A, Ferrucci L, Cruz-Jentoft AJ, Dent E, et al. Sarcopenia: A Time for Action. An SCWD Position Paper. J Cachexia Sarcopenia Muscle. 2019;10(5):956-61.
11. Morley JE, Anker SD, von Haehling S. Prevalence, incidence, and clinical impact of sarcopenia: facts, numbers, and epidemiology-update 2014. J Cachexia Sarcopenia Muscle. 2014;5(4):253-9.
12. von Haehling S, Morley JE, Anker SD. An overview of sarcopenia: facts and numbers on prevalence and clinical impact. J Cachexia Sarcopenia Muscle. 2010;1(2):129-33.
13. Batsis JA, Mackenzie TA, Jones JD, Lopez-Jimenez F, Bartels SJ. Sarcopenia, sarcopenic obesity and inflammation: Results from the 1999-2004 National Health and Nutrition Examination Survey. Clin Nutr. 2016;35(6):1472-83.
14. Volpato S, Bianchi L, Cherubini A, Landi F, Maggio M, Savino E, et al. Prevalence and clinical correlates of sarcopenia in community-dwelling older people: application of the EWGSOP definition and diagnostic algorithm. J Gerontol A Biol Sci Med Sci. 2014;69(4):438-46.

15. Cruz-Jentoft AJ, Baeyens JP, Bauer JM, Boirie Y, Cederholm T, Landi F, et al. Sarcopenia: European consensus on definition and diagnosis: Report of the European Working Group on Sarcopenia in Older People. Age Ageing. 2010;39(4):412-23.
16. Cruz-Jentoft AJ, Bahat G, Bauer J, Boirie Y, Bruyère O, Cederholm T, et al. Sarcopenia: revised European consensus on definition and diagnosis. Age Ageing. 2019;48(1):16-31.
17. Ha Y, Kim D, Han S, Chon YE, Lee YB, Kim MN, et al. Sarcopenia Predicts Prognosis in Patients with Newly Diagnosed Hepatocellular Carcinoma, Independent of Tumor Stage and Liver Function. Cancer Res Treat. 2018;50(3):843-51.
18. Wall BT, Dirks ML, Snijders T, Senden JM, Dolmans J, van Loon LJ. Substantial skeletal muscle loss occurs during only 5 days of disuse. Acta Physiol (Oxf). 2014;210(3):600-11.
19. Baumgartner K, Cooper J, Smith A, St Louis J. Liver Disease: Cirrhosis. FP Essent. 2021;511:36-43.
20. Kim G, Kang SH, Kim MY, Baik SK. Prognostic value of sarcopenia in patients with liver cirrhosis: A systematic review and meta-analysis. PLoS One. 2017;12(10):e0186990.
21. Dasarathy S. Consilience in sarcopenia of cirrhosis. J Cachexia Sarcopenia Muscle. 2012;3(4):225-37.
22. Carey EJ, Lai JC, Wang CW, Dasarathy S, Lobach I, Montano-Loza AJ, et al. A multicenter study to define sarcopenia in patients with end-stage liver disease. Liver Transpl. 2017;23(5):625-33.
23. Tantai X, Liu Y, Yeo YH, Praktiknjo M, Mauro E, Hamaguchi Y, et al. Effect of sarcopenia on survival in patients with cirrhosis: A meta-analysis. J Hepatol. 2022;76(3):588-99.
24. Kondrup J, Nielsen K, Hamberg O. Nutritional therapy in patients with liver cirrhosis. Eur J Clin Nutr. 1992;46(4):239-46.
25. Montano-Loza AJ, Duarte-Rojo A, Meza-Junco J, Baracos VE, Sawyer MB, Pang JX, et al. Inclusion of Sarcopenia Within MELD (MELD-Sarcopenia) and the Prediction of Mortality in Patients With Cirrhosis. Clin Transl Gastroenterol. 2015;6(7):e102.
26. Warner Ii ER, Satapathy SK. Sarcopenia in the Cirrhotic Patient: Current Knowledge and Future Directions. Journal of Clinical and Experimental Hepatology. 2023;13(1):162-77.
27. Heintz-Buschart A, Wilmes P. Human Gut Microbiome: Function Matters. Trends in Microbiology. 2018;26(7):563-74.
28. Jaenicke S, Ander C, Bekel T, Bisdorf R, Dröge M, Gartemann KH, et al. Comparative and joint analysis of two metagenomic datasets from a biogas fermenter obtained by 454-pyrosequencing. PLoS One. 2011;6(1):e14519.
29. Grosicki GJ, Fielding RA, Lustgarten MS. Gut Microbiota Contribute to Age-Related Changes in Skeletal Muscle Size, Composition, and Function: Biological Basis for a Gut-Muscle Axis. Calcif Tissue Int. 2018;102(4):433-42.
30. Lamichhane S, Sen P, Dickens AM, Orešič M, Bertram HC. Gut metabolome meets microbiome: A methodological perspective to understand the relationship between host and microbe. Methods. 2018;149:3-12.
31. Visconti A, Le Roy CI, Rosa F, Rossi N, Martin TC, Mohney RP, et al. Interplay between the human gut microbiome and host metabolism. Nat Commun. 2019;10(1):4505.
32. Paik D, Yao L, Zhang Y, Bae S, D'Agostino GD, Zhang M, et al. Human gut bacteria produce T(H)17-modulating bile acid metabolites. Nature. 2022;603(7903):907-12.
33. Tripathi A, Debelius J, Brenner DA, Karin M, Loomba R, Schnabl B, et al. The gut-liver axis and the intersection with the microbiome. Nat Rev Gastroenterol Hepatol. 2018;15(7):397-411.
34. Lee PC, Lee KC, Yang TC, Lu HS, Cheng TY, Chen YJ, et al. Sarcopenia-related gut microbial changes are associated with the risk of complications in people with cirrhosis. JHEP Rep. 2023;5(1):100619.
35. Kang L, Li P, Wang D, Wang T, Hao D, Qu X. Alterations in intestinal microbiota diversity, composition, and function in patients with sarcopenia. Sci Rep. 2021;11(1):4628.

36. Wang Y, Zhang Y, Lane NE, Wu J, Yang T, Li J, et al. Population-based metagenomics analysis reveals altered gut microbiome in sarcopenia: data from the Xiangya Sarcopenia Study. J Cachexia Sarcopenia Muscle. 2022;13(5):2340-51.
37. Siddharth J, Chakrabarti A, Pannérec A, Karaz S, Morin-Rivron D, Masoodi M, et al. Aging and sarcopenia associate with specific interactions between gut microbes, serum biomarkers and host physiology in rats. Aging (Albany NY). 2017;9(7):1698-720.
38. Liao X, Wu M, Hao Y, Deng H. Exploring the Preventive Effect and Mechanism of Senile Sarcopenia Based on "Gut-Muscle Axis". Front Bioeng Biotechnol. 2020;8:590869.
39. Ticinesi A, Nouvenne A, Cerundolo N, Catania P, Prati B, Tana C, et al. Gut Microbiota, Muscle Mass and Function in Aging: A Focus on Physical Frailty and Sarcopenia. Nutrients. 2019;11(7).
40. Ahluwalia V, Betrapally NS, Hylemon PB, White MB, Gillevet PM, Unser AB, et al. Impaired Gut-Liver-Brain Axis in Patients with Cirrhosis. Sci Rep. 2016;6:26800.
41. Kumar R, Prakash SS, Priyadarshi RN, Anand U. Sarcopenia in Chronic Liver Disease: A Metabolic Perspective. J Clin Transl Hepatol. 2022;10(6):1213-22.
42. Chen Y, Yang F, Lu H, Wang B, Chen Y, Lei D, et al. Characterization of fecal microbial communities in patients with liver cirrhosis. Hepatology. 2011;54(2):562-72.
43. Giannelli V, Di Gregorio V, Iebba V, Giusto M, Schippa S, Merli M, et al. Microbiota and the gut-liver axis: bacterial translocation, inflammation and infection in cirrhosis. World J Gastroenterol. 2014;20(45):16795-810.
44. Kakiyama G, Pandak WM, Gillevet PM, Hylemon PB, Heuman DM, Daita K, et al. Modulation of the fecal bile acid profile by gut microbiota in cirrhosis. J Hepatol. 2013;58(5):949-55.
45. Schmidt TSB, Raes J, Bork P. The Human Gut Microbiome: From Association to Modulation. Cell. 2018;172(6):1198-215.
46. Gilbert JA, Quinn RA, Debelius J, Xu ZZ, Morton J, Garg N, et al. Microbiome-wide association studies link dynamic microbial consortia to disease. Nature. 2016;535(7610):94-103.
47. Wang J, Jia H. Metagenome-wide association studies: fine-mining the microbiome. Nature Reviews Microbiology. 2016;14(8):508-22.
48. Xie G, Wang X, Liu P, Wei R, Chen W, Rajani C, et al. Distinctly altered gut microbiota in the progression of liver disease. Oncotarget. 2016;7(15):19355-66.
49. Wiest R, Lawson M, Geuking M. Pathological bacterial translocation in liver cirrhosis. J Hepatol. 2014;60(1):197-209.
50. Pugin J, Schürer-Maly CC, Leturcq D, Moriarty A, Ulevitch RJ, Tobias PS. Lipopolysaccharide activation of human endothelial and epithelial cells is mediated by lipopolysaccharide-binding protein and soluble CD14. Proc Natl Acad Sci U S A. 1993;90(7):2744-8.
51. Rong YD, Bian AL, Hu HY, Ma Y, Zhou XZ. Study on relationship between elderly sarcopenia and inflammatory cytokine IL-6, anti-inflammatory cytokine IL-10. BMC Geriatr. 2018;18(1):308.
52. Visser M, Pahor M, Taaffe DR, Goodpaster BH, Simonsick EM, Newman AB, et al. Relationship of Interleukin-6 and Tumor Necrosis Factor-α With Muscle Mass and Muscle Strength in Elderly Men and Women: The Health ABC Study. The Journals of Gerontology: Series A. 2002;57(5):M326-M32.
53. Shokri-Mashhadi N, Moradi S, Heidari Z, Saadat S. Association of circulating C-reactive protein and high-sensitivity C-reactive protein with components of sarcopenia: A systematic review and meta-analysis of observational studies. Exp Gerontol. 2021;150:111330.
54. Chaudhari SN, Luo JN, Harris DA, Aliakbarian H, Yao L, Paik D, et al. A microbial metabolite remodels the gut-liver axis following bariatric surgery. Cell Host Microbe. 2021;29(3):408-24.e7.
55. Funabashi M, Grove TL, Wang M, Varma Y, McFadden ME, Brown LC, et al. A metabolic pathway for bile acid dehydroxylation by the gut microbiome. Nature. 2020;582(7813):566-70.
56. Qiu Y, Yu J, Li Y, Yang F, Yu H, Xue M, et al. Depletion of gut microbiota induces skeletal muscle atrophy by FXR-FGF15/19 signalling. Ann Med. 2021;53(1):508-22.

57. Park MY, Kim SJ, Ko EK, Ahn SH, Seo H, Sung MK. Gut microbiota-associated bile acid deconjugation accelerates hepatic steatosis in ob/ob mice. J Appl Microbiol. 2016;121(3):800-10.
58. Aguirre M, Eck A, Koenen ME, Savelkoul PH, Budding AE, Venema K. Diet drives quick changes in the metabolic activity and composition of human gut microbiota in a validated in vitro gut model. Res Microbiol. 2016;167(2):114-25.
59. Frampton J, Murphy KG, Frost G, Chambers ES. Short-chain fatty acids as potential regulators of skeletal muscle metabolism and function. Nat Metab. 2020;2(9):840-8.
60. Oliphant K, Allen-Vercoe E. Macronutrient metabolism by the human gut microbiome: major fermentation by-products and their impact on host health. Microbiome. 2019;7(1):91.
61. Kamimura H, Sato T, Natsui K, Kobayashi T, Yoshida T, Kamimura K, et al. Molecular Mechanisms and Treatment of Sarcopenia in Liver Disease: A Review of Current Knowledge. Int J Mol Sci. 2021;22(3).
62. Schiaffino S, Dyar KA, Ciciliot S, Blaauw B, Sandri M. Mechanisms regulating skeletal muscle growth and atrophy. Febs j. 2013;280(17):4294-314.
63. Li F, Li Y, Duan Y, Hu CA, Tang Y, Yin Y. Myokines and adipokines: Involvement in the crosstalk between skeletal muscle and adipose tissue. Cytokine Growth Factor Rev. 2017;33:73-82.
64. Yoshida T, Delafontaine P. Mechanisms of IGF-1-Mediated Regulation of Skeletal Muscle Hypertrophy and Atrophy. Cells. 2020;9(9).
65. Mavalli MD, DiGirolamo DJ, Fan Y, Riddle RC, Campbell KS, van Groen T, et al. Distinct growth hormone receptor signaling modes regulate skeletal muscle development and insulin sensitivity in mice. J Clin Invest. 2010;120(11):4007-20.
66. Musarò A, McCullagh KJ, Naya FJ, Olson EN, Rosenthal N. IGF-1 induces skeletal myocyte hypertrophy through calcineurin in association with GATA-2 and NF-ATc1. Nature. 1999;400(6744):581-5.
67. Khalil R. Ubiquitin-Proteasome Pathway and Muscle Atrophy. Adv Exp Med Biol. 2018;1088:235-48.
68. Desbois-Mouthon C, Cadoret A, Blivet-Van Eggelpoël MJ, Bertrand F, Cherqui G, Perret C, et al. Insulin and IGF-1 stimulate the beta-catenin pathway through two signalling cascades involving GSK-3beta inhibition and Ras activation. Oncogene. 2001;20(2):252-9.
69. Armstrong DD, Esser KA. Wnt/beta-catenin signaling activates growth-control genes during overload-induced skeletal muscle hypertrophy. Am J Physiol Cell Physiol. 2005;289(4):C853-9.
70. Bian A, Ma Y, Zhou X, Guo Y, Wang W, Zhang Y, et al. Association between sarcopenia and levels of growth hormone and insulin-like growth factor-1 in the elderly. BMC Musculoskelet Disord. 2020;21(1):214.
71. Bogdanovich S, Krag TO, Barton ER, Morris LD, Whittemore LA, Ahima RS, et al. Functional improvement of dystrophic muscle by myostatin blockade. Nature. 2002;420(6914):418-21.
72. Lokireddy S, Mouly V, Butler-Browne G, Gluckman PD, Sharma M, Kambadur R, et al. Myostatin promotes the wasting of human myoblast cultures through promoting ubiquitin-proteasome pathway-mediated loss of sarcomeric proteins. Am J Physiol Cell Physiol. 2011;301(6):C1316-24.
73. Carnac G, Vernus B, Bonnieu A. Myostatin in the pathophysiology of skeletal muscle. Curr Genomics. 2007;8(7):415-22.
74. Sinclair M, Gow PJ, Grossmann M, Angus PW. Review article: sarcopenia in cirrhosis--aetiology, implications and potential therapeutic interventions. Aliment Pharmacol Ther. 2016;43(7):765-77.
75. McFarlane C, Plummer E, Thomas M, Hennebry A, Ashby M, Ling N, et al. Myostatin induces cachexia by activating the ubiquitin proteolytic system through an NF-kappaB-independent, FoxO1-dependent mechanism. J Cell Physiol. 2006;209(2):501-14.
76. Lee SJ. Regulation of muscle mass by myostatin. Annu Rev Cell Dev Biol. 2004;20:61-86.

77. Taylor WE, Bhasin S, Artaza J, Byhower F, Azam M, Willard DH, Jr., et al. Myostatin inhibits cell proliferation and protein synthesis in C2C12 muscle cells. Am J Physiol Endocrinol Metab. 2001;280(2):E221-8.
78. Becker C, Lord SR, Studenski SA, Warden SJ, Fielding RA, Recknor CP, et al. Myostatin antibody (LY2495655) in older weak fallers: a proof-of-concept, randomised, phase 2 trial. Lancet Diabetes Endocrinol. 2015;3(12):948-57.
79. Izumiya Y, Bina HA, Ouchi N, Akasaki Y, Kharitonenkov A, Walsh K. FGF21 is an Akt-regulated myokine. FEBS Lett. 2008;582(27):3805-10.
80. Oost LJ, Kustermann M, Armani A, Blaauw B, Romanello V. Fibroblast growth factor 21 controls mitophagy and muscle mass. J Cachexia Sarcopenia Muscle. 2019;10(3):630-42.
81. Fisher FM, Maratos-Flier E. Understanding the Physiology of FGF21. Annu Rev Physiol. 2016;78:223-41.
82. Jung HW, Park JH, Kim DA, Jang IY, Park SJ, Lee JY, et al. Association between serum FGF21 level and sarcopenia in older adults. Bone. 2021;145:115877.
83. Roh E, Hwang SY, Yoo HJ, Baik SH, Cho B, Park YS, et al. Association of plasma FGF21 levels with muscle mass and muscle strength in a national multicentre cohort study: Korean Frailty and Aging Cohort Study. Age Ageing. 2021;50(6):1971-8.
84. Guo M, Yao J, Li J, Zhang J, Wang D, Zuo H, et al. Irisin ameliorates age-associated sarcopenia and metabolic dysfunction. J Cachexia Sarcopenia Muscle. 2022.
85. Liu S, Cui F, Ning K, Wang Z, Fu P, Wang D, et al. Role of irisin in physiology and pathology. Front Endocrinol (Lausanne). 2022;13:962968.
86. Colaianni G, Cinti S, Colucci S, Grano M. Irisin and musculoskeletal health. Ann N Y Acad Sci. 2017;1402(1):5-9.
87. Peng H, Wang Q, Lou T, Qin J, Jung S, Shetty V, et al. Myokine mediated muscle-kidney crosstalk suppresses metabolic reprogramming and fibrosis in damaged kidneys. Nat Commun. 2017;8(1):1493.
88. Zhao M, Zhou X, Yuan C, Li R, Ma Y, Tang X. Association between serum irisin concentrations and sarcopenia in patients with liver cirrhosis: a cross-sectional study. Sci Rep. 2020;10(1):16093.
89. Boga S, Yildirim AE, Ucbilek E, Koksal AR, Sisman ST, Durak I, et al. The effect of sarcopenia and serum myokines on prognosis and survival in cirrhotic patients: a multicenter cross-sectional study. Eur J Gastroenterol Hepatol. 2022;34(12):1261-8.
90. Nishikawa H, Enomoto H, Nishiguchi S, Iijima H. Liver Cirrhosis and Sarcopenia from the Viewpoint of Dysbiosis. Int J Mol Sci. 2020;21(15).
91. Peng S, Plank LD, McCall JL, Gillanders LK, McIlroy K, Gane EJ. Body composition, muscle function, and energy expenditure in patients with liver cirrhosis: a comprehensive study. Am J Clin Nutr. 2007;85(5):1257-66.
92. Simbrunner B, Trauner M, Reiberger T. Review article: therapeutic aspects of bile acid signalling in the gut-liver axis. Aliment Pharmacol Ther. 2021;54(10):1243-62.
93. Tsien CD, McCullough AJ, Dasarathy S. Late evening snack: exploiting a period of anabolic opportunity in cirrhosis. J Gastroenterol Hepatol. 2012;27(3):430-41.
94. Hanai T, Shiraki M, Nishimura K, Ohnishi S, Imai K, Suetsugu A, et al. Sarcopenia impairs prognosis of patients with liver cirrhosis. Nutrition. 2015;31(1):193-9.
95. Dichi JB, Dichi I, Maio R, Correa CR, Angeleli AY, Bicudo MH, et al. Whole-body protein turnover in malnourished patients with child class B and C cirrhosis on diets low to high in protein energy. Nutrition. 2001;17(3):239-42.
96. Meyer F, Bannert K, Wiese M, Esau S, Sautter LF, Ehlers L, et al. Molecular Mechanism Contributing to Malnutrition and Sarcopenia in Patients with Liver Cirrhosis. Int J Mol Sci. 2020;21(15).
97. Perino A, Demagny H, Velazquez-Villegas L, Schoonjans K. Molecular Physiology of Bile Acid Signaling in Health, Disease, and Aging. Physiol Rev. 2021;101(2):683-731.

98. Thomas C, Pellicciari R, Pruzanski M, Auwerx J, Schoonjans K. Targeting bile-acid signalling for metabolic diseases. Nat Rev Drug Discov. 2008;7(8):678-93.
99. Abrigo J, Campos F, Gonzalez F, Aguirre F, Gonzalez A, Huerta-Salgado C, et al. Sarcopenia Induced by Chronic Liver Disease in Mice Requires the Expression of the Bile Acids Membrane Receptor TGR5. Int J Mol Sci. 2020;21(21).
100. Liu N, Feng J, Lv Y, Liu Q, Deng J, Xia Y, et al. Role of bile acids in the diagnosis and progression of liver cirrhosis: A prospective observational study. Exp Ther Med. 2019;18(5):4058-66.
101. Podda M, Ghezzi C, Battezzati PM, Bertolini E, Crosignani A, Petroni ML, et al. Ursodeoxycholic acid for chronic liver diseases. J Clin Gastroenterol. 1988;10 Suppl 2:S25-31.
102. Attili AF, Angelico M, Cantafora A, Alvaro D, Capocaccia L. Bile acid-induced liver toxicity: relation to the hydrophobic-hydrophilic balance of bile acids. Med Hypotheses. 1986;19(1):57-69.
103. Abrigo J, Gonzalez F, Aguirre F, Tacchi F, Gonzalez A, Meza MP, et al. Cholic acid and deoxycholic acid induce skeletal muscle atrophy through a mechanism dependent on TGR5 receptor. J Cell Physiol. 2021;236(1):260-72.
104. Miura R, Tanaka A, Takikawa H. Urinary bile acid sulfate levels in patients with primary biliary cirrhosis. Hepatol Res. 2011;41(4):358-63.
105. Monte MJ, Marin JJ, Antelo A, Vazquez-Tato J. Bile acids: chemistry, physiology, and pathophysiology. World J Gastroenterol. 2009;15(7):804-16.
106. Šarenac TM, Mikov M. Bile Acid Synthesis: From Nature to the Chemical Modification and Synthesis and Their Applications as Drugs and Nutrients. Front Pharmacol. 2018;9:939.
107. Nimer N, Choucair I, Wang Z, Nemet I, Li L, Gukasyan J, et al. Bile acids profile, histopathological indices and genetic variants for non-alcoholic fatty liver disease progression. Metabolism. 2021;116:154457.
108. Crosignani A, Podda M, Battezzati PM, Bertolini E, Zuin M, Watson D, et al. Changes in bile acid composition in patients with primary biliary cirrhosis induced by ursodeoxycholic acid administration. Hepatology. 1991;14(6):1000-7.
109. Horvatits T, Drolz A, Roedl K, Rutter K, Ferlitsch A, Fauler G, et al. Serum bile acids as marker for acute decompensation and acute-on-chronic liver failure in patients with non-cholestatic cirrhosis. Liver Int. 2017;37(2):224-31.
110. Lu L. Guidelines for the Management of Cholestatic Liver Diseases (2021). J Clin Transl Hepatol. 2022;10(4):757-69.
111. Strasberg SM, Ilson RG. The effect of bile acid synthesis on cholesterol secretion into the bile. Ann Surg. 1975;181(4):458-65.
112. Chiang JY. Bile acid metabolism and signaling. Compr Physiol. 2013;3(3):1191-212.
113. Wahlström A, Sayin Sama I, Marschall H-U, Bäckhed F. Intestinal Crosstalk between Bile Acids and Microbiota and Its Impact on Host Metabolism. Cell Metabolism. 2016;24(1):41-50.
114. Sayin SI, Wahlström A, Felin J, Jäntti S, Marschall HU, Bamberg K, et al. Gut microbiota regulates bile acid metabolism by reducing the levels of tauro-beta-muricholic acid, a naturally occurring FXR antagonist. Cell Metab. 2013;17(2):225-35.
115. Falany CN, Johnson MR, Barnes S, Diasio RB. Glycine and taurine conjugation of bile acids by a single enzyme. Molecular cloning and expression of human liver bile acid CoA:amino acid N-acyltransferase. J Biol Chem. 1994;269(30):19375-9.
116. Teramoto T, Nishio T, Kurogi K, Sakakibara Y, Kakuta Y. The crystal structure of mouse SULT2A8 reveals the mechanism of 7α-hydroxyl, bile acid sulfation. Biochem Biophys Res Commun. 2021;562:15-20.
117. Palmer RH, Bolt MG. Bile acid sulfates. I. Synthesis of lithocholic acid sulfates and their identification in human bile. J Lipid Res. 1971;12(6):671-9.

118. Bathena SP, Mukherjee S, Olivera M, Alnouti Y. The profile of bile acids and their sulfate metabolites in human urine and serum. J Chromatogr B Analyt Technol Biomed Life Sci. 2013;942-943:53-62.
119. Hedenborg G, Norman A. The nature of urinary bile acid conjugates in patients with extrahepatic cholestasis. Scand J Clin Lab Invest. 1984;44(8):725-33.
120. Sinal CJ, Tohkin M, Miyata M, Ward JM, Lambert G, Gonzalez FJ. Targeted disruption of the nuclear receptor FXR/BAR impairs bile acid and lipid homeostasis. Cell. 2000;102(6):731-44.
121. Feng L, Zhang W, Shen Q, Miao C, Chen L, Li Y, et al. Bile acid metabolism dysregulation associates with cancer cachexia: roles of liver and gut microbiome. J Cachexia Sarcopenia Muscle. 2021;12(6):1553-69.
122. Mullish BH, Pechlivanis A, Barker GF, Thursz MR, Marchesi JR, McDonald JAK. Functional microbiomics: Evaluation of gut microbiota-bile acid metabolism interactions in health and disease. Methods. 2018;149:49-58.
123. Marion S, Studer N, Desharnais L, Menin L, Escrig S, Meibom A, et al. In vitro and in vivo characterization of Clostridium scindens bile acid transformations. Gut Microbes. 2019;10(4):481-503.
124. Sato Y, Atarashi K, Plichta DR, Arai Y, Sasajima S, Kearney SM, et al. Novel bile acid biosynthetic pathways are enriched in the microbiome of centenarians. Nature. 2021;599(7885):458-64.
125. Wells JE, Berr F, Thomas LA, Dowling RH, Hylemon PB. Isolation and characterization of cholic acid 7alpha-dehydroxylating fecal bacteria from cholesterol gallstone patients. J Hepatol. 2000;32(1):4-10.
126. Ridlon JM, Kang DJ, Hylemon PB. Isolation and characterization of a bile acid inducible 7alpha-dehydroxylating operon in Clostridium hylemonae TN271. Anaerobe. 2010;16(2):137-46.
127. Batta AK, Salen G, Arora R, Shefer S, Batta M, Person A. Side chain conjugation prevents bacterial 7-dehydroxylation of bile acids. J Biol Chem. 1990;265(19):10925-8.
128. Lucas LN, Barrett K, Kerby RL, Zhang Q, Cattaneo LE, Stevenson D, et al. Dominant Bacterial Phyla from the Human Gut Show Widespread Ability To Transform and Conjugate Bile Acids. mSystems. 2021:e0080521.
129. Russell DW. The enzymes, regulation, and genetics of bile acid synthesis. Annu Rev Biochem. 2003;72:137-74.
130. Winston JA, Rivera A, Cai J, Patterson AD, Theriot CM. Secondary bile acid ursodeoxycholic acid alters weight, the gut microbiota, and the bile acid pool in conventional mice. PLoS One. 2021;16(2):e0246161.
131. Doden H, Sallam LA, Devendran S, Ly L, Doden G, Daniel SL, et al. Metabolism of Oxo-Bile Acids and Characterization of Recombinant 12α-Hydroxysteroid Dehydrogenases from Bile Acid 7α-Dehydroxylating Human Gut Bacteria. Appl Environ Microbiol. 2018;84(10).
132. Li W, Hang S, Fang Y, Bae S, Zhang Y, Zhang M, et al. A bacterial bile acid metabolite modulates T(reg) activity through the nuclear hormone receptor NR4A1. Cell Host Microbe. 2021;29(9):1366-77.e9.
133. Qiu Y, Yu J, Ji X, Yu H, Xue M, Zhang F, et al. Ileal FXR-FGF15/19 signaling activation improves skeletal muscle loss in aged mice. Mech Ageing Dev. 2022;202:111630.
134. Wang H, Chen J, Hollister K, Sowers LC, Forman BM. Endogenous bile acids are ligands for the nuclear receptor FXR/BAR. Mol Cell. 1999;3(5):543-53.
135. Mueller M, Thorell A, Claudel T, Jha P, Koefeler H, Lackner C, et al. Ursodeoxycholic acid exerts farnesoid X receptor-antagonistic effects on bile acid and lipid metabolism in morbid obesity. J Hepatol. 2015;62(6):1398-404.
136. Benoit B, Meugnier E, Castelli M, Chanon S, Vieille-Marchiset A, Durand C, et al. Fibroblast growth factor 19 regulates skeletal muscle mass and ameliorates muscle wasting in mice. Nat Med. 2017;23(8):990-6.

137. Maruyama T, Miyamoto Y, Nakamura T, Tamai Y, Okada H, Sugiyama E, et al. Identification of membrane-type receptor for bile acids (M-BAR). Biochem Biophys Res Commun. 2002;298(5):714-9.
138. Perino A, Pols TW, Nomura M, Stein S, Pellicciari R, Schoonjans K. TGR5 reduces macrophage migration through mTOR-induced C/EBPβ differential translation. J Clin Invest. 2014;124(12):5424-36.
139. Chen H, Ma J, Ma X. Administration of tauroursodeoxycholic acid attenuates dexamethasone-induced skeletal muscle atrophy. Biochem Biophys Res Commun. 2021;570:96-102.
140. Abrigo J, Olguín H, Gutierrez D, Tacchi F, Arrese M, Cabrera D, et al. Bile Acids Induce Alterations in Mitochondrial Function in Skeletal Muscle Fibers. Antioxidants (Basel). 2022;11(9).
141. Cannavino J, Brocca L, Sandri M, Grassi B, Bottinelli R, Pellegrino MA. The role of alterations in mitochondrial dynamics and PGC-1α over-expression in fast muscle atrophy following hindlimb unloading. J Physiol. 2015;593(8):1981-95.
142. Liu HW, Chang YC, Chan YC, Hu SH, Liu MY, Chang SJ. Dysregulations of mitochondrial quality control and autophagic flux at an early age lead to progression of sarcopenia in SAMP8 mice. Biogerontology. 2020;21(3):367-80.
143. Calmus Y, Guechot J, Podevin P, Bonnefis MT, Giboudeau J, Poupon R. Differential effects of chenodeoxycholic and ursodeoxycholic acids on interleukin 1, interleukin 6 and tumor necrosis factor-alpha production by monocytes. Hepatology. 1992;16(3):719-23.
144. Zhao L, Zhang H, Liu X, Xue S, Chen D, Zou J, et al. TGR5 deficiency activates antitumor immunity in non-small cell lung cancer via restraining M2 macrophage polarization. Acta Pharm Sin B. 2022;12(2):787-800.
145. Renga B, Mencarelli A, Cipriani S, D'Amore C, Carino A, Bruno A, et al. The bile acid sensor FXR is required for immune-regulatory activities of TLR-9 in intestinal inflammation. PLoS One. 2013;8(1):e54472.
146. Cipriani S, Mencarelli A, Chini MG, Distrutti E, Renga B, Bifulco G, et al. The bile acid receptor GPBAR-1 (TGR5) modulates integrity of intestinal barrier and immune response to experimental colitis. PLoS One. 2011;6(10):e25637.
147. Guo C, Xie S, Chi Z, Zhang J, Liu Y, Zhang L, et al. Bile Acids Control Inflammation and Metabolic Disorder through Inhibition of NLRP3 Inflammasome. Immunity. 2016;45(4):802-16.
148. Hang S, Paik D, Yao L, Kim E, Trinath J, Lu J, et al. Bile acid metabolites control T(H)17 and T(reg) cell differentiation. Nature. 2019;576(7785):143-8.
149. d'Hennezel E, Abubucker S, Murphy LO, Cullen TW. Total Lipopolysaccharide from the Human Gut Microbiome Silences Toll-Like Receptor Signaling. mSystems. 2017;2(6).
150. Nicastro H, Artioli GG, Costa Ados S, Solis MY, da Luz CR, Blachier F, et al. An overview of the therapeutic effects of leucine supplementation on skeletal muscle under atrophic conditions. Amino Acids. 2011;40(2):287-300.
151. Traub J, Reiss L, Aliwa B, Stadlbauer V. Malnutrition in Patients with Liver Cirrhosis. Nutrients. 2021;13(2).
152. Naseer M, Turse EP, Syed A, Dailey FE, Zatreh M, Tahan V. Interventions to improve sarcopenia in cirrhosis: A systematic review. World J Clin Cases. 2019;7(2):156-70.
153. Buse MG, Reid SS. Leucine. A possible regulator of protein turnover in muscle. J Clin Invest. 1975;56(5):1250-61.
154. Maki T, Yamamoto D, Nakanishi S, Iida K, Iguchi G, Takahashi Y, et al. Branched-chain amino acids reduce hindlimb suspension-induced muscle atrophy and protein levels of atrogin-1 and MuRF1 in rats. Nutr Res. 2012;32(9):676-83.
155. Abumrad NN, Robinson RP, Gooch BR, Lacy WW. The effect of leucine infusion on substrate flux across the human forearm. J Surg Res. 1982;32(5):453-63.

156. Román E, Torrades MT, Nadal MJ, Cárdenas G, Nieto JC, Vidal S, et al. Randomized pilot study: effects of an exercise programme and leucine supplementation in patients with cirrhosis. Dig Dis Sci. 2014;59(8):1966-75.
157. Ascenzi F, Barberi L, Dobrowolny G, Villa Nova Bacurau A, Nicoletti C, Rizzuto E, et al. Effects of IGF-1 isoforms on muscle growth and sarcopenia. Aging Cell. 2019;18(3):e12954.
158. Sinclair M, Grossmann M, Hoermann R, Angus PW, Gow PJ. Testosterone therapy increases muscle mass in men with cirrhosis and low testosterone: A randomised controlled trial. J Hepatol. 2016;65(5):906-13.
159. Yurci A, Yucesoy M, Unluhizarci K, Torun E, Gursoy S, Baskol M, et al. Effects of testosterone gel treatment in hypogonadal men with liver cirrhosis. Clin Res Hepatol Gastroenterol. 2011;35(12):845-54.
160. Wang C, Swerdloff RS, Iranmanesh A, Dobs A, Snyder PJ, Cunningham G, et al. Transdermal testosterone gel improves sexual function, mood, muscle strength, and body composition parameters in hypogonadal men. J Clin Endocrinol Metab. 2000;85(8):2839-53.
161. Sandri M, Sandri C, Gilbert A, Skurk C, Calabria E, Picard A, et al. Foxo transcription factors induce the atrophy-related ubiquitin ligase atrogin-1 and cause skeletal muscle atrophy. Cell. 2004;117(3):399-412.
162. Stitt TN, Drujan D, Clarke BA, Panaro F, Timofeyva Y, Kline WO, et al. The IGF-1/PI3K/Akt pathway prevents expression of muscle atrophy-induced ubiquitin ligases by inhibiting FOXO transcription factors. Mol Cell. 2004;14(3):395-403.
163. Gao S, Zhang G, Zhang Z, Zhu JZ, Li L, Zhou Y, et al. UBR2 targets myosin heavy chain IIb and IIx for degradation: Molecular mechanism essential for cancer-induced muscle wasting. Proc Natl Acad Sci U S A. 2022;119(43):e2200215119.
164. Paumgartner G, Beuers U. Ursodeoxycholic acid in cholestatic liver disease: mechanisms of action and therapeutic use revisited. Hepatology. 2002;36(3):525-31.
165. Hofmann AF. Bile acids as drugs: principles, mechanisms of action and formulations. Ital J Gastroenterol. 1995;27(2):106-13.
166. Liu J, Lu H, Lu YF, Lei X, Cui JY, Ellis E, et al. Potency of individual bile acids to regulate bile acid synthesis and transport genes in primary human hepatocyte cultures. Toxicol Sci. 2014;141(2):538-46.
167. Hillaire S, Ballet F, Franco D, Setchell KD, Poupon R. Effects of ursodeoxycholic acid and chenodeoxycholic acid on human hepatocytes in primary culture. Hepatology. 1995;22(1):82-7.
168. Traub J, Bergheim I, Eibisberger M, Stadlbauer V. Sarcopenia and Liver Cirrhosis-Comparison of the European Working Group on Sarcopenia Criteria 2010 and 2019. Nutrients. 2020;12(2).
169. EASL Clinical Practice Guidelines on nutrition in chronic liver disease. J Hepatol. 2019;70(1):172-93.
170. Tandon P, Low G, Mourtzakis M, Zenith L, Myers RP, Abraldes JG, et al. A Model to Identify Sarcopenia in Patients With Cirrhosis. Clin Gastroenterol Hepatol. 2016;14(10):1473-80.e3.
171. Roller RE, Eglseer D, Eisenberger A, Wirnsberger GH. The Graz Malnutrition Screening (GMS): a new hospital screening tool for malnutrition. Br J Nutr. 2016;115(4):650-7.
172. Amodio P, Bemeur C, Butterworth R, Cordoba J, Kato A, Montagnese S, et al. The nutritional management of hepatic encephalopathy in patients with cirrhosis: International Society for Hepatic Encephalopathy and Nitrogen Metabolism Consensus. Hepatology. 2013;58(1):325-36.
173. Borhofen SM, Gerner C, Lehmann J, Fimmers R, Görtzen J, Hey B, et al. The Royal Free Hospital-Nutritional Prioritizing Tool Is an Independent Predictor of Deterioration of Liver Function and Survival in Cirrhosis. Dig Dis Sci. 2016;61(6):1735-43.
174. Li K, Buchinger TJ, Bussy U, Fissette SD, Johnson NS, Li W. Quantification of 15 bile acids in lake charr feces by ultra-high performance liquid chromatography-tandem mass spectrometry. J Chromatogr B Analyt Technol Biomed Life Sci. 2015;1001:27-34.

175. Kakiyama G, Muto A, Takei H, Nittono H, Murai T, Kurosawa T, et al. A simple and accurate HPLC method for fecal bile acid profile in healthy and cirrhotic subjects: validation by GC-MS and LC-MS. J Lipid Res. 2014;55(5):978-90.
176. Reisinger AC, Posch F, Hackl G, Marsche G, Sourij H, Bourgeois B, et al. Branched-Chain Amino Acids Can Predict Mortality in ICU Sepsis Patients. Nutrients. 2021;13(9).
177. Zakrzewski M, Proietti C, Ellis JJ, Hasan S, Brion MJ, Berger B, et al. Calypso: a user-friendly web-server for mining and visualizing microbiome-environment interactions. Bioinformatics. 2017;33(5):782-3.
178. Chong J, Liu P, Zhou G, Xia J. Using MicrobiomeAnalyst for comprehensive statistical, functional, and meta-analysis of microbiome data. Nat Protoc. 2020;15(3):799-821.
179. Lu Y, Zhou G, Ewald J, Pang Z, Shiri T, Xia J. MicrobiomeAnalyst 2.0: comprehensive statistical, functional and integrative analysis of microbiome data. Nucleic Acids Res. 2023.
180. Pang Z, Chong J, Zhou G, de Lima Morais DA, Chang L, Barrette M, et al. MetaboAnalyst 5.0: narrowing the gap between raw spectra and functional insights. Nucleic Acids Res. 2021;49(W1):W388-w96.
181. Pang Z, Zhou G, Ewald J, Chang L, Hacariz O, Basu N, et al. Using MetaboAnalyst 5.0 for LC-HRMS spectra processing, multi-omics integration and covariate adjustment of global metabolomics data. Nat Protoc. 2022;17(8):1735-61.
182. Bernardi M, Angeli P, Claria J, Moreau R, Gines P, Jalan R, et al. Albumin in decompensated cirrhosis: new concepts and perspectives. Gut. 2020;69(6):1127-38.
183. Wong F. Drug insight: the role of albumin in the management of chronic liver disease. Nat Clin Pract Gastroenterol Hepatol. 2007;4(1):43-51.
184. Garcia-Martinez R, Caraceni P, Bernardi M, Gines P, Arroyo V, Jalan R. Albumin: pathophysiologic basis of its role in the treatment of cirrhosis and its complications. Hepatology. 2013;58(5):1836-46.
185. Stadlbauer V, Mookerjee RP, Wright GA, Davies NA, Jürgens G, Hallström S, et al. Role of Toll-like receptors 2, 4, and 9 in mediating neutrophil dysfunction in alcoholic hepatitis. Am J Physiol Gastrointest Liver Physiol. 2009;296(1):G15-22.
186. van Atteveld VA, Van Ancum JM, Reijnierse EM, Trappenburg MC, Meskers CGM, Maier AB. Erythrocyte sedimentation rate and albumin as markers of inflammation are associated with measures of sarcopenia: a cross-sectional study. BMC Geriatr. 2019;19(1):233.
187. Chen Z, Song C, Yao Z, Sun J, Liu W. Associations between albumin, globulin, albumin to globulin ratio and muscle mass in adults: results from the national health and nutrition examination survey 2011-2014. BMC Geriatr. 2022;22(1):383.
188. Silva-Fhon JR, Rojas-Huayta VM, Aparco-Balboa JP, Céspedes-Panduro B, Partezani-Rodrigues RA. Sarcopenia and blood albumin: A systematic review with meta-analysis. Biomedica. 2021;41(3):590-603.
189. Ponziani FR, Picca A, Marzetti E, Calvani R, Conta G, Del Chierico F, et al. Characterization of the gut-liver-muscle axis in cirrhotic patients with sarcopenia. Liver Int. 2021;41(6):1320-34.
190. Horvath A, Rainer F, Bashir M, Leber B, Schmerboeck B, Klymiuk I, et al. Biomarkers for oralization during long-term proton pump inhibitor therapy predict survival in cirrhosis. Sci Rep. 2019;9(1):12000.
191. Stadlbauer V, Engertsberger L, Komarova I, Feldbacher N, Leber B, Pichler G, et al. Dysbiosis, gut barrier dysfunction and inflammation in dementia: a pilot study. BMC Geriatr. 2020;20(1):248.
192. Matiollo C, Rateke ECM, Moura EQA, Andrigueti M, de Augustinho FC, Zocche TL, et al. Elevated calprotectin levels are associated with mortality in patients with acute decompensation of liver cirrhosis. World J Hepatol. 2022;14(11):1964-76.

193. Kaushal K, Agarwal S, Sharma S, Goswami P, Singh N, Sachdev V, et al. Demonstration of Gut-Barrier Dysfunction in Early Stages of Non-alcoholic Fatty Liver Disease: A Proof-Of-Concept Study. J Clin Exp Hepatol. 2022;12(4):1102-13.
194. Karim A, Iqbal MS, Muhammad T, Ahmad F, Qaisar R. Elevated plasma zonulin and CAF22 are correlated with sarcopenia and functional dependency at various stages of Alzheimer's diseases. Neurosci Res. 2022;184:47-53.
195. Saeki C, Kanai T, Nakano M, Oikawa T, Torisu Y, Saruta M, et al. Low Serum Branched-Chain Amino Acid and Insulin-Like Growth Factor-1 Levels Are Associated with Sarcopenia and Slow Gait Speed in Patients with Liver Cirrhosis. J Clin Med. 2020;9(10).
196. Kukla M, Skladany L, Menżyk T, Derra A, Stygar D, Skonieczna M, et al. Irisin in Liver Cirrhosis. J Clin Med. 2020;9(10).
197. Erridge C, Pridmore A, Eley A, Stewart J, Poxton IR. Lipopolysaccharides of Bacteroides fragilis, Chlamydia trachomatis and Pseudomonas aeruginosa signal via toll-like receptor 2. J Med Microbiol. 2004;53(Pt 8):735-40.
198. Ticinesi A, Mancabelli L, Tagliaferri S, Nouvenne A, Milani C, Del Rio D, et al. The Gut-Muscle Axis in Older Subjects with Low Muscle Mass and Performance: A Proof of Concept Study Exploring Fecal Microbiota Composition and Function with Shotgun Metagenomics Sequencing. Int J Mol Sci. 2020;21(23).
199. Tan H, Zhao J, Zhang H, Zhai Q, Chen W. Novel strains of Bacteroides fragilis and Bacteroides ovatus alleviate the LPS-induced inflammation in mice. Appl Microbiol Biotechnol. 2019;103(5):2353-65.
200. Tan H, Yu Z, Wang C, Zhang Q, Zhao J, Zhang H, et al. Pilot Safety Evaluation of a Novel Strain of Bacteroides ovatus. Front Genet. 2018;9:539.
201. Parker BJ, Wearsch PA, Veloo ACM, Rodriguez-Palacios A. The Genus Alistipes: Gut Bacteria With Emerging Implications to Inflammation, Cancer, and Mental Health. Front Immunol. 2020;11:906.
202. Liu C, Cheung WH, Li J, Chow SK, Yu J, Wong SH, et al. Understanding the gut microbiota and sarcopenia: a systematic review. J Cachexia Sarcopenia Muscle. 2021;12(6):1393-407.
203. Lahiri S, Kim H, Garcia-Perez I, Reza MM, Martin KA, Kundu P, et al. The gut microbiota influences skeletal muscle mass and function in mice. Sci Transl Med. 2019;11(502).
204. Lin H, An Y, Tang H, Wang Y. Alterations of Bile Acids and Gut Microbiota in Obesity Induced by High Fat Diet in Rat Model. J Agric Food Chem. 2019;67(13):3624-32.
205. Kobayashi Y, Hara N, Sugimoto R, Mifuji-Moroka R, Tanaka H, Eguchi A, et al. The Associations between Circulating Bile Acids and the Muscle Volume in Patients with Non-alcoholic Fatty Liver Disease (NAFLD). Intern Med. 2017;56(7):755-62.
206. Tamai Y, Eguchi A, Shigefuku R, Kitamura H, Tempaku M, Sugimoto R, et al. Association of lithocholic acid with skeletal muscle hypertrophy through TGR5-IGF-1 and skeletal muscle mass in cultured mouse myotubes, chronic liver disease rats and humans. Elife. 2022;11.
207. Lee JY, Arai H, Nakamura Y, Fukiya S, Wada M, Yokota A. Contribution of the 7β-hydroxysteroid dehydrogenase from Ruminococcus gnavus N53 to ursodeoxycholic acid formation in the human colon. J Lipid Res. 2013;54(11):3062-9.
208. Thibaut MM, Gillard J, Dolly A, Roumain M, Leclercq IA, Delzenne NM, et al. Bile Acid Dysregulation Is Intrinsically Related to Cachexia in Tumor-Bearing Mice. Cancers (Basel). 2021;13(24).
209. Metges CC. Contribution of microbial amino acids to amino acid homeostasis of the host. J Nutr. 2000;130(7):1857s-64s.
210. Dejong CH, van de Poll MC, Soeters PB, Jalan R, Olde Damink SW. Aromatic amino acid metabolism during liver failure. J Nutr. 2007;137(6 Suppl 1):1579S-85S; discussion 97S-98S.
211. Ribeiro CB, Christofoletti DC, Pezolato VA, de Cássia Marqueti Durigan R, Prestes J, Tibana RA, et al. Leucine minimizes denervation-induced skeletal muscle atrophy of rats through akt/mtor signaling pathways. Front Physiol. 2015;6:73.

212. Hinkle JS, Rivera CN, Vaughan RA. Branched-Chain Amino Acids and Mitochondrial Biogenesis: An Overview and Mechanistic Summary. Mol Nutr Food Res. 2022;66(20):e2200109.
213. Lefevre C, Bindels LB. Role of the Gut Microbiome in Skeletal Muscle Physiology and Pathophysiology. Curr Osteoporos Rep. 2022;20(6):422-32.
214. Sonnenburg JL, Bäckhed F. Diet-microbiota interactions as moderators of human metabolism. Nature. 2016;535(7610):56-64.
215. Salonen A, Lahti L, Salojärvi J, Holtrop G, Korpela K, Duncan SH, et al. Impact of diet and individual variation on intestinal microbiota composition and fermentation products in obese men. Isme j. 2014;8(11):2218-30.
216. Horvath TD, Ihekweazu FD, Haidacher SJ, Ruan W, Engevik KA, Fultz R, et al. Bacteroides ovatus colonization influences the abundance of intestinal short chain fatty acids and neurotransmitters. iScience. 2022;25(5):104158.
217. Pomacu MM, Trașcă MD, Pădureanu V, Bugă AM, Andrei AM, Stănciulescu EC, et al. Interrelation of inflammation and oxidative stress in liver cirrhosis. Exp Ther Med. 2021;21(6):602.
218. Yamamoto Y, Yamashita S. Plasma ratio of ubiquinol and ubiquinone as a marker of oxidative stress. Mol Aspects Med. 1997;18 Suppl:S79-84.
219. Miles MV, Horn PS, Tang PH, Morrison JA, Miles L, DeGrauw T, et al. Age-related changes in plasma coenzyme Q10 concentrations and redox state in apparently healthy children and adults. Clin Chim Acta. 2004;347(1-2):139-44.
220. Ernster L, Dallner G. Biochemical, physiological and medical aspects of ubiquinone function. Biochim Biophys Acta. 1995;1271(1):195-204.
221. Lagendijk J, Ubbink JB, Vermaak WJ. Measurement of the ratio between the reduced and oxidized forms of coenzyme Q10 in human plasma as a possible marker of oxidative stress. Journal of Lipid Research. 1996;37(1):67-75.
222. Powers SK, Ji LL, Kavazis AN, Jackson MJ. Reactive oxygen species: impact on skeletal muscle. Compr Physiol. 2011;1(2):941-69.
223. Steinbrenner H, Speckmann B, Klotz LO. Selenoproteins: Antioxidant selenoenzymes and beyond. Arch Biochem Biophys. 2016;595:113-9.
224. Cai Y, Shen X, Lu L, Yan H, Huang H, Gaule P, et al. Bile acid distributions, sex-specificity, and prognosis in colorectal cancer. Biol Sex Differ. 2022;13(1):61.
225. Jensen EA, Young JA, Mathes SC, List EO, Carroll RK, Kuhn J, et al. Crosstalk between the growth hormone/insulin-like growth factor-1 axis and the gut microbiome: A new frontier for microbial endocrinology. Growth Horm IGF Res. 2020;53-54:101333.
226. Rothschild D, Weissbrod O, Barkan E, Kurilshikov A, Korem T, Zeevi D, et al. Environment dominates over host genetics in shaping human gut microbiota. Nature. 2018;555(7695):210-5.
227. Scepanovic P, Hodel F, Mondot S, Partula V, Byrd A, Hammer C, et al. A comprehensive assessment of demographic, environmental, and host genetic associations with gut microbiome diversity in healthy individuals. Microbiome. 2019;7(1):130.